POLYTECHNIC UNIVERSITY OF MARCHE

Faculty of Medicine and Surgery

Department of Biomedical Sciences and Public Health

PhD course in Biomedical Sciences

XXXVII cycle

Carbapenemase-producing *Klebsiella pneumoniae*: a challenge to global health. Records from University hospitals in Central Italy.

PhD student: Gloria D'Achille

Tutor: Dr. Gianluca Morroni

TABLE OF CONTENTS

1. INTRODUCTION 1

1.1. Carbapenems 2

1.2. *Mechanisms of carbapenem resistance in Enterobacteriaceae* 4

1.2.1.1. Carbapenemases 5

1.2.1.2. Klebsiella pneumoniae carbapenemases 6

1.2.1.3. New Delhi metallo-β-lactamases 8

1.2.1.4. Oxacillinase-48-like carbapenemases 11

1.3. CRE distribution 13

1.4. Therapeutic options 15

2. MATERIAL AND METHODS 19

2.1. Clinical strains 19

2.2. PCR assays 20

2.3. Antibiotics 20

2.3.1. Susceptibility tests 20

2.4. Genomic DNA extraction 21

2.4.1. Genomic DNA quantity evaluation 22

2.4.2. Genomic DNA quality evaluation 22

2.5. Typing assays 22

2.5.1. PFGE 22

2.5.1.1. XbaI digestion 23

2.5.1.2. S1 digestion 23

2.6. WGS 23

2.6.1. Oxford Nanopore technology 24

2.6.1.1. MinION Mk1B 24

2.6.1.2. Library preparation 25

2.6.1.3. Priming and loading the flow cell 25

2.6.2. Illumina technology 26

2.6.2.1. Illumina Miseq 26

2.6.2.2. Library preparation 27

2.6.2.3. Library quality check and dilution to final concentration 28

2.7. MLST 28

2.8. Data analysis 28
3. RESULTS 29
3.1. KPC-Kp 29
3.1.1. Resistance phenotypes 29
3.1.2. Genotyping 32
3.2. OXA-48-Kp 37
3.2.1. Resistance phenotypes 37
3.2.2. Genotyping 38
3.3. *NDM-Kp* 41
3.3.1. Resistance phenotypes 42
3.3.2. Genotyping 42
3.4. OXA-48-NDM-Kp 48
3.4.1. Resistance phenotypes 48
3.4.2. Genotyping 48
3.5. Diffusion of non KPC-producing CR-KP 56
4. DISCUSSION 59
5. CONCLUSIONS 68
6. REFERENCES 70

1. INTRODUCTION

Bacterial antibiotic resistance is nowadays known as one of the most worrying public health threats worldwide. But it wasn't always like that. Almost a century ago, thanks to the Alexander Fleming discovery of penicillin in 1928, the antibiotic era opened up and the concept of modern medicine was completely upset. This antibiotic together with all the subsequently developed suggested a bright future in which we would be able to control and overcome the main part of antimicrobial infections. This prediction was true only for a very short period. Indeed, already in 1940, the first enzyme capable of hydrolyzing and inactivating penicillin was isolated from an *Escherichia coli* strain by Abraham and Chain, introducing the ever-growing penicillinases class *(Hansen, 2021)*. Despite all the efforts on developing new molecules also with different targets and sites of action, bacterial strains seem to always be one step ahead us in rapidly building up different resistance mechanisms. Development of resistance mechanisms and diffusion of antibiotic-resistant strains is related to human bad habits. In fact, the extensive use of antibiotics in agriculture and farms and the administration of inadequate therapies, constantly impress a selective pressure on bacteria that are pushed to develop antibiotic resistance mechanisms to survive. Today we face multidrug-resistant (MDR) microorganisms, defined as strains resistant to at least one agent of three different antibiotic classes *(Magiorakos et al., 2011)*. Both the difficulty of finding a successful therapy and the high number of deaths caused by MDR have a big impact on global economy and society. Fifty thousand MDR-related deaths were counted in 2016 in Europe and USA alone, and these numbers are constantly growing. If we don't find a way to control antibiotic resistance, the global burden of infections will exceed 10 million each year by 2050 *(Montesinos et al., 2024)*. Center for Diseases Control and Prevention (CDC) has estimated as high as 55 billion dollars per year the charge related to antimicrobial resistance only in the USA. These data are probably underestimated because of a lack of complete reports and surveillance *(Duin and Doi, 2017)*. Obviously, antimicrobial resistance (AMR) particularly impacts on debilitated subjects and shows different country distributions linked with types and rates of antibiotics administration. On the other hand, increasing international travel promotes the AMR global spread. Among Gram-negative bacteria, an important role is played by the family of *Enterobacteriaceae*. Members of this group of microorganisms can be normally found in human and animal intestinal tracts. *Klebsiella pneumoniae* and *Escherichia coli* are the most relevant clinical species belonging to *Enterobacteriaceae.* The first one is an environmental bacterium normally found as commensal in human respiratory and gut mucosa while the

second one is one of the most important members of the human intestinal microbiota. In conditions like immunity deficiency, prolonged hospitalization, poor sterility of medical devices, and bad hygiene of healthcare workers, these strains can colonize different districts causing a wide range of disorders, with respiratory and urinary tract infections being the most common. In the worst-case scenario, these bacteria can also overcome the immune defenses of the hosts and spread into the bloodstream causing sepsis. The high infectivity of both *K. pneumoniae* and *E. coli* is linked to various virulence factors that allow them to escape the host's innate immune response but the first cause of therapeutic failure release on their high ability to acquire resistant determinants to β-lactams, in particular to carbapenems.

1.1. Carbapenems

Carbapenems are broad-spectrum bactericidal antibiotics belonging to the group of β-lactams that also includes penicillin, cephalosporins, and monobactams *(Aurilio et al., 2022)*. Their development became necessary when most microorganisms lost their susceptibility to the previous antibiotics of the β-lactams group. In particular, already in the 1960s the emergence of genes coding for different enzymes defined as β-lactamases led to the search for molecules capable of overcome their actions. The first one found in 1976 was the olivanic acid, a natural product of the Gram-positive *Streptomyces clavuligeris*, which acts as broad-spectrum β-lactam. Due to its low penetration in bacterial cells, it was overcome by other more stable molecules like thienamycin. This last one, isolated from *Streptomyces cattleya*, was the first carbapenem and acted as backbone for the others lately developed *(Papp-Wallace et al., 2011)*. Carbapenems are active against both Gram-positive and Gram-negative bacteria inhibiting cell-wall synthesis by acylating their target, the penicillin-binding-proteins (PBPs), a family of membrane-associated proteins involved in peptidoglycan biosynthesis. The absence of peptidoglycan cross-linking results in bacterial cell lysis and death. Carbapenems chemical structure is close to that of penicillin showing a β-lactam ring, but the presence of a carbon atom linked to the C1-position instead of a sulphur one, a C-2 sulphur substituent and a trans-configuration of C5-C6 increase carbapenems spectrum and stability to β-lactamases [figure 1A] *(Armstrong et al., 2021).* The first derivative of thienamycin was imipenem, whose administration in complex microbial infections was allowed in 1985. Due to its deactivation by human kidney dehidropeptidase I (DHP-I), other molecules like meropenem, biapenem, ertapenem and doripenem were advanced [figure 1B] *(Papp-Wallace et al., 2011).*

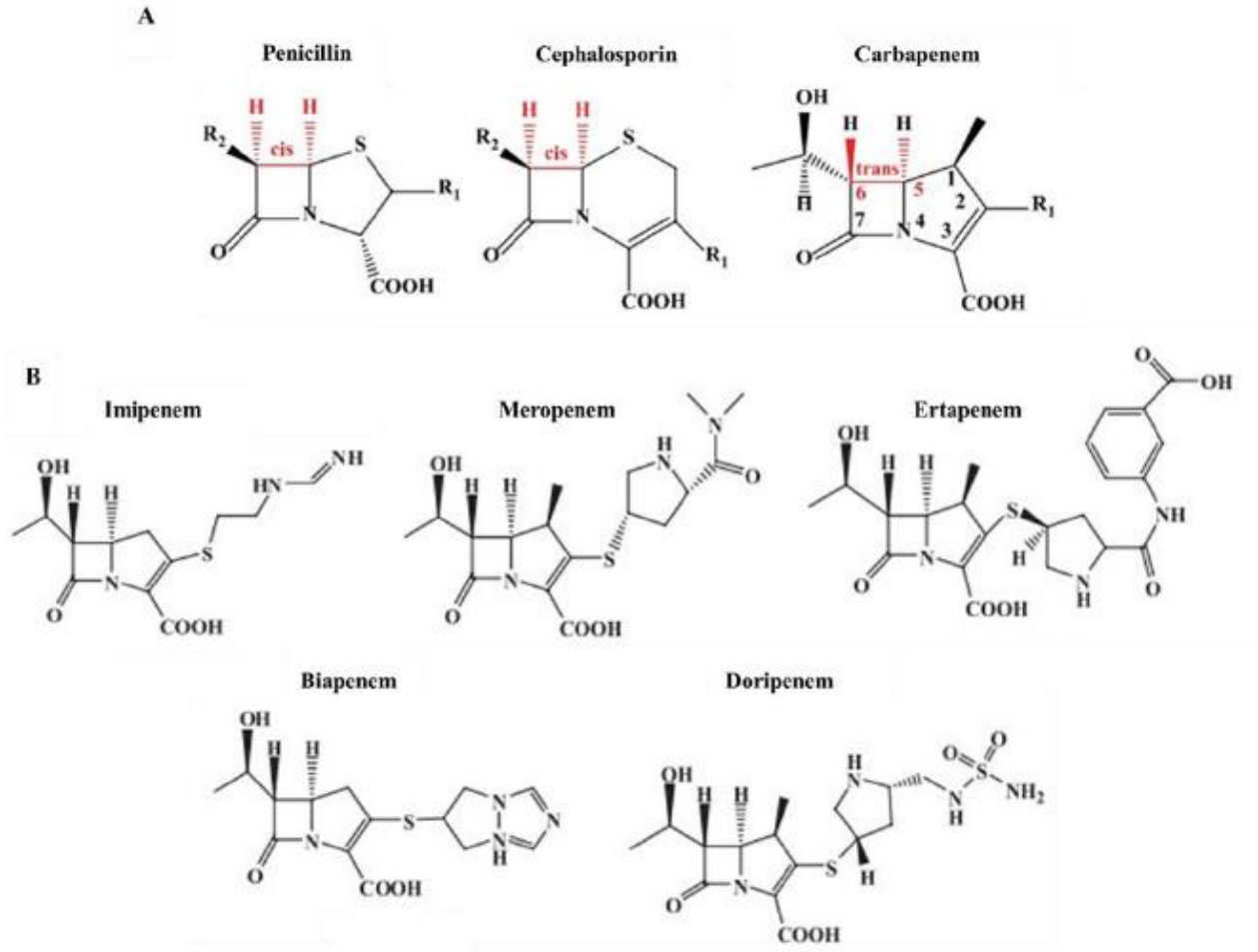

Figure 1. Chemical structures of penicillin, cephalosporin, and carbapenem with a focus on the trans configuration of the C5-C6 bond (A). Chemical structures of clinically available carbapenems (B) (Papp-Wallace et al., 2021).

However, since carbapenems have high rates of renal excretion, avoiding drug accumulation is essential in patients with reduced kidney function *(Armstrong et al., 2021)*. Different carbapenems show a diverse spectrum of activity against pathogens. For example, imipenem is more active against Gram-positive cocci while meropenem is more effective in Gram-negatives and can be used to treat meningitis thanks to its ability to penetrate meninges. Doripenem is useful against *Pseudomonas aeruginosa*, which shows insensibility to ertapenem. Biapenem appears to be better than imipenem on *Enterobacterales* infections. Nevertheless, carbapenems were not applicable to some bacterial species like *Enterococcus faecium*, *Stenotrophomonas maltophilia,* and methicillin-resistant *Staphylococcus aureus* (MRSA). Anyway, carbapenems were considered last-resort treatment in infections sustained by *Enterobacteriaceae* resistant to extended-spectrum cephalosporins and fluoroquinolones but the increase in their usage has led to resistance also to this class of antibiotics.

Furthermore, MDR microorganisms are moving from the nosocomial settings to the community ones thanks to their high ability to maintain their resistant phenotypes also in different habitats *(Duin and Paterson, 2020)*.

1.2. Mechanisms of carbapenem resistance in Enterobacteriaceae

The mechanisms of carbapenems resistance in *Enterobacteriaceae* can be various and include mutations of chromosomally encoded genes or acquisition of resistance genes coding for antibiotic-inactivating enzymes. Indeed, since 2015, CDC has instituted the abbreviation CRE to point carbapenem-resistant *Enterobacteriaceae* while the term CPE includes only the *Enterobacteriaceae* coding for at least one carbapenemase gene. Since carbapenems are diffusible through Gram-negative cell wall, outer membrane proteins play a major role in the entry. Mutations on these porins belonging to the Omp family can avoid drug periplasmic access leading to resistance. In *K. pneumoniae ompK*35 and *ompK*36 are genes coding for two important outer membrane proteins involved in β-lactams entry. In fact, mutations in these genes can lead to antibiotic resistance. In particular, their deletion is involved in carbapenem resistance *(Tsai et al., 2011)*. Another mechanism of carbapenem resistance is efflux pump overexpression which removes antibiotics from the cellular environment *(Meletis, 2016)*. The *K. pneumoniae acrAB* and *oqxAB* multidrug efflux systems are mainly involved in antibiotic- and disinfectant-resistant phenotypes *(Bialek-Davenet et al., 2015)*. Another way to elude carbapenems activity relies on mutations in drug target. Indeed, PBPs mutations are known to avoid carbapenem-targeting *(Aurilio et al., 2022)*. However, the main carbapenem resistance mechanism among *Enterobacteriaceae* is the carbapenemases production: these enzymes are widely diffused due to their localization in mobile genetic elements, such as plasmids, and contribute to the global spread of carbapenem resistance [figure 2].

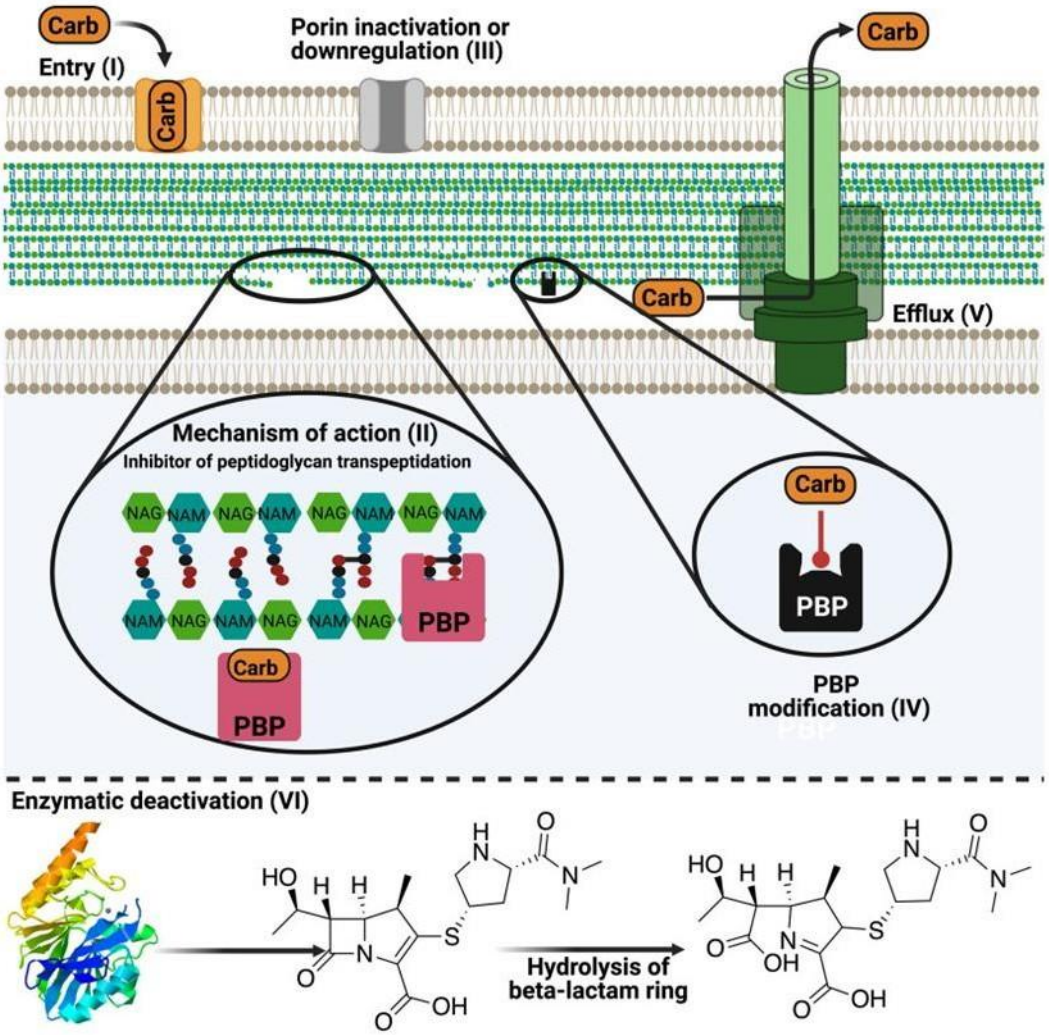

Figure 2. Carbapenems way of entry in bacterial cell (I) and their target (II). Different mechanisms of carbapenem resistance (III-VI) (Armstrong et al., 2021).

1.2.1. Carbapenemases

Carbapenemases are enzymes belonging to the β-lactamases group, an ancient class of enzymes since the first detection goes back to the early 1940s. From that moment on, β-lactamases have constantly challenged the scientific scene by evolving together with the newest antibiotics. Up to now, more than 2,000 different β-lactamases encoding sequences have been identified in both Gram-negative and Gram-positive bacteria *(Hansen, 2021)*. Carbapenemases are β-lactamases extremely versatile, capable of hydrolyse penicillin, cephalosporins, monobactam, and also carbapenems. Moreover, β-lactamase inhibitors available have poor efficiency in blocking their activity *(Queenan and Bush, 2007)*. Initially, carbapenemases were considered species-specific and chromosomally encoded enzymes, but the detection of their genes on plasmids among different organisms revealed their ability to spread and change the global CRE epidemiology *(Diene and Rolain, 2014)*. Different schemes classify β-lactamases according to

their functional or molecular properties. The Ambler classification splits them into 4 groups, named from A to D, depending on their amino acid homology *(Bush, 2018)*. Classes A, C, and D include enzymes with a serine in the active site and were classified as serine-carbapenemases while group B is made up of metallo-β-lactamases (MBLs) with at least one zinc atom in their active site. The various types of carbapenemases belonged to three out of four Ambler's groups: in each Ambler group, there are different family enzymes with multiple allelic variants [table 1]. Moreover, almost all are plasmid-encoded and placed into transposons, allowing them to have a rapid global spread *(Sawa et al., 2020)*. In carbapenem-resistant *K. pneumoniae* (KPCR) and carbapenem-resistant *E. coli* (EcoCR) the carbapenemases mainly detected are *Klebsiella pneumoniae* carbapenemases (KPC), New Delhi metallo-β-lactamases (NDM) and Oxacillinase-48-like carbapenemases (OXA-48) *(Ding et al., 2023).*

Molecular class	Functional group	Enzyme	Hydrolysis profile					Inhibition profile	
			Penicillins	Early cephalosporins	Extended- spectrum cephalosporins	Aztreonam	Carbapenems	EDTA	Clavulanic acid
A	2f	NMC	+	+	+	+	+	-	+
		IMI	+	+	+	+	+	-	+
		SME	+	+	±	+	+	-	+
		KPC	+	+	+	+	+	-	+
		GES	+	+	+	-	±	-	+
B	3	IMP	+	+	+	-	+	+	-
		VIM	+	+	+	-	+	+	-
		GIM	+	+	+	-	+	+	-
		SPM	+	+	+	-	+	+	-
		NDM	+	+	+	-	+	+	-
D	2d	OXA	+	+	±	-	±	-	±

Table 1. Carbapenemases classification and their hydrolysis/inhibition profiles. "+", hydrolysis/inhibition; "-", no hydrolysis/inhibition; "±", variable hydrolysis/inhibition (Queenan and Bush, 2007).

1.2.1.1. Klebsiella pneumoniae carbapenemases

KPC is a group of Ambler class A enzymes, firstly isolated in 1996 on a *K. pneumoniae* clinical strain in North Carolina *(Yigit et al., 2001)*. KPC enzymes show four important conserved motifs (S70-X-X-K73, S130-D131-N132, K234-T/S235-G236, and the Ω-loop) and play their role by acylation and deacylation steps: first the active site S70 forms an acyl-enzyme sticking the carbapenem substrate amid bond and then, E166 and K73 activate a deacylation water molecule to hydrolyse the acyl adduct which is released from the active site [figure 3] *(Jeon et al., 2015).*

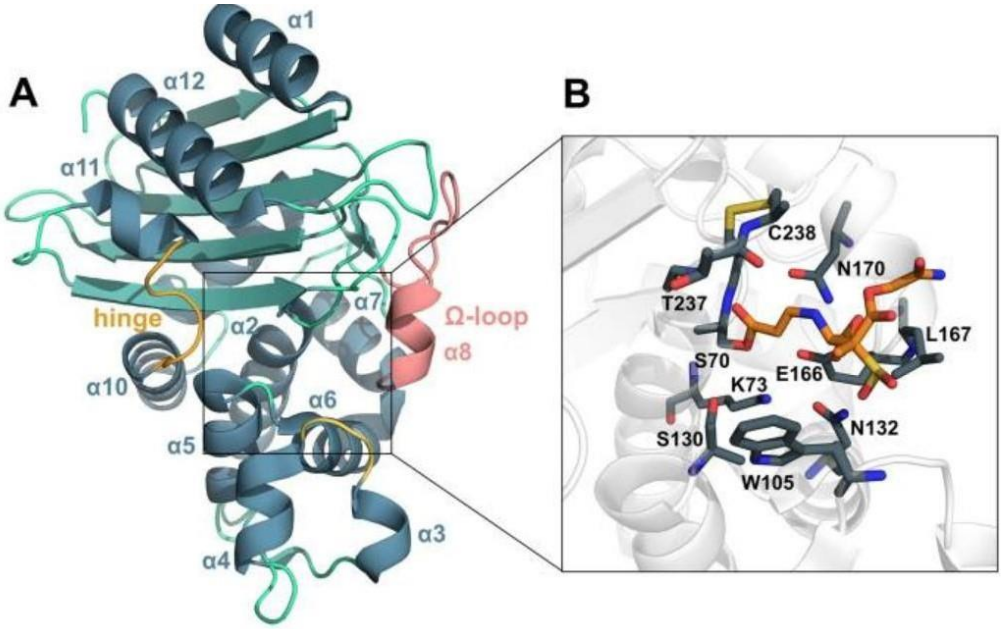

Figure 3. Tertiary structure of KPC-2 carbapenemase (A). Details of the active site: residues involved in ligand binding are in grey while a carbapenem molecule is in orange. The figure shows the covalent link between S70 residue and carbapenem (B). (Galdadas et al, 2018).

From the first detection, KPC-producing *K. pneumoniae* (KPC-Kp) rapidly became endemic in America and then, thanks to its plasmid location, quickly spread and settled in Southern Europe and Asia. Furthermore, *bla*$_{KPC}$ genes are inserted into the Tn*4401*-family transposon, characterized by high levels of transposition also between strains belonging to different species [figure 4] *(Diane and Rolain, 2014)*. In fact, from an initial *K. pneumoniae* exclusivity, today KPC carbapenemase is also found in non-fermenting Gram-negative bacteria like *Pseudomonas aeruginosa* and *Acinetobacter baumannii (Ding et al., 2023).* Since 2019, an increasing number of KPC allelic variants have been recorded, even if the most diffused are *bla*$_{KPC-2}$ and *bla*$_{KPC-3}$ with different prevalences depending on the geographical area: KPC-2 enzymes are widespread in China while both variants are detected in America and Europe. By 2023 in the National Center for Biotechnology Information (NCBI) database 145 *bla*$_{KPC-2}$ and *bla*$_{KPC-3}$ variants were registered *(Ding et al., 2023)*. Some single aminoacidic variants of ancestral genes are responsible for peculiar phenotypes. For instance, *bla*$_{KPC-31}$ is a *bla*$_{KPC-3}$ variant with the D179Y amino acid substitution which confers resistance to ceftazidime-avibactam (CZA) but susceptibility to carbapenems *(Di Pilato et al., 2024)*. The same mutation in *bla*$_{KPC-2}$ brings to *bla*$_{KPC-33}$ allelic variant, with identical antimicrobial behaviour *(Birgy et al., 2024)*. These phenotypes are worrying since CZA, a combination of a third-generation cephalosporin (ceftazidime) with a novel non-β-lactam β-lactamase inhibitor (avibactam) is considered one of the last resort

treatments for KPC-Kp infections and its administration was allowed less than ten years ago. Italy is one of the countries with a major incidence of *bla*$_{KPC}$ allelic variants, together with United States *(Ding et al., 2023)*. Moreover, KPC-Kp is endemic in our country due to the rise and spread of high-risk clones belonging to clonal group CG258 *(Brolund et al., 2019)*. This group consisting of two single locus variant sequence types (ST512 and ST258) was almost the only represented until 2013 *(Conte et al., 2016)* but in the following years, the spread of other clones was observed. In fact, from the surveillance study conducted by Di Pilato and colleagues in 2016 emerged that, even if CG258 was still predominant, other three sequence types came up: ST307, ST101, and ST395. The first two are worldwide spread clones, able to adapt to hospital settings while the last one shows a limited diffusion so far *(Di Pilato et al., 2021)*.

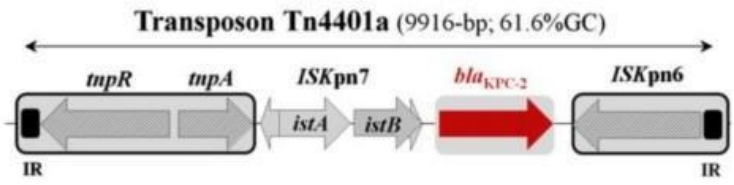

Figure 4. Transposon Tn4401a: mobile genetic element from K. pneumoniae harbouring the bla$_{KPC-2}$ gene. IR, inverted repeat; tnpR, resolvase; tnpA, transposase; IS, insertion sequence; istA, transposase A; istB, transposase B. (Diene and Rolain, 2014).

1.2.1.2. New Delhi metallo-β-lactamases

New Delhi metallo-β-lactamase (NDM) is the latest carbapenemase isolated from a *K. pneumoniae* clinical strain of a Swedish patient who travelled to India in 2009 *(Young et al., 2009).* Belonging to the Ambler class B, this enzyme can hydrolyse penicillin, cephalosporins and carbapenems but not monobactams. Furthermore, both novel and canonical β-lactamase inhibitors like avibactam, clavulanate, sulbactam, and tazobactam are ineffective against MBLs. Only older drugs like colistin or fosfomycin or combination of aztreonam with CZA are potential therapeutic options for MBLs producers *(Di Pilato et al., 2024)*. The MBLs mechanism of substrate hydrolysis is poorly understood and not completely shared by all enzyme families as they differ in their active site structure. NDM carbapenemases have two zinc atoms in their active site: one (Zn1) is linked to three histidine residues (H120, H122, H189) and the other (Zn2) to an aspartate (D124), a cysteine (C208) and a histidine (H250). A water molecule between the two zinc ions is responsible for a nucleophilic attack of the carbapenem carbonyl carbon with amid bond cleavage as a consequence. After β-lactam ring opening, Zn1 is linked to the newly formed carboxylate while Zn2 is associated with the amide nitrogen and the carboxylate of the β-lactam ring. The anionic intermediate thus created is subsequently protonated and the

reaction product is released from the enzyme site [figure 5] *(Feng et al., 2017).*

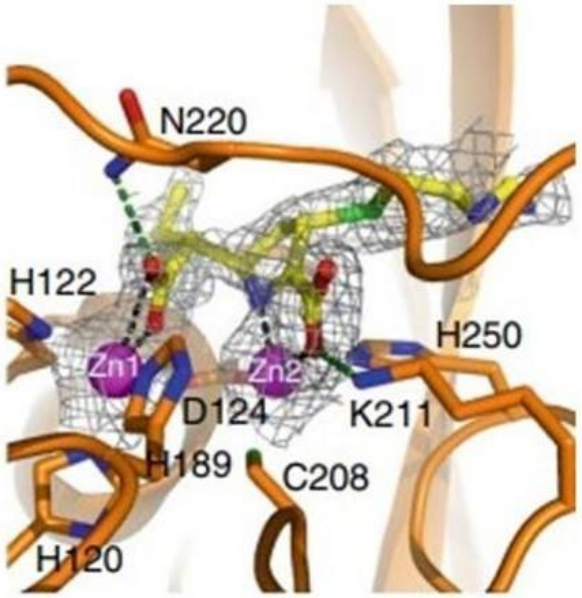

Figure 5. NDM-1 active site with zinc atoms bound by hydrolysed imipenem, coloured in yellow. Metal coordination bonds are black coloured while hydrogen bonds with N220 and K211 are denoted by green dashed lines. (Feng et al., 2017).

bla$_{NDM}$ is a gene frequently associated with mobile elements and can be found in plasmids belonging to different Inc types (e.g. IncFII, IncX), flanked by insertion sequences (e.g. IS*Aba125*, IS*CR1*) or hosted into transposons (e.g. Tn*125*) [figure 6] *(Dong et al., 2022)*. For that reason, *bla*$_{NDM}$ rapidly globally spread not only among the *Enterobacteriaceae* family but also in other non-fermenting species like *Pseudomonas* spp. and *Acinetobacter* spp. Today we can find 24 allelic variants of this gene in more than 60 species belonging to 11 different bacterial families, even if the prevalent carriers are *K. pneumoniae* (NDM-Kp) and *E. coli* (NDM-Eco) *(Wu et al., 2019)*. Although amino acid substitutions do not affect the enzyme active site, few of them can match with peculiar phenotypes. For instance, the V88L mutation highlighted in *bla*$_{NDM-5}$ involves increased carbapenemase activity and higher ertapenem MIC (Minimum Inhibitory Concentration) values compared with the ancestral *bla*$_{NDM-1}$ *(Hornsey et al., 2011)*.

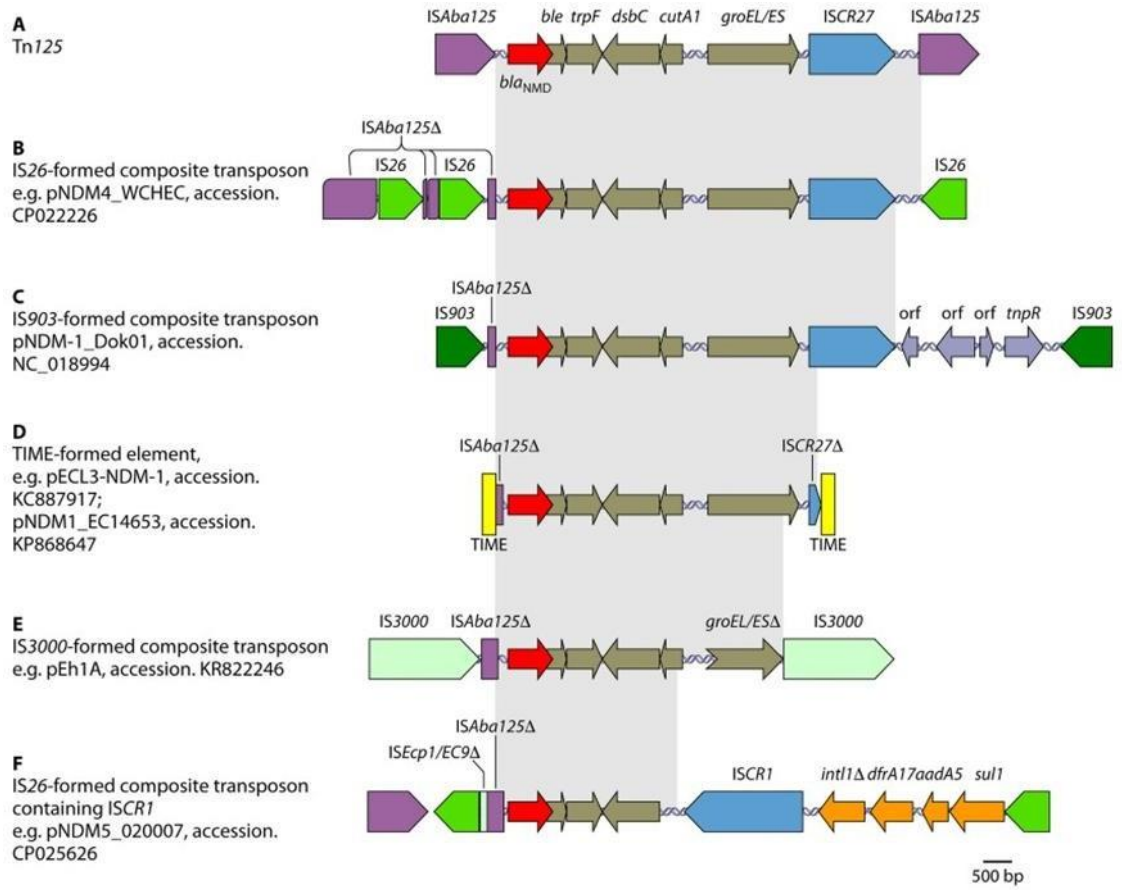

Figure 6. Examples of genetic contexts of bla_{NDM}. IS, insertion sequence; ble, bleomycin; trpF, phosphoribosylanthranilate isomerase; dsbC, dusulfide-isomerases; tnpR, transposon Rn3 resolvase; orf, open reading frame; Δ represents truncated genes or elements. (Wu et al., 2019)

Unlike KPC-Kp described previously, bla_{NDM} spread is not linked to a single prevalent clone but is frequently harboured in certain epidemic strains such as *K. pneumoniae* ST11 and ST147 and *E. coli* ST131 and ST101 *(Hansen et al., 2021)* mainly in Asia, Middle East, North Africa, and certain European regions *(Di Pilato et al., 2024)*. In recent years, NDM-Kp incidence has increased in European hospital settings. For instance, between 2014 and 2016 the Spanish Antibiotic Resistance Surveillance Program registered almost 2% rise in both clinical NDM-Kp and NDM-Eco. The main circulating *K. pneumoniae* clones were ST147, ST101, and ST437 while *E. coli* showed a polyclonal population *(Perez-Vazquez et al., 2019)*. Regarding our country, bla_{NDM-1}-producing *K. pneumoniae* has been responsible for large hospital outbreaks in Northern Italy, Tuscany, since 2018 *(Tavoschi et al., 2020)*. In 2020, another NDM-Kp outbreak was reported in the same hospitals. Even if strains belonged to the identical previous sequence type (ST147), they harboured the different bla_{NDM-9} allelic variant and showed resistance to colistin, fosfomycin, and tigecycline unlike the 2018 clone *(Falcone et al., 2020)*. In Southern Italy, the first outbreak sustained by NDM-1-producing *K. pneumoniae* belonging to ST147 was

recorded between 2020 and 2022 in the Apulia region *(Loconsole et al., 2024)* underlying the high spread of this virulent clone.

1.2.1.3. Oxacillinase-48-like carbapenemases

The Ambler class D includes the oxacillinase enzyme group, featured by a variable hydrolytic profile. OXA-48-like enzymes shows carbapenemases activity independently from porin mutations or the presence of other β-lactamases. The first OXA-48-producing *K. pneumoniae* (OXA-48-Kp) was isolated in Turkey in 2001 and in the following years OXA-48-Kp became endemic in that region *(Tumbarello et al., 2015)* while inter-regional spread characterized Spain, France, Belgium and Romania *(Duin and Doi, 2017)*. Several variants of this gene, differing from one to five mutations, constitute the OXA-48-like subfamily. For instance, OXA-232 has a unique aminoacidic substitution (R214S) while OXA-181 shows four (T104A, N110D, E168Q, and S171A) and OXA-163 presents four deletions (R214, I215, E216, and P217) and one substitution (S220D) *(Boyd et al., 2022)*. Anyway, diversity in the aminoacidic sequence is linked to heterogeneous hydrolysis: for example, OXA-48 carbapenemase has a weaker hydrolytic activity than OXA-181 while OXA-163 doesn't show any carbapenemase hydrolysis activity at all *(Di Pilato et al., 2024)*. OXA-48 is composed of two identical subunits including the active site which shows three conserved motifs and a carbamylated lysine side chain (K34). A unique β-5-β-6 loop conformation is responsible for a tighter active site and for a change in charge distribution which creates a hydrophilic cavity that hosts water molecules. These water molecules are close to the substrate binding site and act as nucleophilic agents reaching the acyl-enzyme bond and resulting in the deacylation step [figure 7] *(Docquier et al., 2009)*. The loss of OXA-163 carbapenemase activity is due to the lack of R214. This residue, indeed, is located in the β-5-β-6 loop of the OXA-48-like enzymes and its deletion brings a change in OXA-163 active site which does not allow carbapenems interactions *(Poirel et al., 2012)*.

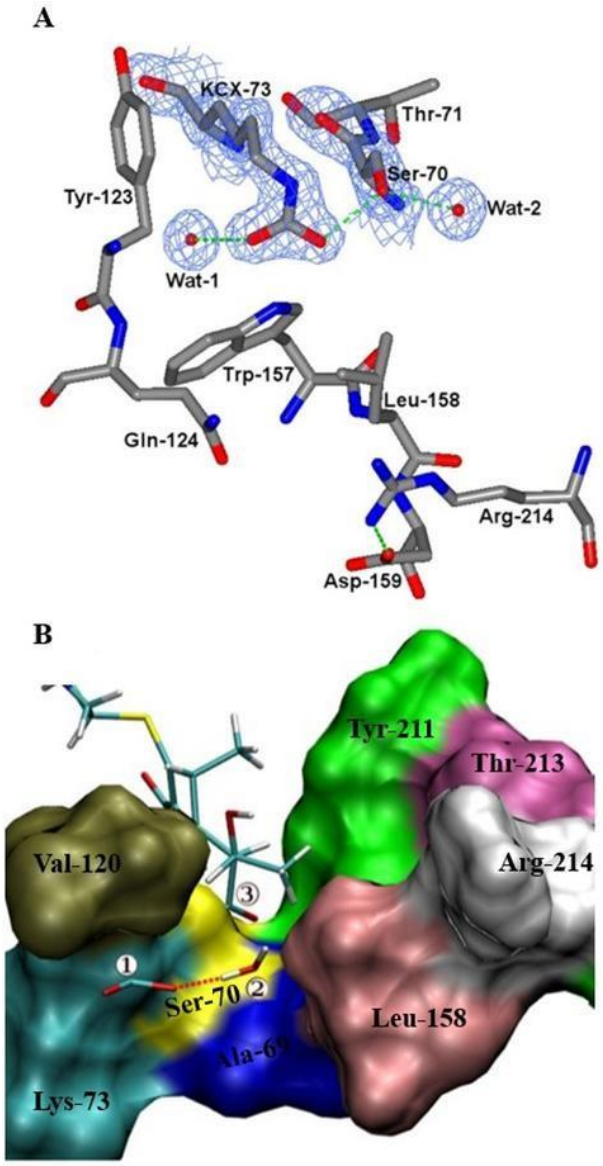

Figure 7. (A) OXA-48 active site residues of relevance. The carbamylated side chain of Lys-73 is shown together with nearby residues and water molecules (red spheres). (B) OXA-48 mechanism of action. Relevant residues of the active site are displayed in different colours and the carbamyl group of Lys-73 is displayed as sticks (label 1). The water molecule involved in the deacylation step is shown in stick representation (label 2) near Lys-73. The meropenem acyl group bound to Ser-70 is pointed out by label 3. In the figure, meropenem adopts a conformation in which the methyl group of the hydroxyethyl substituent is located within the niche formed by the side chains of residues Leu-158 and Thr-213, and the hydroxyl group has moved closer to residue Val-120. In this conformation, water molecule 2 is hydrogen bonded to Lys-73 and is properly oriented to perform the nucleophilic attack on the carbonyl carbon (Docquier et al., 2009).

Even if the progenitor of *bla*$_{\text{OXA-48}}$ is the chromosomally encoded *bla*$_{\text{OXA-54}}$ gene harboured in *Shewanella oneidensis* and the aminoacidic identity between the two genes is about 92% *(Poirel et al. 2004)*, OXA-48-like genes are mainly plasmid located among the *Enterobacteriaceae* family. In particular, these genes are placed into the composite transposon Tn*1999* whose upstream and downstream IS*1999* insertion sequences are probably responsible for OXA-48-like genes mobilization from *S. oneidensis* chromosome to conjugative plasmids. Different plasmids host diverse *bla*$_{\text{OXA-48-like}}$ allelic variants which also have specific geographical distribution. For instance, *bla*$_{\text{OXA-48}}$ is known to be frequently associated with different Tn*1999* transposons on IncL scaffolded plasmids of 60-70 kilobases (kb) and is endemic in North Africa and the Middle East *(Pitout et al., 2019)*. Tn*1999* shows several variants, named from Tn*1999.2* to Tn*1999.5*. Tn*1999.2* is the main cause for dissemination of *bla*$_{\text{OXA-48}}$ through Libya, Turkey,

and the Netherlands [figure 8] *(Hidalgo et al., 2019)*. $bla_{OXA-181}$ is predominantly associated with IncX3 plasmids and it is endemic in the Indian subcontinent and certain sub-Saharan African countries. This mobile element is almost identical also in clones belonging to different sequence types. In fact, the same IncX3 plasmid implicated in a large outbreak sustained by OXA-181-producing *K. pneumoniae* ST307 in South Africa was detected in China and Angola *(Strydom et al., 2020)*. OXA-48-like carbapenemases have been identified in several high-risk international clones. Among these, *K. pneumoniae* ST147 and ST307 and *E. coli* ST38 and ST410 were associated with the global dissemination of OXA-48, OXA-181, OXA-232, and OXA-204 *(Pitout et al., 2019)*.

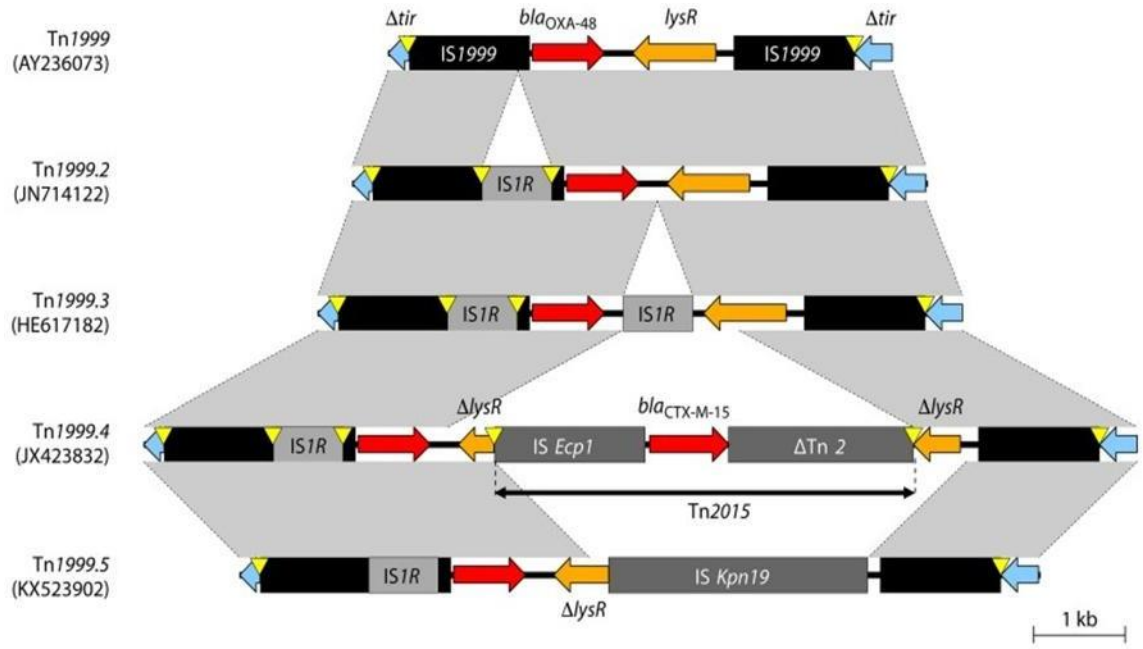

Figure 8. Genetic contest of Tn1999 and its variants within OXA-48-like plasmids. Mobile elements are indicated in black (e.g., IS1999) or grey (others). Genes from background plasmids are depicted with cyan. Yellow triangles indicate target site duplications (Pitout et al., 2019).

1.3. CRE distribution

Resistance to carbapenems has been increasingly reported with different geographic distributions since the beginning of the 1990s *(Gupta et al., 2011)*. More than 90% of CRE strains are represented by KPCR and EcoCR. Before 2001 about 99.9% of *Enterobacteriaceae* clinical strains were susceptible to carbapenems *(Ma et al., 2023)* but then this condition hardly changed. With the increasing awareness of the global CRE impact, different surveillance programs were developed worldwide. For instance, the EARS-Net (European Antimicrobial Resistance Surveillance) is a network that collects clinical data on carbapenem-resistant

invasive high-risk strains across different laboratories in Europe. Between 2005 and 2010 an increasing trend in KPCR was reported in European countries, especially in Greece and Italy which registered an incidence of 49.8% and 12.5% respectively in the last year of the surveillance *(Magiorakos et al., 2013)*. This growing trend goes on also in the following years, as described in the 2016 EARS-Net report, with Greece, Italy and Bulgaria having the highest rate of invasive carbapenem-resistant *K. pneumoniae*. A different situation was shown for *E. coli*, with national percentages ranging between 0% and 0.1% *(ECDC, 2018)*. In 2018, 16 out of 37 participant states (43%) showed regional or inter-regional CRE spread while 4 countries, including Italy, exhibited an endemic situation *(ECDC, 2019)*. The EARS-Net Annual Epidemiological report for 2022 confirmed this trend, with a 49.7% increase in KPCR European incidence compared with 2019 [figure 9] *(ECDC, 2023)*.

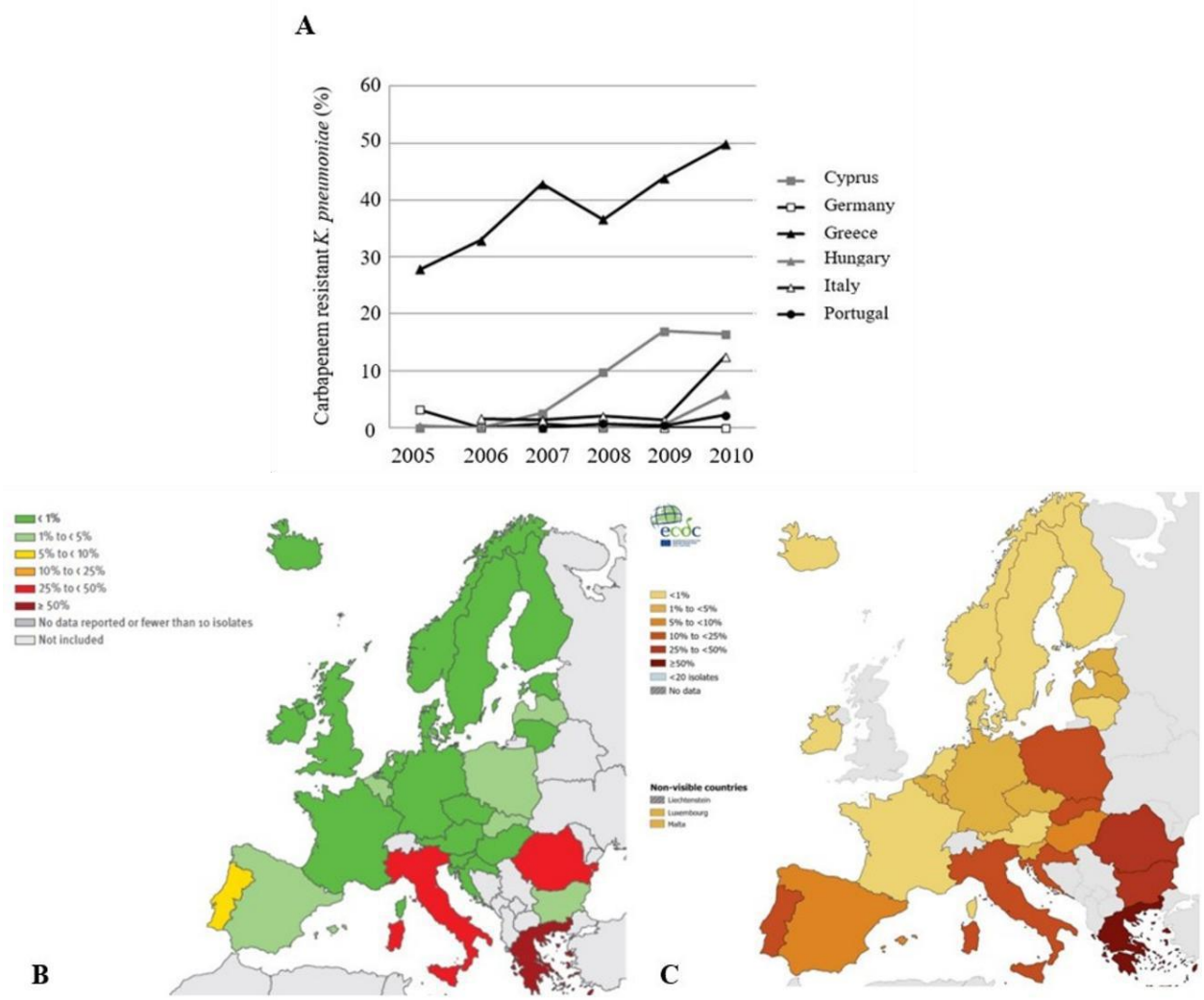

Figure 9. Carbapenem resistant K. pneumoniae incidence from 2005 to 2010 in some European regions (A). Comparison of European KPCR epidemiology in 2016 (B) and 2022 (C). https://www.ecdc.europa.eu/en/about-us/networks/disease-networks-and-laboratory-networks/ears

A global view of the CRE situation is presented by ATLAS (Antimicrobial Testing Leadership and Surveillance), a program that annually monitors the in vitro activity of antibiotics against problematic clinical strains responsible for bloodstream, intraabdominal, respiratory or urinary tract infections, skin/soft tissue infections. The examined regions were divided into 5 groups: APAC (Asia Pacific), EUR (Europe), LATAM (Latin America), MEA (Middle East Africa) and NA (North America). The last ATLAS report is a five-years CRE record, from 2018 to 2022. A growing trend in CRE incidence was detected in almost all the areas. More in detail, the incidence rate increased by 8.2% in LATAM regions and by 4.7% in MEA area. APAC area was characterized by a 2020 peak of 11% while in Europe, after a 2.6% rise until 2021 (growing from 3.9% in 2018 to 6.5% in 2021), in 2022 a 2% drop was detected. Only North America registered a decreasing trend during the study period, moving from 2.6% to 1.1% *(Wise et al., 2024)*. In addition, geographical distribution differs also on the type of carbapenemase produced.

1.4. Therapeutic options

CRE are associated with a high mortality rate because of the limited therapeutic options available. Indeed, carbapenems were considered as last resort treatment in infections sustained by ESBLs-producing Gram-negative bacteria. Therapeutic option choice depends on pathogen antimicrobial susceptibility profile, site of infection, their pharmacokinetics/pharmacodynamics features and possible side effects. Moreover, most drugs available are active against specific carbapenemases resulting ineffective against bacteria exhibiting enzymes of different Ambler classes *(Petrosillo et al., 2019)*. In addition, these microorganisms often show an MDR phenotype making them even more difficult to eradicate. Initially, old drugs no longer in use like colistin were retrieved. At the beginning of the 80s', indeed, its administration was no longer allowed due to its renal toxicity *(Biswas et al., 2012)*. Colistin is a cationic bactericidal polymyxin that binds the lipopolysaccharide (LPS) of the Gram-negative cell wall changing the external membrane permeability with consequent bacterial death [figure 10]. Until 2015, colistin resistance levels were low and mostly caused by rare chromosomal mutations, even if from 2013 insertions sequences in *mgrB* gene were linked to colistin resistant *K. pneumoniae* clinical strains *(Cannatelli et al., 2014)*. More in detail, the insertional inactivation or deletion of the *mgrB* regulator resulted in upregulation of the PhoQ/PhoP signaling system and activation of the *pmrHFIJKLM* operon, leading to colistin resistance by modification of the lipopolysaccharide target *(Cannatelli et al., 2013).* Anyway, in the following years the colistin

resistance rates increased also due to a colistin resistance gene (*mcr-1*). This plasmid-encoded gene was initially detected in China, from strains collected from pigs but then rapidly spread among different species (like *E. coli* and *K. pneumoniae*) and geographical areas *(Havenga et al., 2019)*. Moreover, the worldwide increasing number of CRE infections has led to significant growth in colistin administration which subjected bacteria to a selective pressure. Consequently, bacteria become able to modify their LPS structure and charge inhibiting the LPS-colistin electrostatic interaction *(Petrosillo et al., 2019).*

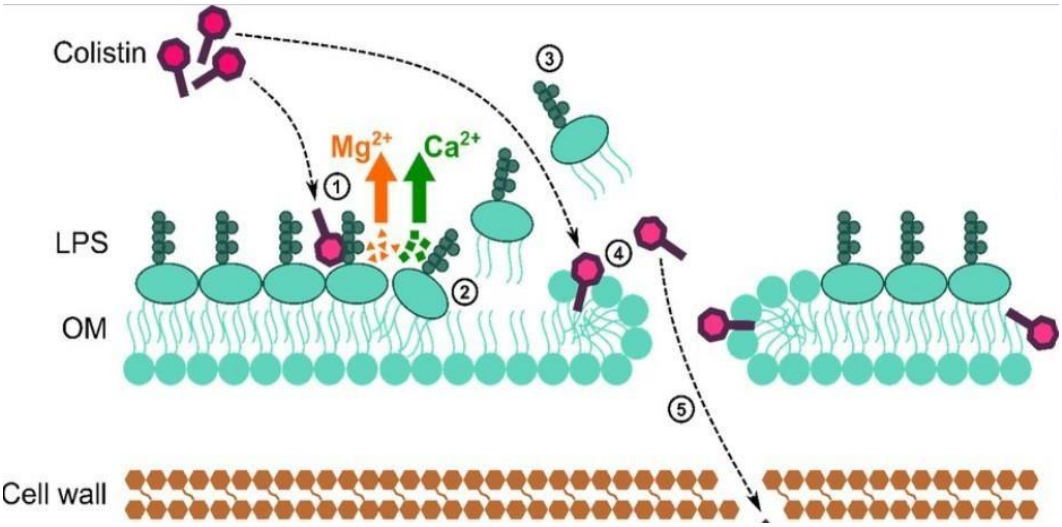

Figure 10. Schematic colistin mechanism of action. OM, outher membrain; LPS, lipopolysaccharide. (Sabnis et al., 2021)

The colistin-resistant *Enterobacteriaceae* incidence rise together with β-lactamases and carbapenemases high spread, promoted new molecules development. One strategy was to combine antimicrobial agents with β-lactamase inhibitors. The novel non-β-lactam β- lactamase inhibitor avibactam works against Ambler class A (e.g. TEM-1, KPC-2, KPC-3), C (e.g. AmpC) and some D (e.g. OXA-10, OXA-48) enzymes, that are not bound by the former β-lactamase inhibitors *(Shirley, 2018)*. Avibactam, unlike clavulanic acid, sulbactam, and tazobactam, is not characterized by a β-lactam core but contains a diazabicyclooctain ring [figure 11A-B]. This molecule acts in a slowly reversible manner: it covalently acylates its target (β-lactamase) but the subsequent deacylation occurs without hydrolysis. In this way, the released avibactam is intact and can block other enzymes [figure 11E] *(Ehmann et al., 2012)*. The coadministration of avibactam with the third-generation cephalosporin ceftazidime in the fixed ratio of 1:4 (commercialized with the name of *Zavicefta*) was allowed by FDA in 2015 for nosocomial pneumonia, urinary tract, and intra-abdominal severe infections and other difficult to treat infections sustained by aerobic Gram-negative bacteria in adults (*European Medicines Agency. Zavicefta: summary of product characteristics. 2018. http://www.ema.europa.eu. Accessed 16*

Mar 2018). Even if *Zavicefta* is really effective against *Pseudomonas aeruginosa* and enterobacteria coding for ESBLs, resistant mutants of KPC-2- or KPC-3-producing *K. pneumoniae* and *Enterobacter cloacae* strains were detected in patients after exposure to ceftazidime-avibactam (CZA). These KPC variants showed one or more amino acid changes in the Ω-loop of the β-lactamase that restore susceptibility to meropenem *(Matesanz and Mensa, 2021)*. Anyway, CZA is not effective against MBLs as they lack the serine residue in their active site: for the treatment of MBL-producing CRE a combination of CZA with the monobactam aztreonam is suggested *(Davido et al., 2017)*. Other therapeutic strategies include the combination of carbapenems with novel β-lactamase inhibitors. Relebactam and vaborbactam are other two non-β-lactam inhibitors that are administrated together with imipenem and meropenem respectively, in severe CRE infections. These inhibitors are active against Ambler class A and C carbapenemases. While relebactam is structurally related to avibactam with the only exception of an additional piperidine ring at the carbonyl group in position 2, vaborbactam shows a peculiar boronic ester ring which increases its potency, as boronic acid is known to be strong serine protease inhibitor [figure 11C-D] *(Zhanel et al., 2017)*.

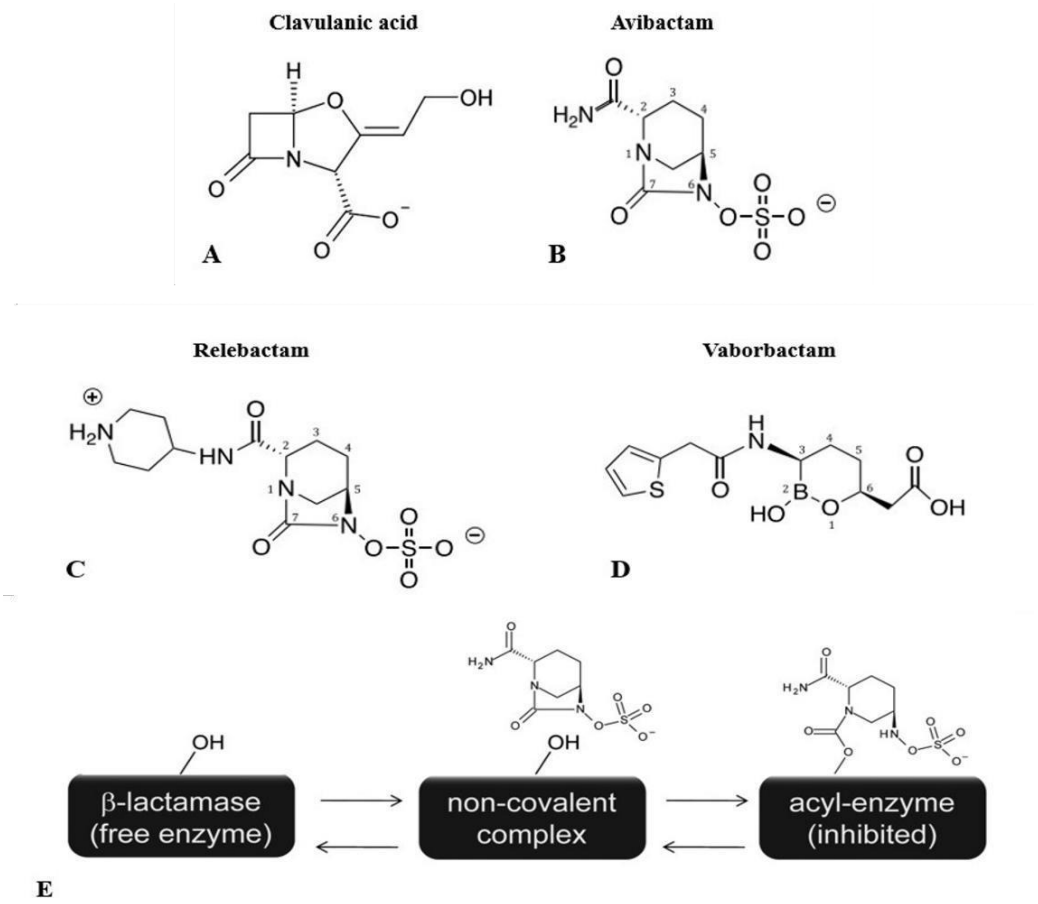

Figure 11. Chemical structures of clavulanic acid (A), avibactam (B), relebactam (C), vaborbactam (D). Schematic illustration of avibactam mechanism of carbapenemase inhibition.

A new perspective was introduced by cefiderocol, a novel siderophore cephalosporin approved by FDA in 2019 for complicated urinary tract infections and in 2020 for hospital acquired pneumoniae sustained by Gram-negative MDR strains *(Yao et al., 2021)*. Cefiderocol (commercial name *Fetroja*) uses a unique mechanism named "trojan horse" strategy to enter bacterial cells. Binding free iron ions in the extracellular space, this molecule undertakes the bacterial iron transport system to cross the bacterial cell wall. Once inside the bacterial cell wall, cefiderocol binds PBPs inhibiting cell wall synthesis [figure 12A] *(Dobias et al., 2017)*. Cefiderocol has a backbone similar to cefepime and ceftazidime but the addition of a chlorocatechol group on the side chain enhances its β-lactamases stability and allows the interactions with bacterial siderophores [figure 12B]. In fact, showing high stability to carbapenemase hydrolysis, cefiderocol is active against *Enterobacteriaceae* producing both serine- and metallo-carbapenemases *(Karakonstantis et al., 2022)*. However, cases of resistance emerging during treatment have already been reported. Even if the cefiderocol resistance mechanism is not yet completely understood, mutations on siderophore receptors (e.g. *piuA*, and *piuD*) or porins (e.g. OmpK35, and Ompk36), and a high copy number of carbapenemase encoding genes are known to increase cefiderocol MIC values *(Simner et al., 2022)*.

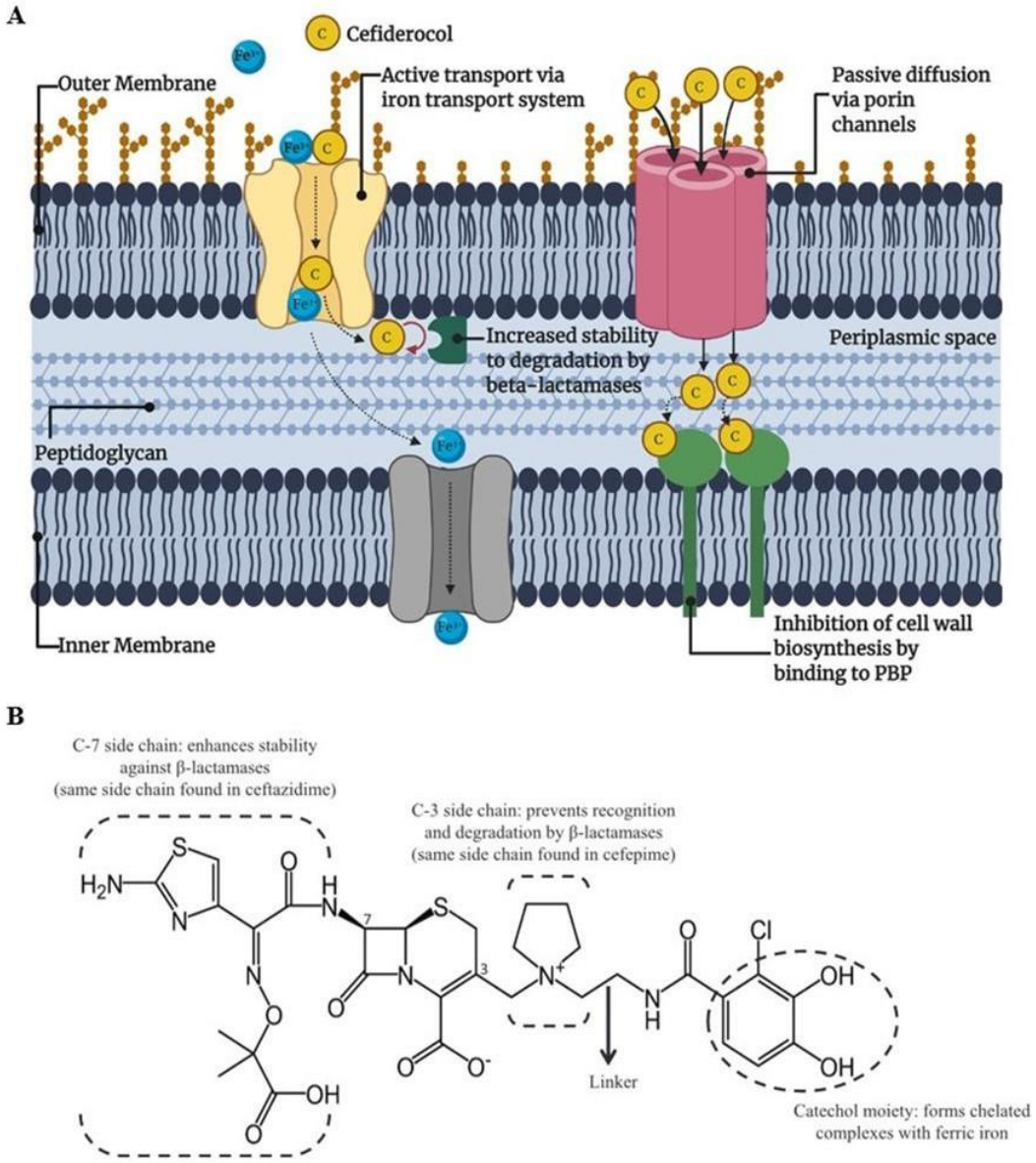

Figure 12. Cefiderocol mechanism of entry in bacterial cells (A). Chemical structure of cefiderocol (B). (Lababidi 2021).

2. MATERIAL AND METHODS

2.1. Clinical strains

A total of 230 carbapenemase-producing clinical *K. penumoniae* were included in this three-year study. Species identification of all bacterial strains was performed by MALDI-TOF mass spectrometry. Samples were collected by three different hospitals: "Azienda Ospedaliera Universitaria Ospedali Riuniti" of Ancona, Marche, "Azienda Ospedaliera" of Perugia, Umbria, and "Azienda Ospedaliera Ospedali Riuniti Marche Nord" of Pesaro and Fano, Marche. All KPC-producing *K. pneumoniae* (Kp-KPC) responsible for BSIs (blood stream infections) collected during the period 2014-2019 from all hospitals mentioned were considered, while all the other

strains coding for different carbapenemases belonged to Ancona hospitalized patients from 2021 to 2023 from different sources with urine culture, and rectal swabs as major types of clinical examinations.

2.2. PCR assays

bla genes presence was initially detected with GeneXpert (Cepheid) and then confirmed with PCR assays with specific primers [table 2]. PCR amplicons were visualized on 1% agarose Tris Acetate EDTA (TAE) based gel, using GeneRuler 100 bp plus DNA ladder (ThermoFisher Scientific) as marker. Gel was coloured with 1xGreen gel (Fisher Molecular Biology), and the applied voltage was 90 V.

Primer	Sequence 5'-3'	Gene	Tm	Product size	Reference
KPC-F	ATGTCACTGTATCGCCGTCT	*bla*KPC	59 °C	893 bp	*Galani et al., 2018*
KPC-R	TTTTCAGAGCCTTACTGCCC				
NDM-F	GGTTTGGCGATCTGGTTTTC	*bla*NDM	59 °C	621 bp	*Poirel et al., 2011*
NDM-R	CGGAATGGCTCATCACGATC				
OXA48-F	TTGGTGGCATCGATTATCGG	*bla*OXA-48	59 °C	743 bp	*Galani et al., 2018*
OXA48-R	GAGCACTTCTTTTGTGATGGC				

Table 2. Primer used for PCR assays to identify bla genes presence. Tm, melting temperature.

2.3. Antibiotics

Antibiotics used for susceptibility tests were provided as powder by Sigma (Sigma-Aldrich). Amikacin (AMK), aztreonam (ATM), avibactam (AVI), cefiderocol (FDC), ceftazidime (CAZ), ciprofloxacin (CIP), colistin (COL), ertapenem (ETP), fosfomycin (FOS), gentamycin (CN), imipenem (IMI), meropenem (MER), tigecycline (TIG), trimethoprim (TMP), and sulfamethoxazole (SMX) were resuspended in adequate solvents to a final concentration of 10 g/L and stocked at -20 °C.

2.3.1. Susceptibility tests

MIC values for fosfomycin were obtained with the agar dilution method in presence of glucose- 6-phosphate at the fixed concentration of 25 mg/L in the medium. MIC values for all the other antibiotics were performed by broth microdilution method. For susceptibility test to ceftazidime-avibactam (CZA), AVI concentration was fixed at 4 mg/L while TMP and SMX were in the ratio 1:19 to test their combination. Regarding FDC, MIC determination was conducted in iron-depleted Muller-Hinton (MH) medium while MH broth was freshly prepared for TIG MIC determination. All these methods followed the EUCAST guidelines

(https://www.eucast.org/ast_of_bacteria) and MIC values were interpreted according to EUCAST *v 13.1* breakpoints (Table 3). *P. aeruginosa* ATCC 27853 (for FDC and MER) and *E. coli* ATCC 25922 strains were used as quality controls.

Antibiotics	***Enterobacteriaceae* breakpoints (mg/L)**	
	Susceptible	**Resistant**
AMK	≤ 8	> 8
ATM	≤ 1	> 4
CIP	≤ 0.25	> 0.5
COL	≤ 2	> 2
CN	≤ 2	> 2
CZA	≤ 8	> 8
ETP	≤ 0.5	> 0.5
FDC	≤ 2	> 2
FOS	≤ 32	> 32
IMI	≤ 2	> 4
MER	≤ 2	> 8
TIG	≤ 0.5	> 0.5
TMP-SMX*	≤ 2	> 4

*Table 3. EUCAST MIC breakpoints for Enterobacteriaceae. *, breakpoints for TMP-SMX are expressed as the TMP concentration.*

2.4. Genomic DNA extraction

Total DNA extraction was performed by *GenElute Bacterial Genomic DNA* kit (Sigma). Bacterial strains were seeded in MacConkey agar (MC) plates and incubated overnight at 37 °C. The day after, bacterial strains were resuspended in 5 ml of saline solution, and 1.5 ml of these suspensions were centrifuged at 12,000 g x 3 minutes. Cell pellets were resuspended in 180 µl of *Lysis Solution T* and incubated for 2 minutes at room temperature after addition of 20 µl of *RNase A Solution*. 20 µl of *Proteinase K* (20 mg/ml, Sigma) were added to the cells which were incubated at 56 °C for 30 minutes and then lysed with 200 µl of *Lysis Solution C* at 56 °C for other 10 minutes. DNA molecules were precipitated with 200 µl of 95% ethanol and then the lysates were loaded in properly prepared columns and centrifugated at 6,500 g for 1 minute. After discarding the eluates, two consecutive washes were performed with 500 µl of *Wash Solution*. The first wash required a 6,500 g x 1 minute centrifuge while the second one a 12,000 g x 3 minutes centrifuge. Columns were transferred in sterile collection tubes and 200 µl of *Elution Solution* followed by a 6,500 g x 1 minute centrifuge has allowed to obtain pure DNA molecules that flow through. Elution step was repeated a second time to increase DNA yield. The obtained genomic DNA was stored at -20 °C.

2.4.1. Genomic DNA quantity evaluation

Qubit 4 fluorometer (Invitrogen) allowed us to check the quantity of the genomic DNA previously extracted. Using the *1X dsDNA High Sensitivity Assay* kit (Invitrogen) double-strand DNA was quantified after performing a calibration with 10 µl of two standardized DNA (the first one concentrated 0 ng/µl and the second one 10 ng/µl) mixed with 190 µl of the *Working Solution*. For DNA quantification 198 µl of the *Working Solution* was mixed with 2 µl of each DNA extracted and incubated 2 minutes at room temperature. DNA concentrations were expressed in ng/µl.

2.4.2. Genomic DNA quality evaluation

Electrophoresis assays were performed to check the quality of extracted DNA. 5 µl of each sample was mixed with DNA Loading Dye (ThermoFisher Scientific) and loaded into a 1% agarose gel. Gel was coloured with 1xGreen gel (Fisher Molecular Biology), and the applied voltage was 90 V. Not smirred DNA prints were considered as good quality DNA, required for next WGS assays.

2.5. Typing assays

Pulsed Field Gel Electrophoresis (PFGE) and *Multi Locus Sequence Typing* (MLST) assays were performed on all samples studied.

2.5.1. PFGE

Bacterial strains were seeded on MC agar plates and after an overnight incubation at 37 °C they were resuspended in 2 ml of *Suspension Buffer* (TRIS-HCl 0.1 M + pH 8.0 EDTA 0.1 M) and diluted to an optical density (OD) between 0.5 and 0.8. The OD was measured at 610 nm. 350 µl of bacterial suspensions properly diluted were combined at 1:1 ratio with melted *Low Melt Agarose* (1.6% Agar and 1% SDS). 100 µl of these preparations were aliquoted on plug-molds and allowed to solidify. Five plugs were prepared for each sample and lysed with 5 ml of *Lysis Buffer* (Tris 50 mM + pH 8.0 EDTA 50 mM + 1% sarcosine) supplemented with 25 µl of *Proteinase K* (20 mg/ml). After an overnight incubation at 56 °C, plugs were subjected to 5 consecutive washes, each followed by a 15 minutes gentle shaking. Two washes were performed with 5 ml of warm water while the remaining three washes were executed with 5 ml of *TE Buffer* (TRIS-HCl 10mM + EDTA 1mM).

2.5.1.1. XbaI digestion

To investigate the restriction profile of bacterial strains, half plug was digested overnight at 37 °C with 30 U of XbaI (ThermoFisher Scientific). DNA digestion was stopped with 500 µl of EDTA 0.5 M and each plug was included in a 1% Pulsed Field Certified Agarose (Bio-Rad) Tris Borate EDTA (TBE) based gel. PFGE assays were performed using Chef Mapper XA System (Bio-Rad) with the following parameters:

- Run time: 20 hours
- Range: 6 V/cm
- Angle: 120 °
- Starting time switch: 2.2 seconds
- Final time switch: 54.2 seconds
- Ramping factor: linear

Once PFGE run ended, gel was coloured with ethidium bromide (0.5 µg/ml) and visualized by transilluminator (Moonlight, Diatech Labline). Restriction profiles have been compared each other and classified according to Tenover criteria *(Tenover et al., 1995)*.

2.5.1.2. S1 digestion

To investigate the number and dimension of plasmids carried out by each sample, half plug was digested for 30 minutes at room temperature with 100 U of S1-nuclease (ThermoFisher Scientific). This enzyme creates nick at the replication origins (ORI) of plasmids allowing their linearization. In this way, a correspondence between gel migration and their molecular weight was possible. Blocking digestion and agarose gel preparation are the same as described in the previous paragraph while run parameters regarding time switch are different:

- Starting time switch: 5 seconds
- Final time switch: 30 seconds

Plasmids dimensions were compared with standardized DNA using two different markers: MidRange PFG Marker (New England BioLabs), ranging from 15 kb to 291 kb, and Lambda PFG Ladder, ranging from 48.5 kb to 1018 kb (New England BioLabs).

2.6. WGS

Whole Genome Sequencing (WGS) of samples studied was performed with two different Next

Generation Sequencing (NGS) techniques: *Oxford Nanopore MinION* and *Illumina MiSeq* technologies.

2.6.1. Oxford Nanopore technology

Oxford Nanopore technology is an NGS method that offers real-time analysis of both DNA and RNA sequences, from short to ultra-long (> 4 Mb) read lengths. This technique does not require template amplification but only pure nucleic acid extraction and library preparation. DNA molecules are read in 5'→3' orientation so single-end reads are obtained as sequencing result. *Oxford Nanopore* sequencing uses flow cells containing an ion-permeable nanopores (α-hemolysins) array on which constant electric voltage flows. Each time a nucleotide goes through a nanopore, a change in the voltage is recorded. This change is base-specific and the basecalling process converts the electricity variation in the corresponding nucleotide. To achieve WGS of sample studied, we used the MinION Mk1B device and the basecalling process was performed by guppy *High-Accuracy* algorithm.

2.6.1.1. MinION Mk1B

MinION Mk1B is a small, portable device (W 105 mm, H 23 mm, D 33 mm) with a 3.0 USB cable that allows its connection to a laptop in which the *MinKNOW* software can be installed for free. Flow cells have standardized dimensions (W 92.4 mm, H 5.8 mm, D 28 mm), contain an array with up to 512 pores and 2048 electrodes in a hexagonal manner, and can be stored at 2-8 °C for three months [figure 13]. Protocols explaining how to wash and store a flow cell are available at https://nanoporetech.com/.

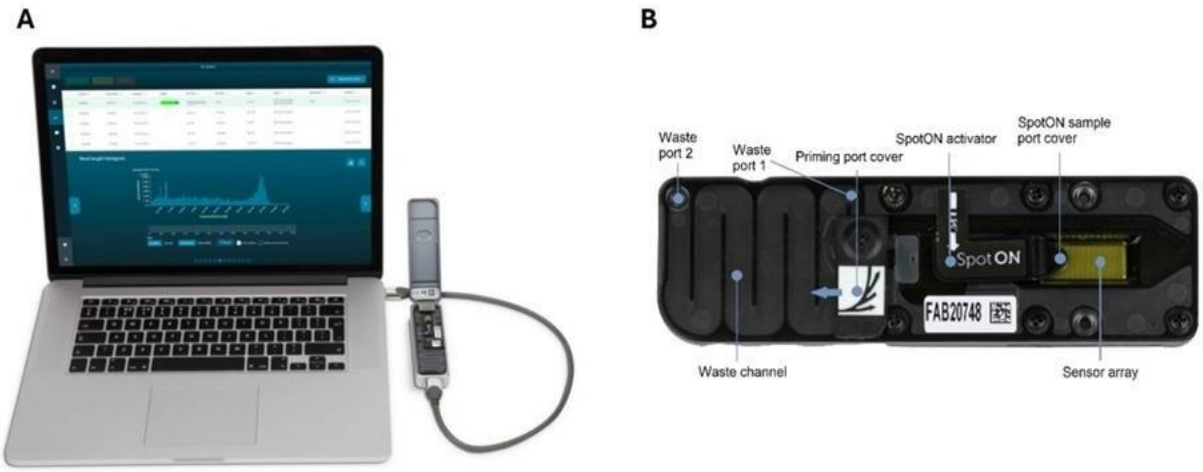

Figure 13. (A) MinION Mk1B device connected to a laptop. (B) Detail of the flow cell with all the components indicated.

2.6.1.2. Library preparation

Library preparation was performed using *Rapid Barcoding Sequencing* kit (SQK-RBK004) which enabled to sequence up to 12 samples in the same run. Each sample was linked to a specific sequencing adapter, a short oligonucleotide indicated as barcode, that allowed us to attribute DNA reads sequenced to the corresponding sample even if samples were pooled together in the same library. Library preparation required about 15 minutes and almost 400 ng of DNA for each sample. Each DNA sample was diluted in a specific tube to a final concentration of 400 ng in a volume of 7.5 µl to which 2.5 µl of different mixture of barcode and *Fragmentation Mix* (RB01-12) were added. These 10 µl were incubated 1 minute at 30 °C and 1 minute at 80 °C to perform the tagmentation and barcoding reactions. Barcoded DNAs were pooled together in a sterile 25 eppendorf and mixed with an equal volume of AMPure XP beads previously resuspended. After incubation for 5 minutes at room temperature, library pool was pelleted on a magnet and washed two times with 200 µl of 70% ethanol. After discarding supernatant, pellet was allowed to dry and then resuspended in 12 µl of 10 mM Tris-HCl pH 7.5-8.0 with 50 mM NaCl and incubated at room temperature for 2 minutes. Beads were pelleted on a magnet and 10 µl of eluate were retained in a new sterile tube in which 1 µl of *Rapid Adapter* (RAP) was added. The prepared library was incubated at room temperature for 5 minutes and then stored on ice until MinION flow cell was ready to be loaded.

2.6.1.3. Priming and loading the flow cell

After having properly placed the flow cell inside the MinION device, the priming port had to be opened and checked for air presence. A P1000 pipette was set at 200 µl, inserted on the priming port and the volume was increased to 230 µl to visualize fluid inside the tip. That meant that no air was present inside the channel of the sensor array. The priming mix was prepared by adding 30 µl of *Flush Tether* (FLT) inside the *Flush Buffer* (FB) tube (EXP-FLP002) and slowly 800 µl were loaded inside the priming port. After 5 minutes of incubation and SpotOn port opening, other 200 µl of priming mix were loaded into the priming port. Thirty-four µl of *Sequencing Buffer* (SQB), 25.5 µl of *Loading Beads* (LB) mixed before use, and 4.5 µl of nuclease-free water were added to the pooled library obtaining a total volume of 75 µl. This 75 µl pool was loaded in a dropwise fashion on the SpotOn port. After closing all ports and the device, the sequencing run could start.

2.6.2. Illumina technology

Illumina technology, also known as sequencing by synthesis (SBS), is a NGS method highly specific and accurate (in the order of Q30). In fact, since DNA molecules are linked to a unique index pair, both strands are read during the sequencing process achieving paired end reads. In addition, DNA templates have to be amplified, so the only way of sequencing error is linked to DNA Polymerase mistakes on base incorporation. This lowers the error rate compared to Nanopore technology and increases sequencing accuracy. Illumina sequencing consists of 3 steps: cluster generation, DNA sequencing, and data analysis. The cluster generation step takes place on the flow cell, a glass with 2 channels on which are bound multiple copies of two different oligonucleotides. These oligonucleotides are complementary to a small region of the adapters linked to DNA fragments. This pairing region is used as priming site for DNA Polymerase reaction and for bridge building. Repeating these steps for thousand times leads to cluster generation. The sequencing chemistry is based on reversible-terminator fluorescently labelled deoxynucleophosphate (dNTP). Only the dNTP complementary to the template strand is incorporated and each time the incorporation occurs, a fluorescent light is registered and then converted in the corresponding base. To achieve WGS of samples studied, Illumina MiSeq instrument was used.

2.6.2.1. Illumina MiSeq

Illumina MiSeq is a benchtop sequencing device (W 68.6 cm, H 52.3 cm, D 56.5 cm) with a slot that hosts the flow cell, another slot for the reagent cartridge and the sequencing buffer, and a touch screen monitor to set parameters and check sequencing status [figure 14]. Reads length, sequencing yield, and duration depend on cartridge type. In fact, different chemistry and kits exist. We used a 2x150 bp v2 cartridge, which allowed us to achieve a maximum of 5.1 Gb of reads up to 150 bp in approximately 24 hours. We sequenced 24 samples in the same run using the *Illumina DNA Prep* kit.



Figure 14. (A) Illumina MiSeq device. (B) Illumina MiSeq flow cell.

2.6.2.2. Library preparation

Library was obtained using the *Illumina DNA Prep* kit which requires almost 3 hours for library preparation and an amount of DNA templates ranging between 100 and 500 ng. We diluted in nuclease-free water our samples to 250 ng in 30 µl of final volume. Once all samples were in the desired concentration, the *Tagmentation Master Mix* (TMM) was prepared in a sterile tube mixing 11 µl x number of samples of *Bead-linked Transposomes* (BLT) and 11 µl x number of samples of *Tagment Buffer 1* (TB1). Twenty µl of TMM were added to each sample which were incubated for 15 minutes at 55 °C. To stop tagmentation, 10 µl of *Tagment Stop Buffer* (TSB) were joined to templates and then they were put at 37 °C for 15 minutes. Tubes containing tagmented DNAs were placed on a magnet and beads were washed three times with 100 µl of *Tagment Wash Buffer* (TWB). To attach indexes (i5 and i7) and sequences required for cluster generation step, tagmented DNAs were subjected to a limited-cycle PCR program after adding 40 µl of *PCR Master Mix* (PCR MM) to the beads. PCR MM consisted of 22 µl x number of samples of *Enhanced PCR Mix* (EPM) and 22 µl x number of samples of nuclease-free water. Before subjecting samples to BLT PCR program, 5 µl of i5 and 5 µl of i7 in samples-specific combinations were added to tagmented DNAs. The BLT PCR program consisted of 1 cycle at 68°C for 3 minutes and 98°C for 3 minutes, 5 cycles at 98°C for 45 seconds, 62°C for 30 seconds and 68°C for 2 minutes, and 1 cycle at 68°C for 1 minute. For the purification step, samples were placed on a magnet and 40 µl of each sample supernatant was transferred in new tubes. After having added 45 µl of *Illumina Purification Beads* (IPB) and 40 µl of nuclease-free water, samples were incubated at room temperature for 5 minutes and then placed on the magnet to collect 125 µl of supernatants and put them in new tubes containing 15 µl of IPB. Following 5

minutes at room temperature, samples were placed again on the magnet and beads were washed two times with 200 µl of 80% ethanol. Beads were allowed to dry and resuspended with 32 µl of *Resuspension Buffer* (RSB). To achieve pure library DNAs, samples were placed for a last time on the magnet and 30 µl of supernatant were transferred in new sterile tubes. Five µl of each sample were pooled together in a new eppendorf.

2.6.2.3. Library quality check and dilution to final concentration

Library was checked for quantity (using *Qubit* fluorometer) and pool size through a capillary electrophoresis using *TapeStation 4150* (Agilent). A D5000 ScreenTape was used, allowing gel separation of samples sizing between 100 and 500 bp with a DNA concentration of 0.1-50 ng/µl. One µl of pooled DNA was mixed with 10 µl of *Sample Buffer*, vortexed for 1 minute, and then placed inside the TapeStation together with a D5000 ScreenTape. To achieve library molarity, quantification of the pool (ng/µl) was divided for the result of pool size (bp) x nucleotide molecular weight (660 g/mol):

$$\text{Molarity} = \frac{\left(\frac{\text{ng}}{\mu\text{l}}\right)}{660\frac{\text{g}}{\text{mol}} \times 600\ \text{bp}}$$

Library pool was diluted to 2 nM and then subjected to a denaturation step: 5 µl of library were combined with 5 µl of NaOH 0.2 M and incubated 5 minutes at room temperature. To dilute the denatured pool at 10 pM, 990 µl of *HT1 Buffer* were added at the previous 10 µl. The last step consisted of a further dilution to 9 pM in a final volume of 600 µl, which was loaded in the appropriate slot in the v2 cartridge.

2.7. MLST

MLST assign a sequence type (ST) to each bacterial strain according to 7 housekeeping genes allelic sequences (*gap*A, *inf*B, *mdh*, *pgi*, *pho*E, *rpo*B, *ton*B). STs were obtained from WGS data using the Institute Pasteur scheme available at http://bigsdb.pasteur.fr/klebsiella/klebsiella.html website.

2.8. Data analysis

Reads obtained by both sequencing methods are supplied in fastq format and have to be assembled to achieve complete sample genomes. After checking for reads quality using *FastQC* program (https://github.com/s-andrews/FastQC), Nanopore long reads were assembled by

Canu v 2.2 and polished by *Medaka v 1.1.0* while hybrid assemblies were performed by *Unicycler v 0.4.8*. The websites *BLAST* (https://blast.ncbi.nlm.nih.gov/Blast.cgi), *Center for Genomic Epidemiology* (http://www.genomicepidemiology.org/services/), and *The Comprehensive Antibiotic Resistance Database* (https://card.mcmaster.ca/home) were used to analyze the resistome and plasmidome. Plasmids were reconstructed by *BRIG 0.95* software after genome annotations using RAST (https://rast.nmpdr.org/) while transposons were depicted with *SnapGene v 6.0.4* and *EasyFig v 2.2.5*. Phylogenetic analysis was performed with *CSI phylogeny 1.4*.

3. RESULTS

3.1. KPC-Kp

During the retrospective multi-center study conducted in the three central Italy hospitals, a total of 167 clinical isolates of KPC-Kp responsible for BSIs were collected from different patients between January 2014 and December 2019. More in detail, 104 strains (named from AN-1 to AN-104) were obtained from the clinical microbiology laboratory of "Ospedali Riuniti" of Ancona; 33 strains (from PR-1 to PR-33) belonged to the "Azienda Ospedaliera" of Perugia, and 30 strains were collected at "Ospedali Riuniti Marche Nord" of Pesaro and Fano (5 from Pesaro named from PS–1 to PS-5, and 25 from Fano named from FA-1 to FA-25) [table 4]. A more detailed description of samples collection and distribution among hospitals during the study period is reported in table 5, together with the annual incidence expressed in percentage.

	Hospitals				**Total per year**	**Annual incidence**
	Ancona	Fano	Pesaro	Perugia		
2014	32	1	0	0	33	19,8%
2015	14	1	3	0	18	10,8%
2016	11	2	0	0	13	7,8%
2017	28	3	0	0	31	18,6%
2018	13	8	1	0	22	13,2%
2019	6	10	1	33	50	29,9%

Table 5. Number of KPC-Kp collected in each hospital included in the study divided per year. The last two columns show the total number of samples harvested every year and their annual incidence.

3.1.1. Resistance phenotypes

Among the 167 KPC-Kp, 68 isolates (40.7%) were resistant to colistin showing MIC values > 2 mg/L. This colistin resistance incidence showed a decreasing trend during the study period,

switching from a 54.5% rate in 2014 (18 out of 33 samples) to a 34% rate in 2019 (17 out of 50 samples) [figure 15]. Moreover, in 2019 the majority of colistin-resistant strains was represented by Perugia's isolates, characterized by an incidence rate of 45.5%. In addition, also the only 3 CZA-resistant *K. pneumoniae* strains (with MIC values ≥ 16 mg/L) belonged to this hospital. MIC values were reported in table 4.

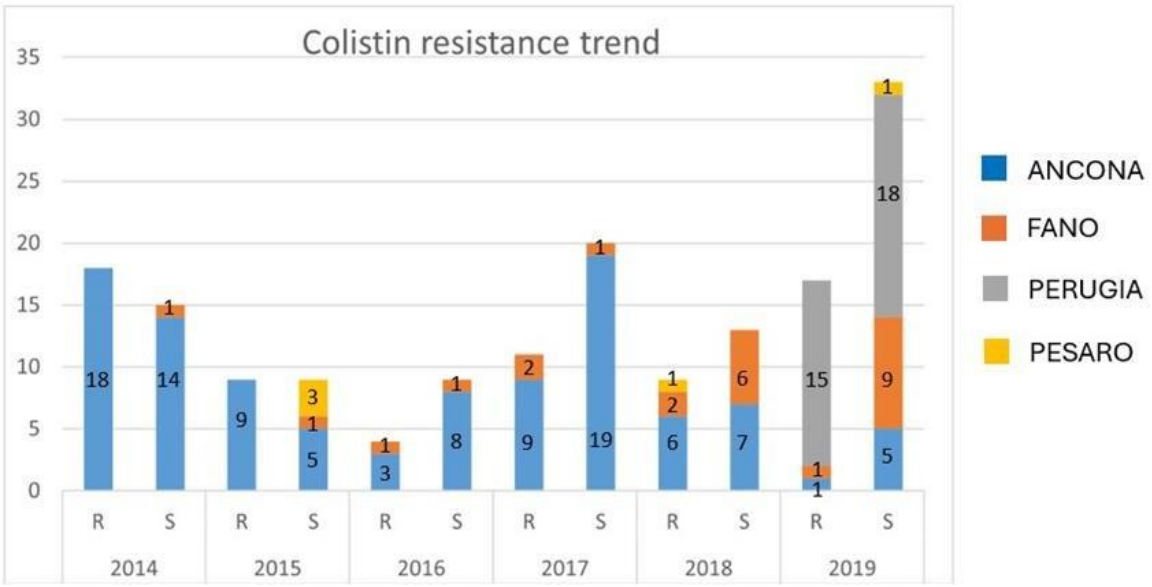

Figure 15. Colistin resistance trend during the study period divided for areas of collection. R, resistant; S, susceptible.

Strain		AN-1	AN-2	AN-3	AN-4	AN-5	AN-6	AN-7	AN-8	AN-9	AN-10	AN-11	AN-12	AN-13	AN-14	AN-15	AN-16	AN-17
Date		2014/01	2014/01	2014/02	2014/02	2014/02	2014/02	2014/03	2014/03	2014/03	2014/03	2014/03	2014/03	2014/04	2014/05	2014/05	2014/06	2014/06
MIC (mg/L)	CZA	4	4	4	4	2	2	2	4	8	8	4	4	2	2	1	8	2
	COL	32	>32	16	2	>32	1	>32	16	2	>32	2	>32	4	4	1	>32	>32
PFGE		A3	A6	A6	A3	#1	#1	A7	A6	A3	A3	K	A3	A3	A6	A6	$	#1

Strain		AN-18	AN-19	AN-20	AN-21	AN-22	AN-23	AN-24	AN-25	AN-26	AN-27	AN-28	AN-29	AN-30	AN-31	AN-32	AN-33	AN-34
Date		2014/06	2014/06	2014/07	2014/07	2014/07	2014/07	2014/08	2014/08	2014/08	2014/08	2014/08	2014/08	2014/08	2014/09	2014/12	2015/04	2015/05
MIC (mg/L)	CZA	8	1	2	1	1	4	2	2	1	4	1	4	2	8	4	2	2
	COL	1	1	2	0.5	1	>32	0.5	4	0.5	8	1	32	16	1	32	2	>32
PFGE		A6	#1	#4	#1	A6	K	#1	A6	#1	£	€	&	&	A3	A3	A6	A6

Strain		AN-35	AN-36	AN-37	AN-38	AN-39	AN-40	AN-41	AN-42	AN-43	AN-44	AN-45	AN-46	AN-47	AN-48	AN-49	AN-50	AN-51
Date		2015/06	2015/08	2015/08	2015/08	2015/09	2015/09	2015/09	2015/09	2015/09	2015/08	2015/11	2015/12	2016/01	2016/02	2016/04	2016/05	2016/06
MIC (mg/L)	CZA	4	2	4	4	8	8	8	1	4	2	2	4	8	4	8	8	4
	COL	4	2	16	1	>32	>32	>32	2	16	4	2	4	2	8	1	1	4
PFGE		A6	A6	A6	A3	A6	A6	A3	A6	A3	A3	A3	A3	A1	A2	B1	A5	C

Strain		AN-52	AN-53	AN-54	AN-55	AN-56	AN-57	AN-58	AN-59	AN-60	AN-61	AN-62	AN-63	AN-64	AN-65	AN-66	AN-67	AN-68
Date		2016/06	2016/07	2016/09	2016/10	2016/11	2016/11	2017/01	2017/01	2017/01	2017/03	2017/04	2017/04	2017/05	2017/05	2017/05	2017/06	2017/06
MIC (mg/L)	CZA	2	2	8	4	8	8	8	8	2	4	8	4	4	8	4	1	2
	COL	0.12	0.12	0.5	16	0.25	0.12	0.12	0.25	0.12	8	0.5	2	32	8	0.25	0.5	0.5
PFGE		D1	E1	A3	A4	A4	D2	D1	A5	D2	F1	A1	A4	A2	G	A4	A4	H2

Strain		AN-69	AN-70	AN-71	AN-72	AN-73	AN-74	AN-75	AN-76	AN-77	AN-78	AN-79	AN-80	AN-81	AN-82	AN-83	AN-84	AN-85
Date		2017/06	2017/06	2017/06	2017/06	2017/07	2017/09	2017/09	2017/10	2017/10	2017/10	2017/10	2017/11	2017/11	2017/12	2017/12	2017/12	2017/12
MIC (mg/L)	CZA	4	8	8	8	4	8	1	8	4	4	8	8	8	8	4	8	4
	COL	16	16	8	0.12	32	4	0.5	0.25	0.5	4	0.25	0.25	0.25	0.12	1	0.25	≤0.06
PFGE		E1	A1	F2	1	A4	A4	J	D1	A5	K	L	D2	A5	A6	M	A7	A1

Strain		AN-86	AN-87	AN-88	AN-89	AN-90	AN-91	AN-92	AN-93	AN-94	AN-95	AN-96	AN-97	AN-98	AN-99	AN-100	AN-101	AN-102
Date		2018/01	2018/01	2018/01	2018/01	2018/01	2018/01	2018/04	2018/05	2018/05	2018/08	2018/10	2018/10	2018/11	2019/04	2019/06	2019/06	2019/07
MIC (mg/L)	CZA	4	4	8	8	2	4	8	2	4	4	8	2	4	8	8	4	2
	COL	4	1	>32	1	0.12	4	>32	0.25	0.5	≤0.06	0.12	8	8	≤0.06	2	0.12	0.25
PFGE		A4	N	A1	A4	D1	G	A6	O	A4	F3	E2	E2	E2	A4	A1	P	Q

Strain		AN-103	AN-104	PR-1	PR-2	PR-3	PR-4	PR-5	PR-6	PR-7	PR-8	PR-9	PR-10	PR-11	PR-12	PR-13	PR-14	PR-15
Date		2019/08	2019/08	2019/01	2019/01	2019/02	2019/04	2019/04	2019/05	2019/05	2019/06	2019/06	2019/07	2019/06	2019/07	2019/07	2019/07	2019/08
MIC (mg/L)	CZA	8	8	4	4	16	8	8	4	0.5	1	4	2	16	32	2	8	8
	COL	0.25	16	0.5	4	0.5	1	16	2	16	16	1	8	1	1	32	>32	>32
PFGE		R	S	B1	W	B2	T	B1	U	@	@	B1	V	B2	B2	W	W	W

Strain		PR-16	PR-17	PR-18	PR-19	PR-20	PR-21	PR-22	PR-23	PR-24	PR-25	PR-26	PR-27	PR-28	PR-29	PR-30	PR-31	PR-32
Date		2019/09	2019/09	2019/09	2019/09	2019/09	2019/09	2019/09	2019/09	2019/10	2019/10	2019/10	2019/11	2019/11	2019/11	2019/11	2019/11	2019/12
MIC (mg/L)	CZA	8	4	2	8	2	2	8	4	2	8	4	8	4	8	8	8	8
	COL	>32	32	2	16	4	0.5	1	1	>32	4	1	4	0.5	0.5	1	0.5	1
PFGE		W	X	B1	W	Y	B1	B1	B1	A3	W	B1	W	B1	B1	B1	B1	@

Strain		PR-33	FA-1	FA-2	FA-3	FA-4	FA-5	FA-6	FA-7	FA-8	FA-9	FA-10	FA-11	FA-12	FA-13	FA-14	FA-15	FA-16
Date		2019/12	2014/09	2015/05	2016/06	2016/08	2017/08	2017/11	2017/12	2018/02	2018/02	2018/04	2018/05	2018/06	2018/07	2018/08	2018/11	2019/01
MIC (mg/L)	CZA	2	4	4	2	2	8	4	4	4	4	4	1	1	2	2	2	2
	COL	1	0.06	0.12	16	0.25	>32	4	0.12	>32	0.12	0.5	0.25	0.25	0.12	>32	0.06	0.12
PFGE		Z	A7	A7	A6	A6	A7	A7	A7	A7	A7	A7	A7	A7	A7	A7	-	#2

Strain		FA-17	FA-18	FA-19	FA-20	FA-21	FA-22	FA-23	FA-24	FA-25	PS-1	PS-2	PS-3	PS-4	PS-5
Date		2019/02	2019/02	2019/03	2019/05	2019/07	2019/07	2019/07	2019/08	2019/12	2015/09	2015/09	2015/11	2018/06	2019/07
MIC (mg/L)	CZA	2	2	2	2	1	2	2	1	4	4	4	8	4	2
	COL	>32	0.06	0.12	0.25	0.12	0.12	0.25	0.25	32	0.25	0.25	2	2	0.25
PFGE		#1	#1	#3	#1	#1	A4	#1	A4	#4	A7	?	A7	A7	!

Table 4. KPC-Kp with date of collection, MIC values, and XbaI restriction profile. Red cells, MIC resistant values.

3.1.2. Genotyping

PFGE assays highlighted 50 different pulsotypes with 2 major clusters [table 4]. The restriction profile indicated as cluster A was present in all hospitals and it was the most common restriction profile detected in Ancona, with an incidence of 54.8%. Cluster B, however, featured only Perugia's isolates, counting 16 out of 33 samples collected (48.5%). One sample for each pulsotype detected was subjected to WGS by Oxford Nanopore technology. Among the 50 strains sequenced, MLST pointed out 11 different STs, with ST512 (40%) and ST307 (30%) as the most represented. These STs were found in all the areas studied, except for Pesaro which lacked ST307. Another common ST found was ST101, with an incidence rate of 14%. Even if this ST was found only in Ancona and Pesaro, a strictly related one, the ST2502, which differs only for the *rpoB* allelic variant, was found among Perugia isolates. This sequence type was newly discovered by Arena and colleagues during a CRE surveillance in Florence, Italy, in 2016 *(Arena et al., 2020)*. Phylogenetic tree, built using AN-16 as reference, showed that the genetic distance among ST512 samples was low while ST307 and ST101 strains exhibited a slightly higher variability [figure 16]. These observations were confirmed by SNPs matrix that highlighted a minimum of 22 and a maximum of 251 SNPs between ST512 strains and ranged from 63 to 448 and from 124 to 496 SNPs among ST307 and ST101 strains, respectively. *bla*$_{KPC}$ genes were plasmid located on the same well-characterized transposon Tn*4401* on all samples studied. In most cases, cones showed one *bla*$_{KPC}$ copy but four samples harboured two copies of the gene. Among these, two isolates (AN-78, and PS-5) exhibited the two *bla*$_{KPC}$ genes in the same plasmid while in the remaining (AN-29, and AN-83) the gene was in two different plasmids. Three allelic variants of the carbapenemase encoding gene were detected among samples: 45 strains encoded for *bla*$_{KPC-3}$ (90%), 4 samples, all belonging to ST307, for *bla*$_{KPC-2}$ (8%), and the remaining one (also resistant to CZA) for *bla*$_{KPC-66}$ (2%). Plasmids carrying *bla*$_{KPC}$ genes were different in size, ranging from 86 to 266 kb, and in incompatibility groups, even if the most represented were IncFIB(pQIL) and IncFII(K), with an incidence of 68%. Nine samples carried only the *bla*$_{KPC}$ encoding plasmid while the remaining 41 showed at least two plasmids. Regarding antibiotic resistance genes other than carbapenemases, all samples presented the chromosomally encoded *fosA* gene and different *bla*$_{SHV}$ allelic variants related to the ST. More in detail, ST307 isolates carried the *bla*$_{SHV-28}$, ST101 the *bla*$_{SHV-1}$, and ST512 the *bla*$_{SHV-11}$ or *bla*$_{SHV-182}$ allelic variants. Complete resistomes and genetic characteristics of

all clones studied are reported in table 6.

Of the 50 KPC-Kp sequenced, 25 isolates resulted resistant to colistin, but no one coded for the *mcr* gene. On the other hand, the wild type *mgrB* regulator featured only in 6 isolates (24%), while in 2 others was not detected (8%), and in the remaining ones was interrupted by insertion sequences (68%). More in detail, 15 isolates (60%) showed the *mgrB* gene interrupted by an *IS5*-like insertion sequence while in the remaining 2 isolates (8%) the insertional inactivation depended on *IsKpn14* element [table 7]. Both these two *mgrB* allelic variants were described by Cannatelli and colleagues in 2013 and 2014, respectively (accession numbers: HG008893, and KJ129604).

Col-R strains	**Year**	***mgrB***
AN-16	2014	Insertional inactivation, IS*5*-like
AN-27	2014	Insertional inactivation, IS*5*-like
AN-29	2014	Insertional inactivation, IS*5*-like
AN-48	2016	Insertional inactivation, IS*5*-like
AN-51	2016	WT
AN-55	2016	Insertional inactivation, IS*5*-like
AN-61	2017	Insertional inactivation, IS*5*-like
AN-71	2017	Insertional inactivation, IS*5*-like
AN-74	2017	Insertional inactivation, IS*5*-like
AN-78	2017	Insertional inactivation, IS*5*-like
AN-91	2018	Insertional inactivation, IS*5*-like
AN-92	2018	Insertional inactivation, IS*5*-like
AN-98	2018	Insertional inactivation, IS*5*-like
AN-104	2019	WT
FA-3	2016	Insertional inactivation, IS*5*-like
FA-5	2017	Insertional inactivation, IS*5*-like
FA-17	2019	WT
FA-25	2019	WT
PR-7	2019	Δ*mgrB*
PR-8	2019	WT
PR-10	2019	Insertional inactivation, IS*Kpn14*
PR-15	2019	Insertional inactivation, IS*Kpn14*
PR-17	2019	Δ*mgrB*
PR-20	2019	WT
PR-24	2019	Insertional inactivation, IS*5*-like

Table 7. mgrB sequences detected in colistin resistant KPC-Kp sequenced. WT, wild type; ΔmgrB, gene not detected.

Strains	ST	antibiotic resistance genes									plasmid incompatibility group	***bla*KPC carrying plasmid**	
		beta-lactams	quinolones	aminoglycosides	tetracyclines	fosfomycin	folate	macrolides	phenicols	efflux pump		incompatibility group	size (kb)
AN-16	512	***bla*KPC-3**; *bla*SHV-11; *bla*TEM-1	*oqx*A; *oqx*B; *aac*(6')-Ib-cr	*aac*(6')-Ib; *aac*(6')-Ib-cr; *aph*(3')-Ia; *aad*A2	-	*fos*A6	*oqx*A; *oqx*B; *sul*1; *dfr*A12	*mph*(A)	*oqx*A; *oqx*B; *cat*A1	*kpn*E; *kpn*F; *kpn*G	IncFIB(pQil); IncFII(K); IncFIB(K); ColRNAI	IncFIB(pQil); IncFII(K)	115
AN-27	512	***bla*KPC-3**; *bla*SHV-1; *bla*TEM-1	*oqx*A; *oqx*B	*aac*(6')-Ib; *aad*A2	-	*fos*A6	*oqx*A; *oqx*B; *sul*1	-	*oqx*A; *oqx*B	*kpn*E; *kpn*F; *kpn*G	IncFIB(pQil); IncFII(K)	IncFIB(pQil); IncFII(K)	113
AN-28	14	***bla*KPC-3**; *bla*SHV-1; bla$_{SHV-28}$; *bla*TEM-1	*oqx*A; *oqx*B; qnrB19	*aph*(6)-Id; *aph*(3'')-Ib	-	*fos*A6	*oqx*A; *oqx*B; *sul*1	-	*oqx*A; *oqx*B	*kpn*E; *kpn*F; *kpn*G	IncFIB(pQil); IncFII(K); ColRNAI	IncFIB(pQil); IncFII(K)	113
AN-29	512	***bla*KPC-3***; *bla*SHV-11; *bla*TEM-1	*oqx*A; *oqx*B; *aac(6')-Ib-cr*	*aac*(6')-Ib; *aac*(6')-Ib-cr; *aph*(3')-Ia; *aad*A2	-	*fos*A6	*oqx*A; *oqx*B; *sul*1; *dfr*A12	*mph*(A)	*oqx*A; *oqx*B	*kpn*E; *kpn*F; *kpn*G; *ompk*37	IncFIB(pQil); IncFII(K); IncFIB(K); ColRNAI	IncFIB(pQil); IncFII(K) + IncFIB(K); IncFII(K)	219+112
AN-48	512	***bla*KPC-3**; *bla*SHV-11;	*oqx*A; *oqx*B; *aac*(6')-Ib-cr	*aac*(6')-Ib; *aac*(6')-Ib-cr; *aph*(3')-Ia; *aad*A2	-	*fosA6* (Q130P, D138E)	*oqx*A; *oqx*B; *sul*1; *dfr*A12	*mph*(A)	*oqx*A; *oqx*B; *cat*A1	*kpn*E; *kpn*F; *kpn*G	IncFIB(pQil); IncFIB(K); IncFII(K); ColRNAI; IncX3	IncFIB(pQil); IncFII(K)	100
AN-49	512	***bla*KPC-3**; *bla*SHV-11; *bla*TEM-1	*oqx*A; *oqx*B; *aac*(6')-Ib-cr	*aac*(6')-Ib; *aac*(6')-Ib-cr; *aph*(3')-Ia; *aad*A2	-	*fosA6* (Q130P, D138E)	*oqx*A; *oqx*B; *sul*1; *dfr*A12	*mph*(A)	*oqx*A; *oqx*B; *cat*A1	*kpn*E; *kpn*F; *kpn*G	IncFIB(pQil); IncFII(K); IncFIB(K); ColRNAI	IncFIB(pQil); IncFII(K)	118
AN-50	512	***bla*KPC-3**; *bla*SHV-182; *bla*TEM-1	*oqx*A; *oqx*B; *aac*(6')-Ib-cr	*aac*(6')-Ib; *aac*(6')-Ib-cr; *aph*(3')-Ia; *aad*A2	-	*fosA6* (Q130P, D138E)	*oqx*A; *oqx*B; *sul*1; *dfr*A12	*mph*(A)	*oqx*A; *oqx*B; *cat*A1	*kpn*E; *kpn*F; *kpn*G	IncFIB(K); IncFII(K); IncFIB(pQil); ColRNAI; IncX3	IncFIB(pQil); IncFII(K)	113
AN-51	37	***bla*KPC-3**; ***bla*OXA-1**; *bla*CTX-M-15; *bla*TEM-1; *bla*SHV-11	*oqx*A; *oqx*B; *aac*(6')-Ib-cr; *qnr*B1	*aac*(6')-Ib-cr	-	*fosA6* (I89V, Q130P)	*oqx*A; *oqx*B	-	*oqx*A; *oqx*B	*kpn*E; *kpn*F; *kpn*G	IncFIB(pQil); IncFII(K); IncFIB(K); ColRNAI	IncFIB(pQil); IncFII(K)	114
AN-53	101	***bla*KPC-3**; *bla*SHV-1; *bla*TEM-1	*oqx*A; *oqx*B	*arm*A		*fos*A6	*oqx*A; *oqx*B; *sul*1; *dfr*A5	mph(E)	*oqx*A; *oqx*B; *cat*A1	*kpn*E; *kpn*F; *kpn*G; *ompk*37	IncFIB(pQil); IncFII(K); IncX1	IncFIB(pQil); IncFII(K)	113
AN-55	512	***bla*KPC-3**; *bla*SHV-11; *bla*TEM-1	*oqx*A; *oqx*B	*aac*(6')-Ib; *aph*(3')-Ia; *aad*A2b	-	*fos*A6	*oqx*A; *oqx*B; *sul*1; *dfr*A14	*mph*(A)	*oqx*A; *oqx*B; *cat*A1	*kpn*F; *kpn*G; KpnH	IncFIB(K); IncFII(K); IncFIB(pQIL); ColRNAI; IncX3	IncFIB(pQil); IncFII(K)	114
AN-58	512	***bla*KPC-3**; *bla*SHV-11; *bla*TEM-1	*oqx*A; *oqx*B; *aac*(6')-Ib-cr	*aac*(6')-Ib; *aac*(6')-Ib-cr; *aad*A2	-	*fos*A6	*oqx*A; *oqx*B; *sul*1	-	*oqx*A; *oqx*B	*kpn*E; *kpn*F; *kpn*G	IncFIB(pQil); IncFII(K); ColRNAI	IncFIB(pQil); IncFII(K)	117
AN-61	101	***bla*KPC-3**; *bla*SHV-1; *bla*TEM-1	*oqx*A; *oqx*B	*arm*A	-	*fosA5* (M29T, A86V, A138D)	*oqx*A; *oqx*B; *sul*1; *dfr*A5	*msr*(E); *mph*(E)	*oqx*A; *oqx*B; *cat*A1	*kpn*F; *kpn*G	IncFIB(K); IncFII(K); ColRNAI; Col440II	IncFIB(pQil); IncFII(K)	76
AN-67	512	***bla*KPC-3**; *bla*SHV-11	*oqx*A; *oqx*B; *aac*(6')-Ib-cr	*aac*(6')-Ib; *aad*A2; *aph*(3')-Ia	-	*fos*A6	*oqx*A; *oqx*B; *sul*1	-	*oqx*A; *oqx*B	*kpn*E; *kpn*F; *kpn*G	IncFII(K); IncFIB(K); ColRNAI; IncX3	IncFIB(K); IncFII(K)	161

AN-68	512	***bla*$_{KPC-3}$**; *bla*$_{SHV-11}$	*oqx*A; *oqx*B; *aac*(6')-Ib-cr	*aac*(6')-Ib-cr; *aac*A4; *aad*A2b	-	*fosA5* (M29T)	*oqx*A; *oqx*B; *sul*1	-	*oqx*A; *oqx*B	*kpn*E; *kpn*F; *kpn*G	IncFII(K); IncFIB(K); ColRNAI; IncX3	IncFIB(K); IncFII(K)	160
AN-71	101	***bla*$_{KPC-3}$**; *bla*$_{SHV-1}$	*oqx*A; *oqx*B	*arm*A	-	*fos*A6	*oqx*A; *oqx*B; *sul*1; *dfr*A5	*msr*(E); *mph*(E)	*oqx*A; *oqx*B	*kpn*E; *kpn*F; *kpn*G; *ompk*37	IncFIB(K); IncFII(K); ColRNAI; Col440II	IncFIB(K); IncFII(K)	198
AN-72	512	***bla*$_{KPC-3}$**; *bla*$_{SHV-11}$; *bla*$_{TEM-1}$	*oqx*A; *oqx*B; *aac*(6')-Ib-cr	*aac*(6')-Ib; *aac*(6')-Ib-cr; *aph*(3')-Ia; *aad*A2	-	*fos*A6	*oqx*A; *oqx*B; *sul*1; *dfr*A12	*mph*(A)	*oqx*A; *oqx*B; *cat*A1	*kpn*E; *kpn*F; *kpn*G	IncFIB(pQil); IncFII(K); IncFIB(K); IncFIB(pNDM-MAR); IncHI1B(pNDM-MAR); ColRNAI	IncFIB(pQil); IncFII(K)	94
AN-75	405	***bla*$_{KPC-3}$**; *bla*$_{CTX-M-15}$; *bla*$_{OXA-1}$; *bla*$_{TEM-1}$; *bla*$_{SHV-76}$	*oqx*A; *oqx*B; *aac*(6')-Ib-cr; *qnr*B1	*aac*(6')-Ib-cr; *str*A; *str*B	*tet*(A)	*fosA6* (Q130P)	*oqx*A; *oqx*B; *dfr*A14	-	*oqx*A; *oqx*B	*kpn*E; *kpn*F	IncFIB(pQil); IncFII(K); IncFIB(K)	IncFIB(pQil); IncFII(K)	113
AN-78	512	***bla*$_{KPC-3}$***; *bla*$_{SHV-11}$;	*oqx*A; *oqx*B; *aac*(6')-Ib-cr	*aac*(6')-Ib; *aac*(6')-Ib-cr; *aad*A2b	-	*fosA6* (Q130P)	*oqx*A; *oqx*B; *sul*1	-	*oqx*A; *oqx*B	*kpn*E; *kpn*F; *kpn*G	IncFII(K); IncFIB(K); ColRNAI	IncFIB(K); IncFII(K)	174
AN-79	307	***bla*$_{KPC-3}$**; *bla*$_{SHV-28}$; *bla*$_{TEM-1}$; *bla*$_{OXA-1}$	*oqx*A; *oqx*B; *aac*(6')-Ib-cr; *qnr*B1	*aac*(6')-Ib-cr; *aac*(3)-IIa; *str*A; *str*B	-	*fosA6* (Q130P)	*oqx*A; *oqx*B; *sul*2; *dfr*A14	-	*oqx*A; *oqx*B	*kpn*E; *kpn*F; *kpn*G	IncFIB(pQil); IncFII(K); IncFIB(K)	IncFIB(pQil); IncFII(K)	113
AN-80	512	***bla*$_{KPC-3}$**; *bla*$_{SHV-182}$; *bla*$_{TEM-1}$	*oqx*A; *oqx*B; *aac*(6')-Ib-cr	*aac*(6')-Ib-cr; *aac*A4; *aad*A2; *aph*(3')-Ia	-	*fosA6* (I91V, Q130P, D138E)	*oqx*A; *oqx*B; *sul*2; *dfr*A14	*mph*(A)	*oqx*A; *oqx*B; *cat*A1	*kpn*E; *kpn*F; *kpn*G	IncFIB(pQil); IncFII(K); IncFIB(K); ColRNAI	IncFIB(pQil); IncFII(K)	113
AN-83	307	***bla*$_{KPC-3}$*; *bla*$_{SHV-28}$; *bla*$_{TEM-1}$; *bla*$_{OXA-1}$	*oqx*A; *oqx*B; *aac*(6')-Ib-cr; *qnr*B1	*aac*(3)-IIa; *aac*(6')-Ib-cr	*tet*(A)	*fosA6* (Q130P)	*oqx*A; *oqx*B; *dfr*A14	-	*oqx*A; *oqx*B	-	IncFIB(pQil); IncFII(K); IncFIB(K)	IncFIB(pQil); IncFII(K); IncFIB(K)	200+113
AN-87	307	***bla*$_{KPC-3}$**: *bla*$_{SHV-28}$; *bla*$_{TEM-1}$; *bla*$_{OXA-1}$	*oqx*A; *oqx*B; *aac*(6')-Ib-cr; *qnr*B1	*aac*(3)-IIa; *aac*(6')-Ib-cr	*tet*(A)	*fosA6* (Q130P)	*oqx*A; *oqx*B; *dfr*A14	-	*oqx*A; *oqx*B	*kpn*E; *kpn*F; *kpn*G	IncFIB(pQil); IncFII(K); IncFIB(K)	IncFIB(pQil); IncFII(K); IncFIB(K)	345
AN-91	101	***bla*$_{KPC-3}$**; *bla*$_{SHV-1}$	*oqx*A; *oqx*B	*arm*A	-	*fosA6* (A86V, Q130P, Q139E)	*oqx*A; *oqx*B; *sul*1; *dfr*A5	*msr*(E); *mph*(E)	*oqx*A; *oqx*B; *cat*A1	*kpn*E; *kpn*F; *kpn*G; *ompk*37	IncFIB(K); IncFII(K); ColRNAI; Col440II	IncFIB(K); IncFII(K)	199
AN-92	512	***bla*$_{KPC-3}$**: *bla*$_{SHV-11}$; *bla*$_{TEM-1}$; *bla*$_{OXA-9}$	*oqx*A; *oqx*B; *aac*(6')-Ib-cr	*aac*(6')-Ib; *aac*(6')-Ib-cr; *aph*(3')-Ia; *aad*A2	-	*fosA5* (M29T)	*oqx*A; *oqx*B; *sul*1; *dfr*A12	*mph*(A)	*oqx*A; *oqx*B; *cat*A1	*kpn*E; *kpn*F; *kpn*G	IncFIB(pQil); IncFII(K); IncFIB(K); ColRNAI	IncFIB(pQil); IncFII(K)	113
AN-93	307	***bla*$_{KPC-2}$**; *bla*$_{CTX-M-15}$; *bla*$_{SHV-28}$; *bla*$_{TEM-1}$; *bla*$_{OXA-1}$	*oqx*A; *oqx*B; *aac*(6')-Ib-cr; *qnr*B1	*aac*(6')-Ib-cr	-	*fosA6* (A78V, Q130P)	*oqx*A; *oqx*B; *dfr*A14	-	*oqx*A; *oqx*B	*kpn*E; *kpn*F; *kpn*G	IncFIB(K); IncFII(K)	IncFIB(K); IncFII(K)	266
AN-95	101	***bla*$_{KPC-3}$**; *bla*$_{SHV-11}$; *bla*$_{TEM-1}$	*oqx*A; *oqx*B	*arm*A	-	*fos*A6	*oqx*A; *oqx*B; *sul*1; *dfr*A5	*mph*(A)	*oqx*A; *oqx*B; *cat*A1	*kpn*E; *kpn*F; *kpn*G	IncFIB(pQil); IncFII(K); IncFIB(K); ColRNAI; Col440II	IncFIB(pQil); IncFII(K)	96
AN-98	101	***bla*$_{KPC-3}$**; *bla*$_{SHV-11}$	*oqx*A; *oqx*B	*arm*A	-	*fosA6* (A86V, Q130P, Q139E)	*oqx*A; *oqx*B	*msr*(E); *mph*(E)	*oqx*A; *oqx*B	*kpn*E; *kpn*F	IncFIB(K); IncFII(K); ColRNAI; Col440II	IncFIB(K); IncFII(K)	179
AN-100	512	***bla*$_{KPC-3}$**; *bla*$_{SHV-11}$	*oqx*A; *oqx*B	*aac*(6')-Ib-cr	-	*fosA5* (M29T)	*oqx*A; *oqx*B	-	*oqx*A; *oqx*B	*kpn*E; *kpn*F; *kpn*G	IncFIB(pQil); IncFII(K); IncFIB(K)	IncFIB(pQil); IncFII(K); IncFIB(K)	167

AN-101	1519	***bla*KPC-3**; *bla*SHV-182; *bla*TEM-1	*oqx*A; *oqx*B	*aac*(6')-Ib-cr	-	*fosA5* (M29T)	*oqx*A; *oqx*B	-	*oqx*A; *oqx*B	*kpn*E; *kpn*F; *kpn*G	IncFIB(pQil); IncFII(K)	IncFIB(pQil); IncFII(K)	120
AN-102	307	***bla*KPC-2**; *bla*SHV-28; *bla*TEM-1; *bla*OXA-1	*oqx*A; *oqx*B	-	-	*fosA6* (Q130P)	*oqx*A; *oqx*B	-	*oqx*A; *oqx*B	*kpn*E; *kpn*F	IncFIB(pQil); IncFII(K)	IncFIB(pQil); IncFII(K)	113
AN-103	307	***bla*KPC-3**; *bla*CTX-M-15; *bla*SHV-28; *bla*TEM-1; *bla*OXA-1	*oqx*A; *oqx*B; *aac*(6')-Ib-cr	*aac*(6')-Ib-cr; *aac*(3)-IIa; *str*A; *str*B	-	*fosA6* (Q130P)	*oqx*A; *oqx*B; *sul*2; *dfr*A14	-	*oqx*A; *oqx*B	*kpn*E; *kpn*F	IncFIB(pQil); IncFII(K); IncFIB(K)	IncFIB(pQil); IncFII(K)	100
AN-104	307	***bla*KPC-2**; *bla*CTX-M-15; *bla*SHV-28; *bla*TEM-1; *bla*OXA-1	*oqx*A; *oqx*B; *aac*(6')-Ib-cr; *qnr*B1	*aac*(6')-Ib-cr; *aac*(3)-IIa; *str*A; *str*B	-	*fos*A6	*oqx*A; *oqx*B; *sul*2; *dfr*A14	-	*oqx*A; *oqx*B	*kpn*E; *kpn*F; *kpn*G	IncFIB(pQil); IncFII(K); IncFIB(K); ColRNAI; Col440II	IncFIB(pQil); IncFII(K)	107
PR-4	29	***bla*KPC-3**; *bla*SHV-187; *bla*TEM-1	*oqx*A; *oqx*B	-	-	*fosA6* (Q130P, V135E)	*oqx*A; *oqx*B	-	*oqx*A; *oqx*B	*kpn*E; *kpn*F; *kpn*G; *ompk*37	IncFIB(pQil); IncFIB(K); IncFII(K); IncFIB(pNDM-MAR); IncFII(pkP91); Col440I	IncFIB(pQil); IncFII(K)	112
PR-6	512	***bla*KPC-3**; *bla*SHV-11; *bla*TEM-1	*oqx*A; *oqx*B; *aac*(6')-Ib-cr	*aac*(6')-Ib; *aac*(6')-Ib-cr; *aph*(3')-Ia; *aad*A2	-	*fos*A6	*oqx*A; *oqx*B; *sul*1; *dfr*A12	*mph*(A)	*oqx*A; *oqx*B; *cat*A1	*kpn*E; *kpn*F; *kpn*G	IncFIB(K); IncFII(K); IncFIB(pQil); ColRNAI; IncX3	IncFIB(pQil); IncFII(K)	113
PR-8	307	***bla*KPC-3**; *bla*CTX-M-15; *bla*SHV-28; *bla*TEM-1; *bla*OXA-10; *bla*CMY-16	*oqx*A; *oqx*B; *aac*(6')-Ib-cr	*aac*(6')-Ib-cr; *aac*(6')-Ib3; *aac*(3)-IIa; *aad*A1; *str*A; *aph*(3)-Ia; *str*B	*tet*(A)	*fos*A6	*oqx*A; *oqx*B; *sul*1; *sul*2; *dfr*A14	-	*oqx*A; *oqx*B; *flo*R; *cml*A5	*kpn*E; *kpn*F; *kpn*G	IncFIB(pQil); IncFII(K); IncC	IncFIB(pQil); IncFII(K)	113
PR-10	512	***bla*KPC-66**; *bla*TEM-1; *bla*SHV-11	*oqx*A; *oqx*B; *aac*(6')-Ib-cr	*aac*(6')-Ib-cr; *aac*A4; *aad*A2; *aph*(3')-Ia	-	*fosA5* (M29T)	*oqx*A; *oqx*B; *sul*1; *dfr*A12	*mph*(A)	*oqx*A; *oqx*B; *cat*A1	*kpn*E; *kpn*F; *kpn*G	IncFIB(pQil); IncFIB(K); IncFII(K); Col440I; IncX3	IncFIB(pQil); IncFII(K)	113
PR-11	307	***bla*KPC-3**; *bla*CTX-M-15; *bla*SHV-28; *bla*TEM-1; *bla*OXA-10; *bla*CMY-16	*oqx*A; *oqx*B; *aac*(6')-Ib-cr	*aac*(6')-Ib-cr; *aac*(6')-Ib3; *aac*(3)-IIa; *aad*A1; *str*A; *aph*(3)-Ia; *str*B	*tet*(A)	*fosA6* (Q130P)	*oqx*A; *oqx*B; *sul*1; *sul*2; *dfr*A14	-	*oqx*A; *oqx*B; *flo*R; *cml*A1	*kpn*E; *kpn*F	IncFIB(K); IncFIB(pQIL); IncFII(K); IncC	IncFIB(pQil); IncFII(K)	113
PR-15	2502	***bla*KPC-3**; *bla*SHV-1 *bla*TEM-1	*oqx*A; *oqx*B	*arm*A	-	*fosA6* (A86V, Q130P, Q139E)	*oqx*A; *oqx*B	*msr*(E); *mph*(E)	*oqx*A; *oqx*B	*kpn*E; *kpn*F; *ompk*37	IncFIB(K); IncFII(K); IncR; ColRNAI; Col440II	IncFIB(pQil); IncFII(K)	86
PR-17	711	***bla*KPC-3**; *bla*CTX-M-15; *bla*OXA-1; *bla*TEM-1; *bla*SHV-187	*oqx*A; *oqx*B; *aac*(6')-Ib-cr; *qnr*B1	*aac*(6')-Ib-cr; *aac*(3)-IIa; *str*A; *str*B	-	*fosA6* (Q130P, V135E)	*oqx*A; *oqx*B; *sul*2; *dfr*A14	-	*oqx*A; *oqx*B	*kpn*E; *kpn*F; *kpn*G; *ompk*37	IncFIB(pQil); IncFII(K); IncFIB(K); ColRNAI; Col440II; IncR	IncFII(K); IncFIB(K); IncR	92
PR-20	101	***bla*KPC-3**; *bla*SHV-1; *bla*TEM-1	*oqx*A; *oqx*B	*arm*A	-	*fos*A6	*oqx*A; *oqx*B; *sul*1; *dfr*A5	*mph*(E)	*oqx*A; *oqx*B; *cat*A1	*kpn*E; *kpn*F; *kpn*G; *ompk*37	IncFIB(pQil); IncFII(K); IncFIB(K); ColRNAI; Col440II	IncFIB(pQil); IncFII(K)	113
PR-24	512	***bla*KPC-3**; *bla*OXA-9; *bla*TEM-1; *bla*SHV-182	*oqx*A; *oqx*B; *aac*(6')-Ib-cr	*aac*(6')-Ib; *aac*(6')-Ib-cr; *aph*(3')-Ia; *aad*A2	-	*fosA5* (M29T, F137L)	*oqx*A; *oqx*B; *sul*1	-	*oqx*A; *oqx*B	*kpn*E; *kpn*F; *kpn*G	IncFIB(pQil); IncFII(K); ColRNAI	IncFIB(pQil); IncFII(K)	115

PR-33	512	***bla*$_{KPC-3}$; *bla*$_{SHV-11}$**	*oqx*A; *oqx*B; *aac*(6')-Ib-cr	*aac*(6')-Ib-cr	-	*fosA6* (Q130P, V135E)	*oqx*A; *oqx*B	-	*oqx*A; *oqx*B	*kpn*E; *kpn*F; *kpn*G	IncFIB(K); IncFII(K); ColRNAI; IncX3	IncFIB(K); IncFII(K)	163
FA-5	512	***bla*$_{KPC-3}$; *bla*$_{SHV-11}$**	*oqx*A; *oqx*B; *aac*(6')-Ib-cr	*aac*(6')-Ib; *aad*A2	-	*fosA6* (I91V, Q130P, D138E)	*oqx*A; *oqx*B; *sul*1	-	*oqx*A; *oqx*B	*kpn*F; *kpn*G	IncFII(K); IncFIB(K); ColRNAI	IncFIB(K); IncFII(K)	164
FA-15	307	***bla*$_{KPC-3}$; *bla*$_{CTX-M-15}$; *bla*$_{OXA-1}$; *bla*$_{TEM-1}$; *bla*$_{SHV-28}$**	*oqx*A; *oqx*B; *aac*(6')-Ib-cr; *qnr*B1	*aac*(6')-Ib-cr; *str*A; *str*B	-	*fos*A6	*oqx*A; *oqx*B; *sul*2; *dfr*A14	-	*oqx*A; *oqx*B	*kpn*E; *kpn*F; *kpn*G	IncFIB(pQil); IncFII(K); IncFIB(K)	IncFIB(pQil); IncFII(K)	103
FA-16	307	***bla*$_{KPC-3}$; *bla*$_{CTX-M-15}$; *bla*$_{OXA-1}$; *bla*$_{TEM-1}$; *bla*$_{SHV-28}$**	*oqx*A; *oqx*B; *aac*(6')-Ib-cr; *qnr*B1	*aac*(6')-Ib-cr; *aac*(3)-IIa; *str*A; *str*B	*tet*(A)	*fosA6* (Q130P)	*oqx*A; *oqx*B; *sul*2; *dfr*A14	-	*oqx*A; *oqx*B	*kpn*E; *kpn*F; *kpn*G	IncFIB(pQil); IncFII(K); IncFIB(K)	IncFIB(pQil); IncFII(K)	103
FA-17	307	***bla*$_{KPC-2}$; *bla*$_{CTX-M-15}$; *bla*$_{OXA-1}$; *bla*$_{TEM-1}$; *bla*$_{SHV-28}$**	*oqx*A; *oqx*B; *aac*(6')-Ib-cr; *qnr*B1	*aac*(6')-Ib-cr; *aac*(3)-IIa; *str*A; *str*B	*tet*(A)	*fosA6* (Q130P)	*oqx*A; *oqx*B; *sul*2; *dfr*A14	-	*oqx*A; *oqx*B	*kpn*E; *kpn*F; *kpn*G	IncFIB(pQil); IncFII(K); IncFIB(K)	IncFIB(pQil); IncFII(K)	114
FA-19	307	***bla*$_{KPC-2}$; *bla*$_{OXA-1}$; *bla*$_{TEM-171}$; *bla*$_{SHV-28}$**	*oqx*A; *oqx*B; *aac*(6')-Ib-cr	*aac*(3)-IIa; *aac*(6')-Ib-cr	-	*fosA6* (Q130P)	*oqx*A; *oqx*B; *dfr*A14	-	*oqx*A; *oqx*B; *cat*B3	*kpn*E; *kpn*F	IncFIB(pQil); IncFII(K); IncFIB(K)	IncFIB(pQil); IncFII(K); IncFIB(K)	265
FA-25	307	***bla*$_{KPC-2}$; *bla*$_{CTX-M-15}$; *bla*$_{OXA-1}$; *bla*$_{SHV-28}$**	*oqx*A; *oqx*B; *aac*(6')-Ib-cr; *qnr*B1	*aac*(6')-Ib-cr	-	*fosA6* (Q130P)	*oqx*A; *oqx*B; *dfr*A14	-	*oqx*A; *oqx*B	*kpn*E; *kpn*F; *kpn*G	IncFIB(K); IncFII(K)	-	46
PS-4	512	***bla*$_{KPC-3}$; *bla*$_{SHV-11}$; *bla*$_{TEM-1}$**	*oqx*A; *oqx*B	*aph*(3')-Ia; *aad*A2	-	*fosA6* (I91V, Q130P, D138E)	*oqx*A; *oqx*B; *sul*1; *dfr*A12	*mph*(A)	*oqx*A; *oqx*B; *cat*A1	*kpn*E; *kpn*F; *kpn*G	IncFIB(K); ColRNAI; IncR	IncR	76
PS-5	395	***bla*$_{KPC-3}$*; *bla*$_{CTX-M-15}$; *bla*$_{OXA-1}$; *bla*$_{TEM-1}$; *bla*$_{SHV-11}$**	*oqx*A; *oqx*B; *aac*(6')-Ib-cr; *qnr*S1	*aad*A1; *aad*B; *aac*(6')-Ib-cr	-	*fosA6* (Q130P, D138E)	*oqx*A; *oqx*B; *sul*1	-	*oqx*A; *oqx*B; *cat*A1; *cat*B3	*kpn*E; *kpn*F; *kpn*G	IncFIB(pQil); IncFIB(K); IncFII(K); IncFIB(pNDM-MAR); IncHI1B(pNDM-MAR)	IncFIB(pQil); IncFII(K)	103

*Table 6. Genetic features of KPC-Kp sequenced achieved with WGS analysis. *, two copies of the gene.*

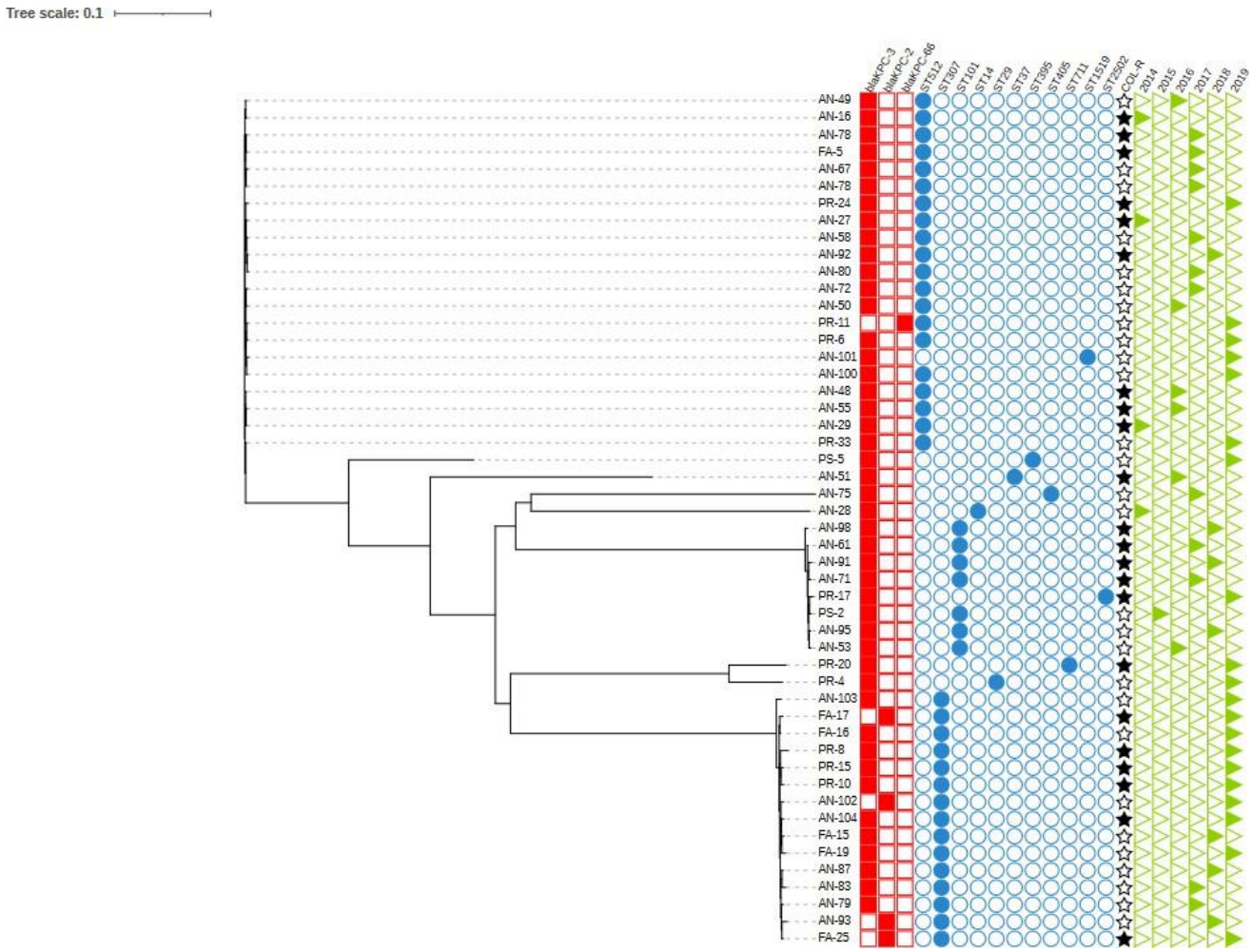

Figure 16. Phylogenetic tree and genetic characteristics of KPC-Kp sequenced.

3.2. OXA-48-Kp

Between December 2021 and June 2022 eight OXA-48-Kp (named from O-1 to O-8) were collected from different patients and in different wards at "Ospedali Riuniti" of Ancona. Among these, 6 were recovered from rectal swabs (75%), 1 from blood culture (12.5%) and the remaining one from urine culture (12.5%) [table 8].

3.2.1. Resistance phenotypes

All samples were resistant to carbapenems (ETP: MIC values > 2 mg/L; IMI: MIC values ≥ 8 mg/L; MER: MIC values of 16 mg/L), CIP (MIC values > 2 mg/L), TIG (MIC values ≥ 2 mg/L), and TMP-SXT (MIC values > 16 mg/L) and susceptible to AMK, COL, CZA, and FDC. Regarding ATM and CAZ, only two isolates (O-5 and O-6) showed susceptible phenotypes, with MIC values of 0.5 mg/L for the monobactam and 1 mg/L for the cephalosporin. For these two drugs, the resistance rate among the clones studied was 75%. MIC values were reported in table 8.

Sample	Date	Sources	MIC (mg/L)											PFGE
	(y/m)		AMK	CIP	TIG	TMP-SXT	FDC	COL	ATM	MER	ETP	CZA	CAZ	IMI	XbaI
O-1	2021/12	blood colture	8	>2	4	>16	0.5	2	>32	16	>2	1	>32	8	A1
O-2	2022/01	rectal swab	8	>2	4	>16	2	1	>32	16	>2	1	>32	8	A1
O-3	2022/01	rectal swab	8	>2	4	>16	0.5	1	>32	16	>2	1	>32	8	A1
O-4	2022/01	rectal swab	8	>2	4	>16	0.5	2	>32	16	>2	1	>32	8	A1
O-5	2022/04	rectal swab	2	>2	2	>16	<0.03	2	0.5	16	>2	0.5	1	16	A2
O-6	2022/04	rectal swab	1	>2	2	>16	<0.03	2	0.5	16	>2	0.5	1	8	A2
O-7	2022/05	rectal swab	4	>2	4	>16	0.5	2	>32	16	>2	1	>32	16	A2
O-8	2022/06	urine culture	8	>2	4	>16	1	2	>32	16	>2	1	>32	>32	A2

Table 8. OXA-48-Kp with date and source of collection, MIC values, and XbaI restriction profile. Red cells indicate MIC resistant values.

3.2.2. Genotyping

XbaI-PFGE pointed out two strictly related pulsotypes (each one represented by 4 isolates), differing for a single restriction band, reported in table 8. S1-PFGE revealed that all strains carried 2 different plasmids: 6 strains showed one element of ~ 250 kb and another of ~ 55 kb while the remaining two isolates (O-5 and O-6) presented a slightly different plasmid profile. More in detail, in both strains the smaller plasmid was ~ 45 kb long while only in O-6 the bigger one was of ~ 180 kb. WGS, conducted with Oxford Nanopore technology, assigned the ST395 to all isolates and confirmed the plasmid profile detected by S1-PFGE with an additional Col plasmid of 4 kb. bla_{OXA-48} gene was carried in a 7 kb transposon, located on an IncR plasmid of 57 kb in all isolates except for O-5 and O-6 in which the plasmid was 50 kb long, lacking a genetic element of ~ 8 kb. The IncR plasmid showed 99.93% Identity with a pRIVM plasmid of an OXA-48-Kp from a 2021 bacterial surveillance in the Netherlands (Accession number CP068905.1) [figure 17]. The IncR plasmids carried other resistance genes such as bla_{TEM-1B}, *tet*(A), *qnrS1*, *sul1*, and *dfrA1.* All isolates shared the same antibiotic resistance genes but O-5 and O-6 lacked $bla_{CTX-M-15}$, bla_{OXA-1}, and *aac*(6')-Ib-cr which were encoded on the 8 kb element missing in these two samples. The complete resistomes were listed in table 9.

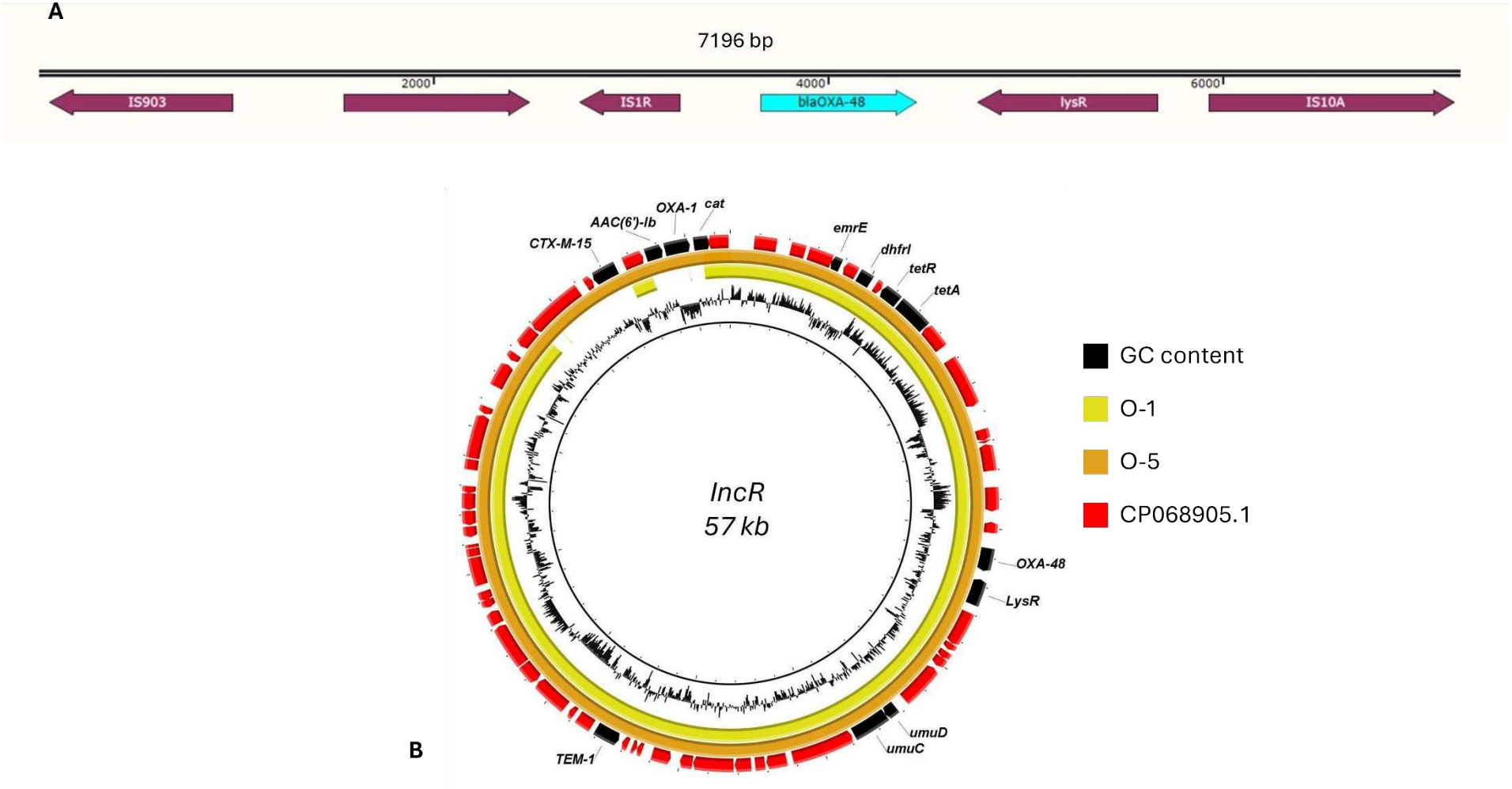

Figure 17. (A) OXA-48 transposon. lysR, lysine regulator; ORF without denomination, hypothetical protein. (B) Comparison of O-1 and O-5 IncR plasmids with CP0c8S05.1. Black ORFs represent antibiotic resistance genes.

Strain	ST	antibiotic resistance genes					efflux pump	plasmid incompatibility group	*bla*$_{OXA}$ carrying plasmid	
		beta-lactams	quinolones	aminoglycosides	folate	phenicols			incompatibility group	size (kb)
O-1	395	***bla*$_{OXA-48}$;** *bla*$_{TEM-1}$; *bla*$_{OXA-1}$; *bla*$_{SHV-11}$; *bla*$_{CTX-M-15}$	*oqx*A; *oqx*B; *qnrS*1	*aac*(6')-Ib-cr	*dfrA*1; *sul*1	*catB*3	*kpn*E; *kpn*F; *kpn*G	IncHI1B; IncR; Col4401II	IncR	57
O-2	395	***bla*$_{OXA-48}$;** *bla*$_{TEM-1}$; *bla*$_{OXA-1}$; *bla*$_{SHV-11}$; *bla*$_{CTX-M-15}$	*oqx*A; *oqx*B; *qnrS*1	*aac*(6')-Ib-cr	*dfrA*1; *sul*1	*catB*3	*kpn*E; *kpn*F; *kpn*G	IncHI1B; IncR; Col4401II	IncR	57
O-3	395	***bla*$_{OXA-48}$;** *bla*$_{TEM-1}$; *bla*$_{OXA-1}$; *bla*$_{SHV-11}$; *bla*$_{CTX-M-15}$	*oqx*A; *oqx*B; *qnrS*1	*aac*(6')-Ib-cr	*dfrA*1; *sul* 1	*catB*3	*kpn*E; *kpn*F; *kpn*G	IncHI1B; IncR; Col4401II	IncR	57
O-4	395	***bla*$_{OXA-48}$;** *bla*$_{TEM-1}$; *bla*$_{OXA-1}$; *bla*$_{SHV-11}$; *bla*$_{CTX-M-15}$	*oqx*A; *oqx*B; *qnrS*1	*aac*(6')-Ib-cr	*dfrA*1; *sul* 1	*catB*3	*kpn*E; *kpn*F; *kpn*G	IncHI1B; IncR; Col4401II	IncR	57
O-5	395	***bla*$_{OXA-48}$;** *bla*$_{TEM-1}$; *bla*$_{SHV-11}$;	*oqx*A; *oqx*B; *qnrS*1	-	*dfrA*1; *sul*1	*catB*3	*kpn*E; *kpn*F; *kpn*G	IncHI1B; IncR; Col4401II	IncR	50
O-6	395	***bla*$_{OXA-48}$;** *bla*$_{TEM-1}$; *bla*$_{SHV-11}$;	*oqx*A; *oqx*B; *qnrS*1	-	*dfrA*1; *sul*1	*catB*3	*kpn*E; *kpn*F; *kpn*G	IncHI1B; IncR; Col4401II	IncR	50
O-7	395	***bla*$_{OXA-48}$;** *bla*$_{TEM-1}$; *bla*$_{OXA-1}$; *bla*$_{SHV-11}$; *bla*$_{CTX-M-15}$	*oqx*A; *oqx*B; *qnrS*1	*aac*(6')-Ib-cr	*dfrA*1; *sul*1	*catB*3	*kpn*E; *kpn*F; *kpn*G	IncHI1B; IncR; Col4401II	IncR	57
O-8	395	***bla*$_{OXA-48}$;** *bla*$_{TEM-1}$; *bla*$_{OXA-1}$; *bla*$_{SHV-11}$; *bla*$_{CTX-M-15}$	*oqx*A; *oqx*B; *qnrS*1	*aac*(6')-Ib-cr	*dfrA*1; *sul*1	*catB*3	*kpn*E; *kpn*F; *kpn*G	IncHI1B; IncR; Col4401II	IncR	57

Table 9. Genetic features of OXA-48-Kp sequenced achieved with WGS analysis.

Phylogenetic analysis showed that samples were strictly related each other, even if O-8 exhibited an increased genetic distance from the rest of the group, as indicated by the longest tree branch. O-3 and O-4, instead, seemed to be the closest sample. These observations were confirmed by SNPs matrix: samples showed from a minimum of 14 to a maximum of 43 SNPs. In particular, the highest SNPs number were detected in O-8 (43 SNPs with both O-2 and O-7 isolates) while the lowest value featured between O-3 and O-4 [figure 18].

A

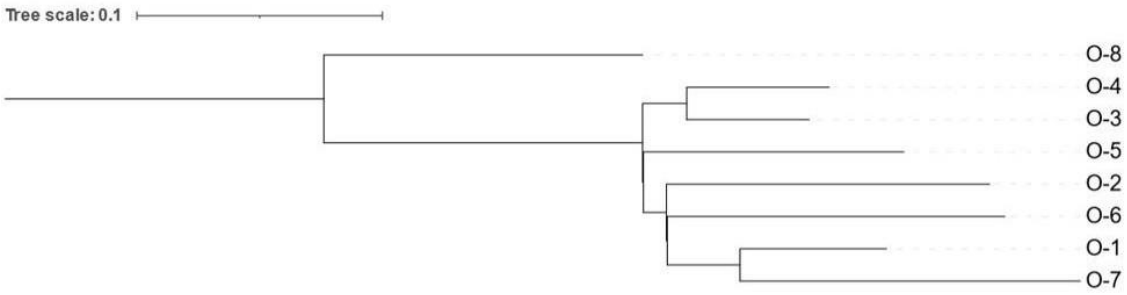

B

	O-2	O-3	O-4	O-5	O-6	O-7	O-8	O-1
O-2	0	22	26	28	33	34	43	27
O-3	22	0	14	22	27	30	31	23
O-4	26	14	0	24	25	26	35	21
O-5	28	22	24	0	29	30	39	25
O-6	33	27	25	29	0	35	42	24
O-7	34	30	26	30	35	0	43	23
O-8	43	31	35	39	42	43	0	38
O-1	27	23	21	25	24	23	38	0

Figure 18. (A) OXA-48-Kp phylogenetic tree. O-1 was used as reference. (B) OXA-48-Kp SNPs matrix. Orange cells, maximum SNPs number; green cells, minimum SNPs number.

3.3. NDM-Kp

A total of 17 NDM-Kp were isolated between November 2021 and September 2023 from 10 different patients at "Ospedali Riuniti" of Ancona. Strains belonging to different patients were named from N-1 to N-10 while NDM-Kp belonging to the same patient were tagged with letters in alphabetical order following dates of isolation [table 10]. The most frequent biological sample was rectal swab (47%) while other sources were urine samples (23.5%), urinary catheters (11.8%), blood cultures (11.8%), and catheter tip (5.9%).

3.3.1. Resistance phenotypes

All isolates showed resistance to CZA (MIC values > 32 mg/L), ETP (MIC values > 2 mg/L), and MER (MIC values > 32 mg/L). Different situations were highlighted for other antibiotics tested: 15 samples were resistant to IMI (88.2%), 14 to ATM (82.3%), only 6 to FDC (35.3%) and none showed resistance to COL (0%). MIC values were reported in table 10.

Sample	Patient	Date (y/m)	Sources	MIC (mg/L)							PFGE
				FDC	COL	ATM	MER	ETP	CZA	IMI	XbaI
N-1	1	2021/11	rectal swab	1	2	>32	>32	>2	>32	0.5	A
N-2	2	2022/04	UC	2	1	>32	>32	>2	>32	16	B
N-3A	3	2022/05	blood	1	2	>32	>32	>2	>32	16	C
N-3B	3	2022/05	blood	4	2	>32	>32	>2	>32	16	C
N-4	4	2022/05	urine culture	4	2	>32	>32	>2	>32	32	D
N-5A	5	2022/06	rectal swab	2	2	>32	>32	>2	>32	32	D
N-6	6	2022/06	rectal swab	4	1	>32	>32	>2	>32	32	D
N-7A	7	2022/06	rectal swab	0.5	2	>32	>32	>2	>32	16	D
N-7B	7	2022/06	UC	8	1	0.25	>32	>2	>32	32	D
N-8	8	2022/07	rectal swab	1	2	>32	>32	>2	>32	>32	E
N-5B	5	2022/08	rectal swab	16	1	>32	>32	>2	>32	32	D
N-9	9	2022/10	rectal swab	>32	0.5	>32	>32	>2	>32	>32	F
N-7C	7	2023/07	urine culture	1	2	0.5	>32	>2	>32	>32	G
N-7D	7	2023/07	CP	0.5	2	>32	>32	>2	>32	0.5	G
N-7E	7	2023/08	urine culture	0.5	1	2	>32	>2	>32	32	D
N-10A	10	2023/08	rectal swab	1	1	>32	>32	>2	>32	>32	H
N-10B	10	2023/09	urine culture	1	2	>32	>32	>2	>32	>32	H

Table 10. NDM-Kp with date and source of collection, MIC values, and XbaI restriction profile. UC, urinary catheter; CP, catheter tip. Cells coloured in red are for MIC resistant values.

3.3.2. Genotyping

XbaI-PFGE assays highlighted 8 different pulsotypes indicated in table 10 as letters from A to H. Pulsotype D was the most represented, counting 7 out of 17 isolates, and occurred from May 2022 to August 2023. Strains collected from the same patient belonged to the same pulsotype except for patient 7, which had 5 different isolations during 1 year frame. In fact, its first two isolates (N-7A and N-7B) were classified as D pulsotype, the third (N-7C) and fourth (N-7D) were G and the last one (N-7E) was D again. One sample for each patient and 3 different strains from patient N-7 (for a total of 12 samples) were further investigated, subjecting them to S1 digestion and WGS analysis with both Nanopore and Illumina technologies. S1 digestion highlighted a heterogeneous plasmid profile, differing in number (ranging from zero to three plasmids for strains) and in size (from ~ 43 to ~ 340 kb). This plasmid profile was confirmed by WGS analysis, which pointed out that bla_{NDM} gene was plasmid-encoded in 10 out of 12 strains. Most of these plasmids (40%) were characterized by only IncFIB replicon (N-4, N-5A, N-6, and N-7B) or IncFIB together with IncHI1B (20%) (N-1, and N-3A), two (N-2, and N-8) were recombinant IncFIA-repB plasmids (20%), one (N-9) was a recombinant IncFII-repB plasmid (10%) and the last one (N-10A) was a IncFII plasmid (10%). These mobile elements showed different dimensions, ranging from 79 to 374 kb [table 11]. N-1 and N-3A plasmids shared 99% identity with a bla_{NDM-5} *K. pneumoniae* (ON-1) carrying plasmid that will be described in

the next paragraph. N-2 and N-8, instead, showed 100% of both coverage and identity with a *K. pneumoniae* plasmid deposited on NCBI (Accession number CP106888.1). N-9 plasmid was 104 kb long and exhibited 100% identity and 93% coverage with a ST147 *K. pneumoniae* plasmid P1 (Accession number OW967816.1) not coding for bla_{NDM} gene. N-4, N-5A, N-6, and N-7B showed slightly identical NDM-carrying plasmids which shared 99.99% identity but only 66% of coverage with a 125.7 kb long plasmid of a *K. pneumoniae* non-coding for bla_{NDM} (Accession number CP135509.1). N-10A plasmid, lastly, had 100% coverage and 99.95% identity with the ST147 *K. pneumoniae* pCC1410-1 plasmid coding for bla_{NDM-5} (Accession number KT25788.1) [figure 20]. MLST analysis conferred 5 different STs to the 12 isolates: ST11, ST147, ST307, ST395, and ST437. More in detail, ST307 and ST437 counted one strain each (8.3%) (N-3A, and N-10A respectively) while ST11 and ST147 two (16.6% each) (N-2 and N-8, and N-1 and N-9 respectively). The remaining 6 isolates belonged to ST395 (50%), 3 of which were isolated from patient 7. Two bla_{NDM} allelic variants were detected among samples: bla_{NDM-1} featured STs 11, 147, and 307 (5 out of 12 isolates, corresponding to 41.7%) while bla_{NDM-5} characterized STs 395 and 437 (7 out of 12 isolates, amounting to 58.3% incidence). bla_{NDM} genes were always located on Tn*125-like* transposons, (chromosomally integrated on N-7C and N-7E) that showed differences among samples except for the bleomycin resistance gene *ble* and the phosphoribosyl anthranilate isomerase gene *trpF* which were always positioned next to bla_{NDM} [figure 19]. ST11 transposons were flanked by ISAba3000 from one side and Tn*3* transposase from the other while ST395 ones were delimited by ISAba125 and ISCR insertion sequences. ST147 samples did not share the same transposon structure: N-9 element was flanked by two ISAba3000 while N-1 transposon by IS6 from one side and ISAba125 on the other side. N-3A transposon was the same as N-1 while N-10A showed two tandem copies of an ISCR/IS6 transposon. Regarding resistance genes other than carbapenemases, all samples coded for antibiotic resistance genes to aminoglycosides, quinolones, folate, and fosfomycin while only ST307 exhibited *tet*A gene, for tetracycline resistance. Strains belonging to STs 147, 307, and 437 showed resistance genes for rifamycin and macrolides, excluding N-1 which did not carry any macrolides resistance gene. Phenicol resistance genes were not detected in STs 147, and 437 while regarding beta-lactams genes a heterogenous situation was depicted. bla_{TEM-1} was present in all samples but N-9 (ST147) and N-10A (ST437), while $bla_{CTX-M-15}$ was missing in 3 out of 6 ST395 samples (all belonging to patient N-7). In all these isolates no bla_{OXA} allelic variants were detected, while bla_{OXA-1} was present in the remaining sample except for N-1 featured by bla_{OXA-9}. However, all samples were characterized by bla_{SHV} genes whose variants were ST-related: bla_{SHV-11} featured STs 147, 395, and

437 (75%), *bla*$_{SHV-12}$ was present in ST11 samples (16.7%), and *bla*$_{SHV-28}$ was showed by ST307 (8.3%). Complete resistomes were reported in table 11.

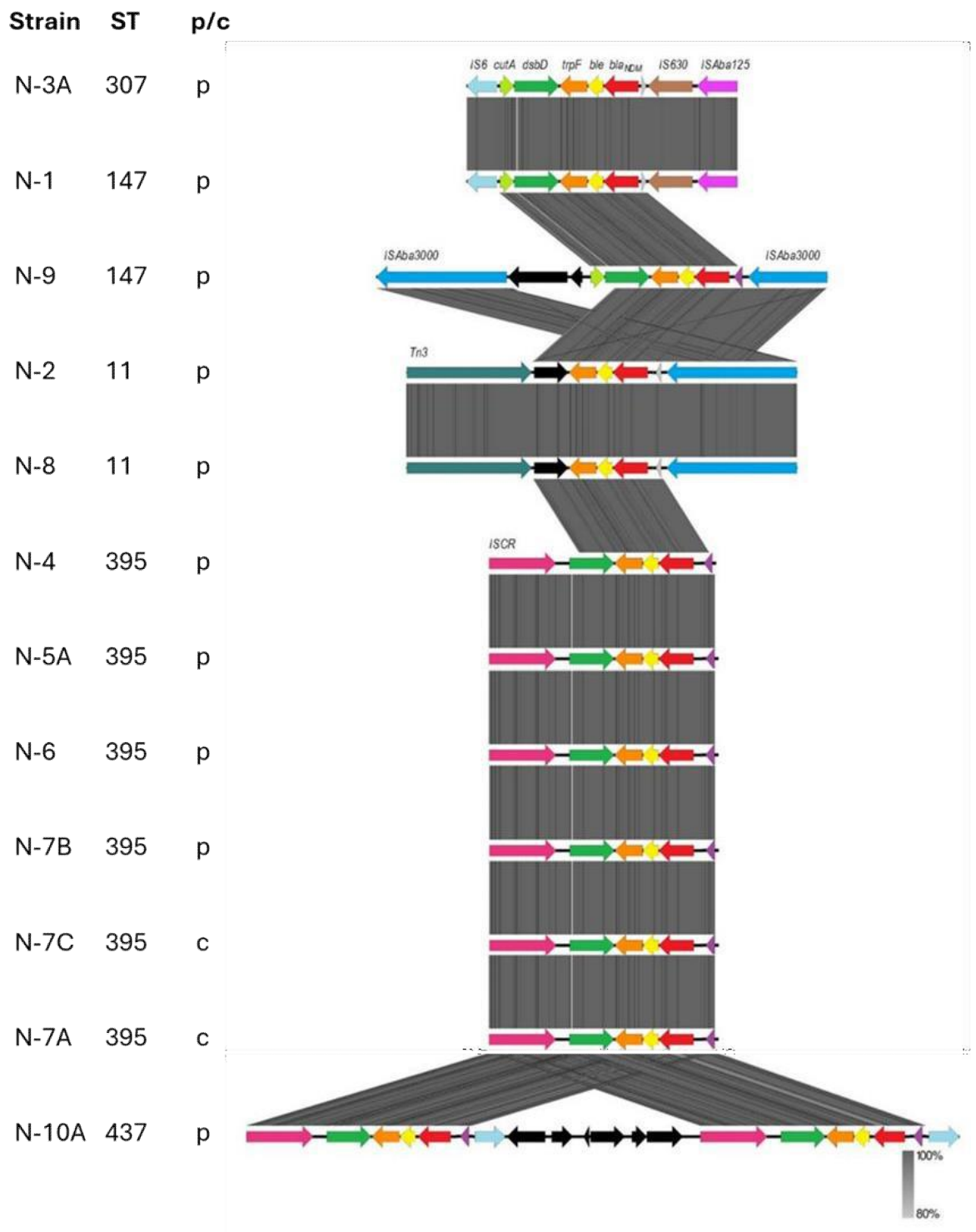

Figure 19. NDM-Kp transposons. p, plasmid location; c, chromosomal location; dsbD, cytochrome c-type biogenesis protein; cutA, periplasmic divalent cation tolerance protein.

Strain	ST	antibiotic resistance genes										efflux pump	plasmid incompatibility group	*bla*NDM plasmid	
		beta-lactams	bleomycin	quinolones	aminoglycosides	tetracycline	macrolide	fosfomycin	folate	phenicols	rifamicin			incompatibility group	size (kb)
N-1	147	***bla*NDM-1**; *bla*TEM-1; *bla*CTX-M-15; *bla*OXA-9; *bla*SHV-11	*ble*MBL	*oqx*A; *oqx*B; *qnrB*1	*aac*(6')-Ib; *aac*(6')-Ib-cr; *armA*; *aph* 3')-VI; *aadA* 1	-	-	*fosA6 (Q130P)*	*sul*1; *sul*2	-	*arr*3	*kpn*E; *kpn*F; *kpn*G; *ompk*37	IncFIB; IncH1B; IncR	IncFIB; IncH1B	374
N-2	11	***bla*NDM-1**; *bla*TEM-1; *bla*CTX-M-15; *bla*OXA-1; *bla*SHV-12	*ble*MBL	*oqx*A; *oqx*B; *qnrB*19	*aac*(6')-Ib; *aac*(3)-IIa *aac*(6')-Ib-cr; *aadB*; *aph* (3')-Ia;	-	-	fosA6 (I91V, Q130P, D138E)	*dfrA*14	*catB*3	-	*kpn*E; *kpn*F; *kpn*G	IncFIA; repB; IncL; ColRNAI	IncFIA; repB	79
N-3A	307	***bla*NDM-1**; *bla*TEM-1; *bla*CTX-M-15; *bla*OXA-1; *bla*SHV-28	*ble*MBL	*oqx*A; *oqx*B; *qnrS*1; *qnrB*1	*aac(*6')-Ib-cr; *strA*; *strB*; *aph(*3')-VI; *rmtF*	*tet*A	*msr*E; *mph*E	*fosA 6 (Q130P)*	*sul*1; *sul*2; *dfrA*5; *dfrA*14	*catB*3	*arr*2	*kpn*E; *kpn*F; *kpn*G	IncFIB; IncH1B; IncFII	IncFIB; IncH1B	360
N-4	395	***bla*NDM-5**; *bla*TEM-1; *bla*CTX-M-15; *bla*OXA-1; *bla*SHV-11	*ble*MBL	*oqx*A; *oqx*B; *qnrB*1	*aac* 6')-Ib-cr; *aadA*2; *rmtB*; *aac*(3)-IId	-	-	*fosA6 (Q130P, D138E)*	*sul*1; *dfrA*12	*catA*1	-	*kpn*E; *kpn*F; *kpn*G	IncFIB	IncFIB	95
N-5A	395	***bla*NDM-5**; *bla*TEM-1; *bla*CTX-M-15; *bla*OXA-1; *bla*SHV-11	*ble*MBL	*oqx*A; *oqx*B; *qnrB*1	*aac*(6')-Ib-cr; *aadA*2; *rmtB*; *aac*(3)-IId	-	-	*fos6 (Q130P, D138E)*	*sul*1; *dfrA*12	*catB*3	-	*kpn*E; *kpn*F	IncFIB	IncFIB	108
N-6	395	***bla*NDM-5**; *bla*TEM-1; *bla*CTX-M-15; *bla*OXA-1; *bla*SHV-11	*ble*MBL	*oqx*A; *oqx*B; *qnrB*1	*aac*(6')-Ib-cr; *aadA*2; *rmtB*; *aac*(3)-IId	-	-	*fosA6 (Q130P, D138E)*	*sul*1; *dfrA*12	*catB*3	-	*kpn*E; *kpn*F; *kpn*G	IncFIB	IncFIB	108
N-7B	395	***bla*NDM-5**; *bla*TEM-1; *bla*SHV-11	*ble*MBL	*oqx*A; *oqx*B	*aadA*2; *aac*(3)-IId	-	-	*fosA6 (Q130P, D138E)*	*sul*1; *dfrA*12	*catA*1	-	*kpn*E; *kpn*F; *kpn*G	IncFIB	IncFIB	108
N-8	11	***bla*NDM-1**; *bla*TEM-1; *bla*CTX-M-15; *bla*OXA-1; *bla*SHV-12	*ble*MBL	*oqx*A; *oqx*B; *qnrB*19	*aac*(6')-Ib; *aac*(3)-IIa *aac*(6')-Ib-cr; *aadB*; *aph*(3')-Ia;	-	-	*fosA*6 (I91V, Q130P, D138E)	*dfrA*14	*catB*3	-	*kpn*E; *kpn*F; *kpn*G	IncFIA; repB; IncL; ColRNAI	IncFIA; repB	79
N-9	147	***bla*NDM-1**; *bla*CTX-M-15; *bla*SHV-11	*ble*MBL	*oqx*A; *oqx*B; *qnrB*1	*strA; strB*	-	*mph*A	*fosA6 (Q130P, D138E)*	*sul*1; *dfrA*14	-	*arr*2	*kpn*E; *kpn*F; *kpn*G; *ompk*37	IncFII; repB; IncR	IncFII; repB	104
N-7C	395	***bla*NDM-5**; *bla*TEM-1; *bla*SHV-11	*ble*MBL	*oqx*A; *oqx*B; *qnrB*1	*aadA2*; *aac*(3)-IId	-	-	*fosA6 (Q130P, D138E)*	*sul*1; *dfrA*12	*catA*1	-	*kpnE*; *kpn*F; *kpn*G	-	-	-
N-7E	395	***bla*NDM-5**; *bla*TEM-1; *bla*SHV-11	*ble*MBL	*oqx*A; *oqx*B; *qnrB*1	*aadA*2; *rmt*B	-	-	*fosA6 (Q130P, D138E)*	*sul*1; *dfrA*12	*catB*3	-	*kpn*E; *kpn*F; *kpn*G	-	-	-
N-10A	437	***bla*NDM-5**; *bla*CTX-M-15; *bla*SHV-11	*ble*MBL	*oqx*A; *oqx*B;	*aadA*2; *rmt*F	-	*erm*B	*fosA6* (I91V, Q130P, D138E)	*sul*1; *dfrA*12	-	*arr*2	*kpn*E; *kpn*F; *kpn*G	IncFIB; IncFII; IncR; Col	IncFII	84

Table 11. Genetic features of NDM-Kp sequenced achieved with WGS analysis.

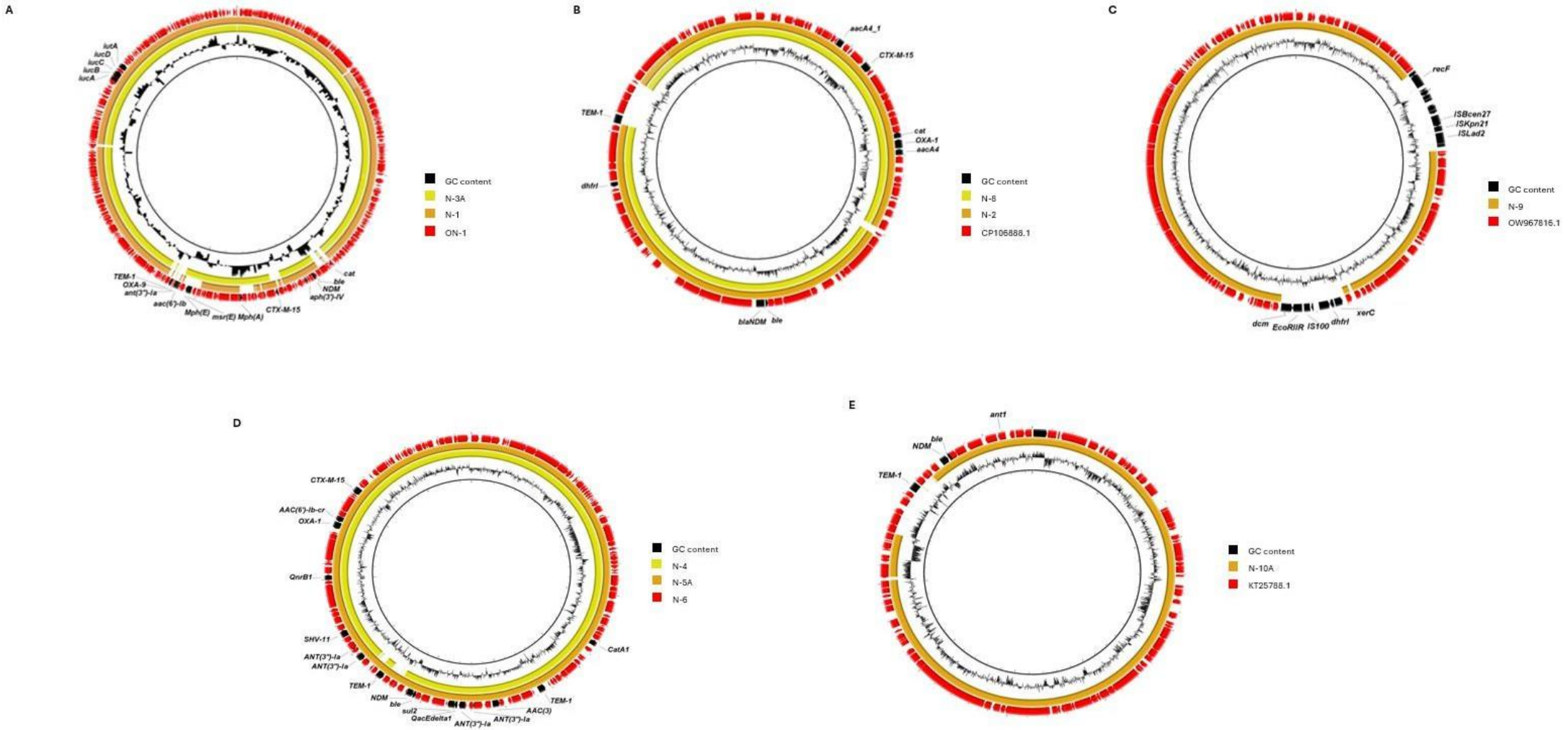

Figure 20. (A) Comparison of IncFIB/IncH1IB plasmids with those of a OXA-48-NDM-Kp of this study. Black arrows, antibiotic resistance genes. (B) Comparison of ST11 plasmids with the best match on NCBI. Black arrows, antibiotic resistance genes. (C) Comparison of N-9 plasmid with the best match on NCBI. Black arrows, ORF missing in our plasmid. (D) Comparison of ST395 plasmids. Black arrows, antibiotic resistance genes. (E) Comparison of N-10A with the best match on NCBI. Black arrows, antibiotic resistance genes.

Phylogenetic tree of the NDM-Kp sequenced showed the presence of branches with different lengths, of which the shorter ones linked strains belonging to the same ST [figure 21]. These observations were confirmed by SNPs matrix which showed that N-3A was the most different sample, with a minimum of 18,120 SNPs with N-1 and reaching a maximum of 19,809 SNPs with sample N-10A. The two ST11 samples, indeed, were close to each other, showing only 8 SNPs, while among ST147 slightly higher differences (159 SNPs) were highlighted. A heterogeneous situation was detected among ST395 isolates, which differed from a minimum of 2 SNPs (between N-4 and N-6) to a maximum of 266 SNPs (between N-7B and N-7C), even if they made up a well-defined cluster. The closest isolates to N-10A (ST437) were ST11 ones, with ~6,230 SNPs, while the farthest was ST307 sample, with 19,809 SNPs.

A

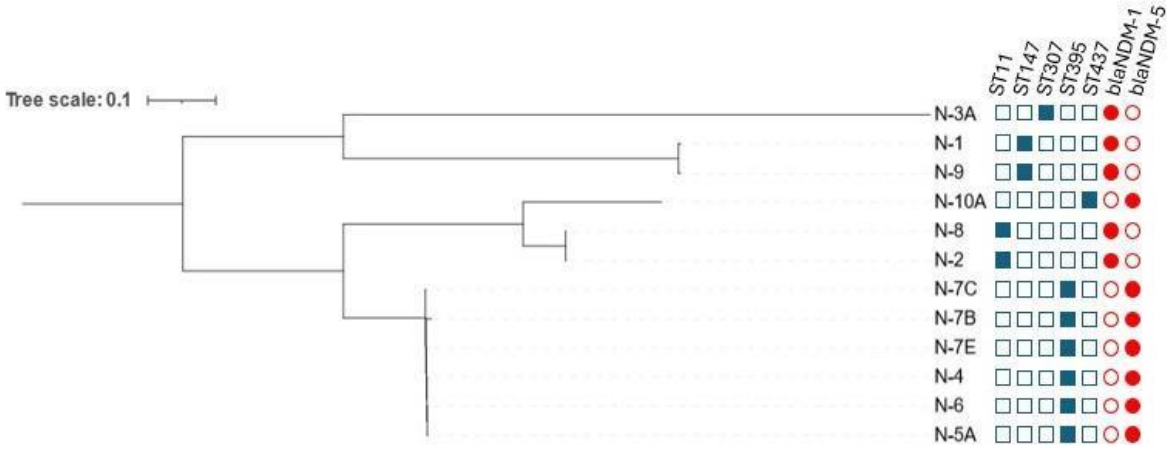

B

	N-2	N-3A	N-4	N-5A	N-6	N-7B	N-8	N-9	N-7C	N-7E	N-10A	N-1
N-2	0	19775	9466	9470	9468	9686	8	18455	9464	9466	6233	18464
N-3A	19775	0	19116	19120	19116	19112	19773	18121	19122	19116	19809	18120
N-4	9466	19116	0	6	2	252	9466	15878	64	10	11775	15887
N-5A	9470	19120	6	0	4	256	9468	15882	68	14	11779	15891
N-6	9468	19116	2	4	0	252	9466	15878	64	10	11775	15887
N-7B	9686	19112	252	256	252	0	9684	15696	266	250	11975	15705
N-8	8	19773	9466	9468	9466	9684	0	18453	9462	9464	6231	18462
N-9	18455	18121	15878	15882	15878	15696	18453	0	15864	15876	18652	159
N-7C	9464	19122	64	68	64	266	9462	15864	0	58	11751	15871
N-7E	9466	19116	10	14	10	250	9464	15876	58	0	11775	15885
N-10A	6233	19809	11775	11779	11775	11975	6231	18652	11751	11775	0	18661
N-1	18464	18120	15887	15891	15887	15705	18462	159	15871	15885	18661	0

Figure 21. (A) Phylogenetic tree and genetic characteristics of NDM-Kp sequenced. Tree was built using N-1 as reference. (B) SNPs matrix. Green cells, minimum SNPs number; orange cells, maximum SNPs number.

3.4. OXA-48-NDM-Kp

A total of 38 *K. pneumoniae* coding for both OXA-48 and NDM carbapenemases were collected during one year frame, between September 2022 and September 2023. Among these, 36 samples (indicated from ON-1 to ON-36) were isolated at "Ospedali Riuniti" of Ancona while the remaining two isolates belonged to patients recovered at Jesi (ON-J) and Civitanova Marche (ON-C) hospitals. Samples were collected from different sources, with rectal swabs and urine culture as main matrices, counting 16 (42.1%) and 13 (34.2%) isolates respectively [table 12].

3.4.1. Resistance phenotypes

A totally resistant phenotype regarding all the antibiotics tested was shown in 13 out of 38 samples (34.2%). Of the 25 remaining isolates, 2 were susceptible to colistin, 15 to cefidercol, and 8 to both these antibiotics. The resistance rates to these drugs stood at 73.6% (28 out of 38 samples) and 39.5% (15 out of 38 samples) respectively. Colistin susceptibility was detected among clones harvested between May and June 2023 and during the last month of study while regarding cefiderocol the susceptibility was a more diffuse phenomenon. MIC values for all the antibiotics tested were reported in table 12.

3.4.2. Genotyping

XbaI PFGE highlighted two distinct restriction profiles, indicated as A and B, each one with one strictly related pulsotype named A1 and B1 respectively [table 12]. Group A counted 18 samples (47.4%) and was the unique pulsotype detected until March 2023. Moreover, the only A1 sample (2.6%) harvested in January 2023 belonged to the Jesi patient. Group B, instead, counted 16 samples (42.1%) that totally replaced the A pulsotype from March to May and from August to September 2023. The strictly related B1 group, counting 3 samples (7.9%), featured only in August 2023. One sample for each month of the study period and almost one sample for each pulsotype highlighted every month, amounting to a total of 17 samples, was subjected to WGS analysis with a hybrid method.

Sample	Date (y/m)	Sources	MIC (mg/L)									PFGE
			FDC	COL	ATM	MER	ETP	CZA	IMI	CN	AMK	XbaI
ON-1	2022/09	urine culture	16	32	>32	>32	>2	>32	>32	>32	>32	A
ON-2	2022/09	BA	16	16	>32	>32	>2	>32	>32	>32	>32	A
ON-3	2022/09	BA	>32	>32	>32	>32	>2	>32	>32	>32	>32	A
ON-4	2022/10	rectal swab	2	32	>32	>32	>2	>32	>32	>32	>32	A
ON-5	2022/11	rectal swab	4	32	>32	>32	>2	>32	>32	>32	>32	A
ON-6	2022/11	rectal swab	1	>32	>32	>32	>2	>32	>32	>32	>32	A
ON-7	2022/11	rectal swab	1	32	>32	>32	>2	>32	>32	>32	>32	A
ON-8	2022/12	urine culture	8	8	>32	>32	>2	>32	>32	>32	>32	A
ON-J	2023/01	blood	2	>32	>32	>32	>2	>32	>32	>32	>32	A1
ON-9	2023/01	urine culture	4	32	>32	>32	>2	>32	>32	>32	>32	A
ON-C	2023/02	BAL	8	>32	>32	>32	>2	>32	>32	>32	>32	A
ON-10	2023/02	rectal swab	1	16	>32	>32	>2	>32	>32	>32	>32	A
ON-11	2023/03	BA	0.5	32	>32	>32	>2	>32	>32	>32	>32	A
ON-12	2023/03	rectal swab	1	32	>32	>32	>2	>32	>32	>32	>32	B
ON-13	2023/03	urine culture	>32	32	>32	>32	>2	>32	>32	>32	>32	B
ON-14	2023/04	urine culture	>32	32	>32	>32	>2	>32	>32	>32	>32	B
ON-15	2023/04	urine culture	>32	32	>32	>32	>2	>32	>32	>32	>32	B
ON-16	2023/04	urine culture	>32	32	>32	>32	>2	>32	>32	>32	>32	B
ON-17	2023/04	urine culture	>32	32	>32	>32	>2	>32	>32	>32	>32	B
ON-18	2023/04	rectal swab	>32	32	>32	>32	>2	>32	>32	>32	>32	B
ON-19	2023/05	rectal swab	2	16	>32	>32	>2	>32	>32	>32	>32	B
ON-20	2023/05	UC	2	2	>32	>32	>2	>32	>32	>32	>32	B
ON-21	2023/06	rectal swab	1	1	>32	>32	>2	>32	>32	>32	>32	A
ON-22	2023/06	urine culture	0.5	1	>32	>32	>2	>32	>32	>32	>32	B
ON-23	2023/06	urine culture	4	1	>32	>32	>2	>32	>32	>32	>32	B
ON-24	2023/06	urine culture	2	1	>32	>32	>2	>32	>32	>32	>32	B
ON-25	2023/06	urine culture	2	2	>32	>32	>2	>32	>32	>32	>32	A
ON-26	2023/06	rectal swab	1	0.5	>32	>32	>2	>32	>32	>32	>32	A
ON-27	2023/07	rectal swab	1	8	>32	>32	>2	>32	>32	>32	>32	A
ON-28	2023/07	rectal swab	1	>32	>32	>32	>2	>32	>32	>32	>32	A
ON-29	2023/07	rectal swab	2	>32	>32	>32	>2	>32	>32	>32	>32	A
ON-30	2023/08	rectal swab	1	>32	>32	>32	>2	>32	>32	>32	>32	B1
ON-31	2023/08	rectal swab	1	>32	>32	>32	>2	>32	>32	>32	>32	B1
ON-32	2023/08	wound	1	4	>32	>32	>2	>32	>32	>32	>32	B
ON-33	2023/08	UC	1	>32	>32	>32	>2	>32	>32	>32	>32	B1
ON-34	2023/09	blood	2	2	>32	>32	>2	>32	>32	>32	>32	B
ON-35	2023/09	urine culture	2	1	>32	>32	>2	>32	>32	>32	>32	B
ON-36	2023/09	rectal swab	>32	1	>32	>32	>2	>32	>32	>32	>32	B

Table 12. OXA-NDM-Kp with date and source of collection, MIC values, and XbaI restriction profile. BA, bronco aspirate; BAL, broncho-alveolar lavage; UC, urinary catheter. Cells coloured in red are for MIC resistant values.

The MLST scheme assigned the ST383 to all isolates and WGS confirmed the presence of both *bla*$_{OXA-48}$ and *bla*$_{NDM-5}$ allelic variants on conserved transposons. *bla*$_{OXA-48}$ gene was always located on a 5.7 kb long mobile element flanked by two IS10A insertion sequences. This element was located on an IncL plasmid of 67 kb, highly conserved in all samples and showing 100% identity with the ST383 OXA-NDM-Kp plasmid of a Qatar study (accession number CP091815.1). *bla*$_{NDM-5}$ gene, instead, was always next to the bleomycin resistance coding gene *ble* and was localized on a 10 kb mobile element flanked by IS110A by one side and ISAba125 by the other. This element was plasmid located on 10 out of 17 samples (58.8%) and chromosomally encoded on the remaining 7 isolates (41.2%). In all samples also a recombinant IncFIB-IncHI1B plasmid was featured but it was not completely conserved. In fact, in the 10 isolates characterized by plasmid localized *bla*$_{NDM-5}$ the IncFIB-IncHI1B element was 367 kb long and showed 99.9% Identity with another Kp plasmid of the same Qatar study previously mentioned (Accession number CP091814.1) [figure 22]. Among the remaining 7 samples, this plasmid was 331 kb long in 5 strains and 245 kb long in the other 2. The 331 kb plasmid lacked a region of 38.5 kb (indicated as sequence A) flanked by two copies of IS26, which included the *bla*$_{NDM-5}$ transposon. In addition to sequence A, in the 245 kb plasmid other 89.2 kb (sequence B), flanked by IS6 from one side and IS1D from the other, were missing [figure 23]. Sequence A was chromosomally encoded in all 7 samples while sequence B was not present in the 2 isolates with the 245 kb plasmid. In these 2 samples, instead, antibiotic resistance genes such as *aac* (6')-Ib, *bla*$_{OXA-9}$, and *bla*$_{TEM-1}$ were not present, since they were coded in sequence B. The complete resistome of the samples sequenced was reported in table 13.

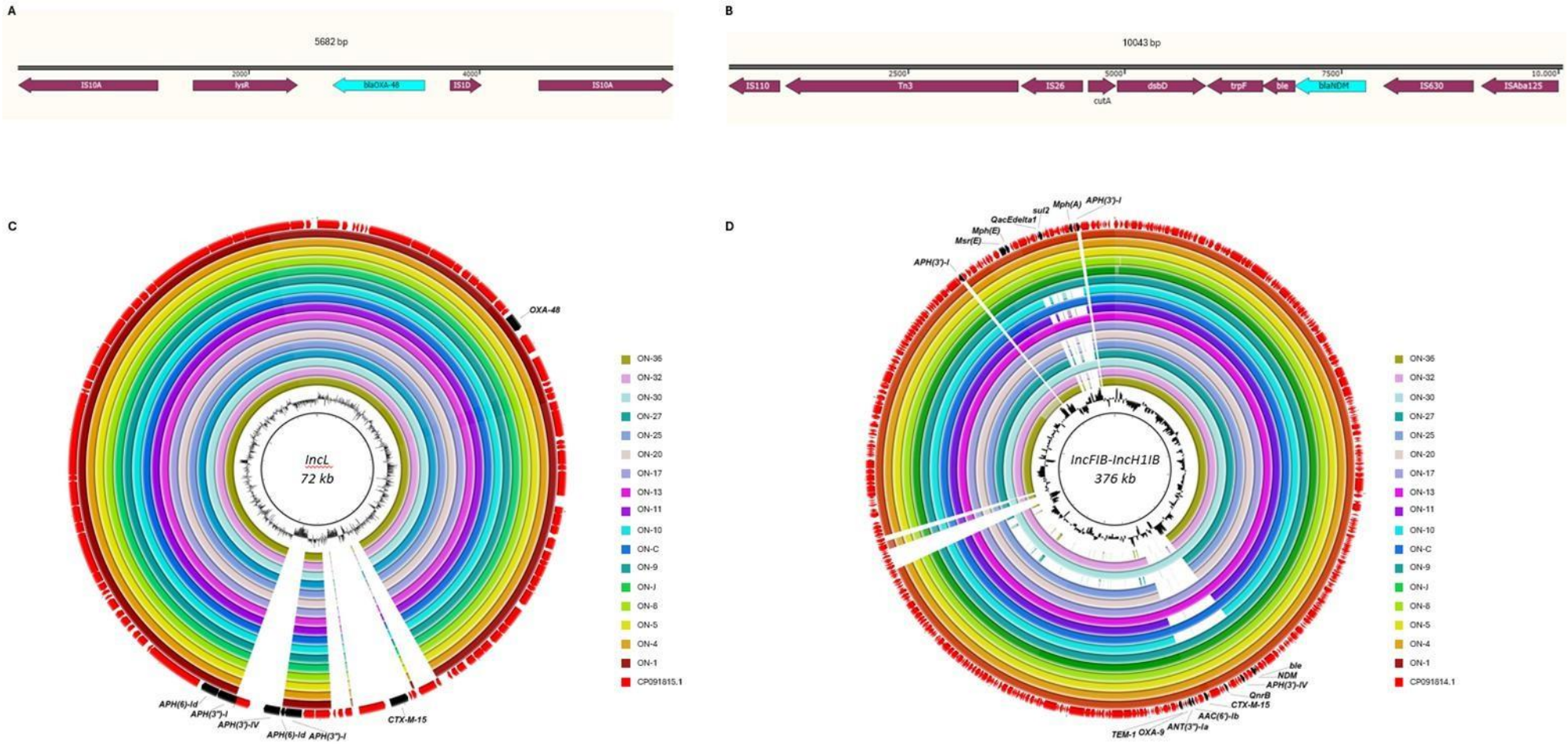

Figure 22. (A) OXA-48-Kp transposon. (B) NDM-Kp transposon. (C) Comparison of IncL plasmids with CP091815.1. Black arrows, antibiotic resistance genes. (D) Comparison of IncFIB-IncH1IB plasmids with CP091814.1. Black arrows, antibiotic resistance genes.

A

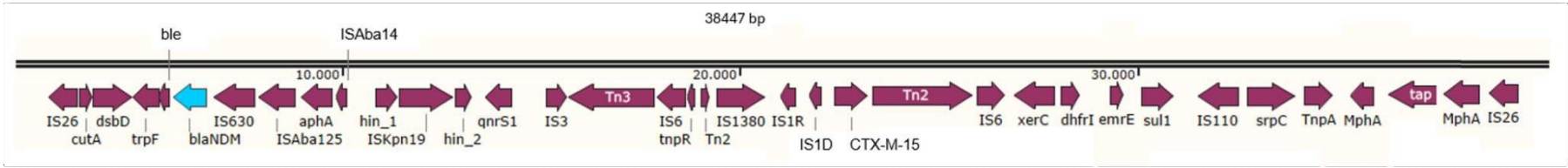

B

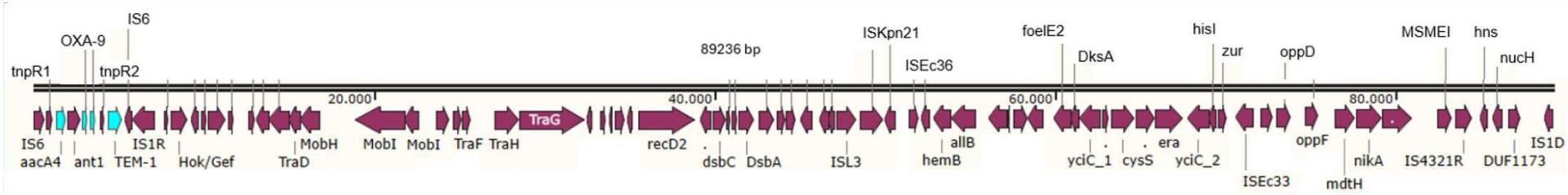

Figure 23. (A) Representation of sequence A. Cyan ORF, bla_{NDM} gene. (B) Representation of sequence B. Cyan ORFs, antibiotic resistance genes missing in samples with 245 kb NDM plasmid.

Strain	ST	antibiotic resistance genes									efflux pumps	bla_{NDM} carrying plasmid		bla_{OXA} carrying plasmid	
		beta-lactams	bleomycin	quinolones	aminoglycosides	tetracyclines	macrolides	fosfomycin	folate	phenicols		incompatibility group	size (kb)	incompatibility group	size (kb)
ON-1	383	**bla_{NDM-5}; bla_{OXA-48};** $bla_{CTX-M-15}$; bla_{TEM-1}; bla_{SHV-1}; $bla_{\Delta OXA-9}$	*ble*$_{MBL}$	*oqx*A; *oqx*B; *qnr*S1	*aac*(6')-Ib; *aac(*6')-Ib-cr; *str*A; *str*B; *arm*A; *aad*A1; *aph*(3')-VI	*tet*A	*mph*A; *mph*E; *mrs*E	*fos*A6 (Q130P, Q139E)	*oqx*A; *oqx*B; *sul*1; *sul*2; *dfr*A5	*cat*A1	*kpn*E; *kpn*F; *kpn*G; *ompk*37	IncFIB; IncHI1B	366	IncL	67
ON-4	383	**bla_{NDM-5}; bla_{OXA-48};** $bla_{CTX-M-15}$; bla_{TEM-1}; bla_{SHV-1}; $bla_{\Delta OXA-9}$	*ble*$_{MBL}$	*oqx*A; *oqx*B; *qnr*S1	*aac*(6')-Ib; *aac(*6')-Ib-cr; *str*A; *str*B; *arm*A; *aad*A1; *aph*(3')-VI	*tet*A	*mph*A; *mph*E; *mrs*E	*fos*A6 (Q130P, Q139E)	*oqx*A; *oqx*B; *sul*1; *sul*2; *dfr*A5	*cat*A1	*kpn*E; *kpn*F; *kpn*G; *ompk*37	IncFIB; IncHI1B	366	IncL	67
ON-5	383	**bla_{NDM-5}; bla_{OXA-48};** $bla_{CTX-M-15}$; bla_{TEM-1}; bla_{SHV-1}; $bla_{\Delta OXA-9}$	*ble*$_{MBL}$	*oqx*A; *oqx*B; *qnr*S1	*aac*(6')-Ib; *aac(*6')-Ib-cr; *str*A; *str*B; *arm*A; *aad*A1; *aph*(3')-VI	*tet*A	*mph*A; *mph*E; *mrs*E	*fos*A6 (Q130P, Q139E)	*oqx*A; *oqx*B; *sul*1; *sul*2; *dfr*A5	*cat*A1	*kpn*E; *kpn*F; *kpn*G; *ompk*37	IncFIB; IncHI1B	366	IncL	67
ON-8	383	**bla_{NDM-5}; bla_{OXA-48};** $bla_{CTX-M-15}$; bla_{TEM-1}; bla_{SHV-1}; $bla_{\Delta OXA-9}$	*ble*$_{MBL}$	*oqx*A; *oqx*B; *qnr*S1	*aac*(6')-Ib; *aac(*6')-Ib-cr; *str*A; *str*B; *arm*A; *aad*A1; *aph*(3')-VI	*tet*A	*mph*A; *mph*E; *mrs*E	*fos*A6 (Q130P, Q139E)	*oqx*A; *oqx*B; *sul*1; *sul*2; *dfr*A5	*cat*A1	*kpn*E; *kpn*F; *kpn*G; *ompk*37	IncFIB; IncHI1B	366	IncL	67
ON-J	383	**bla_{NDM-5}; bla_{OXA-48};** $bla_{CTX-M-15}$; bla_{TEM-1}; bla_{SHV-1}; $bla_{\Delta OXA-9}$	*ble*$_{MBL}$	*oqx*A; *oqx*B; *qnr*S1	*aac*(6')-Ib; *aac(*6')-Ib-cr; *str*A; *str*B; *arm*A; *aad*A1; *aph*(3')-VI	*tet*A	*mph*A; *mph*E; *mrs*E	*fos*A6 (Q130P, Q139E)	*oqx*A; *oqx*B; *sul*1; *sul*2; *dfr*A5	*cat*A1	*kpn*E; *kpn*F; *kpn*G; *ompk*37	IncFIB; IncHI1B	366	IncL	67
ON-9	383	**bla_{NDM-5}; bla_{OXA-48};** $bla_{CTX-M-15}$; bla_{TEM-1}; bla_{SHV-1}; $bla_{\Delta OXA-9}$	*ble*$_{MBL}$	*oqx*A; *oqx*B; *qnr*S1	*aac*(6')-Ib; *aac(*6')-Ib-cr; *str*A; *str*B; *arm*A; *aad*A1; *aph*(3')-VI	*tet*A	*mph*A; *mph*E; *mrs*E	*fos*A6 (Q130P, Q139E)	*oqx*A; *oqx*B; *sul*1; *sul*2; *dfr*A5	*cat*A1	*kpn*E; *kpn*F; *kpn*G; *ompk*37	IncFIB; IncHI1B	366	IncL	67
ON-C	383	**bla_{NDM-5}; bla_{OXA-48};** $bla_{CTX-M-15}$; bla_{TEM-1}; bla_{SHV-1}; $bla_{\Delta OXA-9}$	*ble*$_{MBL}$	*oqx*A; *oqx*B; *qnr*S1	*aac*(6')-Ib; *aac(*6')-Ib-cr; *str*A; *str*B; *arm*A; *aad*A1; *aph*(3')-VI	*tet*A	*mph*A; *mph*E; *mrs*E	*fos*A6 (Q130P, Q139E)	*oqx*A; *oqx*B; *sul*1; *sul*2; *dfr*A5	*cat*A1	*kpn*E; *kpn*F; *kpn*G; *ompk*37	IncFIB; IncHI1B	331	IncL	67
ON-10	383	**bla_{NDM-5}; bla_{OXA-48};** $bla_{CTX-M-15}$; bla_{TEM-1}; bla_{SHV-1}; $bla_{\Delta OXA-9}$	*ble*$_{MBL}$	*oqx*A; *oqx*B; *qnr*S1	*aac*(6')-Ib; *aac(*6')-Ib-cr; *str*A; *str*B; *arm*A; *aad*A1; *aph*(3')-VI	*tet*A	*mph*A; *mph*E; *mrs*E	*fos*A6 (Q130P, Q139E)	*oqx*A; *oqx*B; *sul*1; *sul*2; *dfr*A5	*cat*A1	*kpn*E; *kpn*F; *kpn*G; *ompk*37	IncFIB; IncHI1B	366	IncL	67
ON-11	383	**bla_{NDM-5}; bla_{OXA-48};** $bla_{CTX-M-15}$; bla_{TEM-1}; bla_{SHV-1}; $bla_{\Delta OXA-9}$	*ble*$_{MBL}$	*oqx*A; *oqx*B; *qnr*S1	*aac*(6')-Ib; *aac(*6')-Ib-cr; *str*A; *str*B; *arm*A; *aad*A1; *aph*(3')-VI	*tet*A	*mph*A; *mph*E; *mrs*E	*fos*A6 (Q130P, Q139E)	*oqx*A; *oqx*B; *sul*1; *sul*2; *dfr*A5	*cat*A1	*kpn*E; *kpn*F; *kpn*G; *ompk*37	IncFIB; IncHI1B	331	IncL	67
ON-13	383	**bla_{NDM-5}; bla_{OXA-48};** $bla_{CTX-M-15}$; bla_{TEM-1}; bla_{SHV-1}; $bla_{\Delta OXA-9}$	*ble*$_{MBL}$	*oqx*A; *oqx*B; *qnr*S1	*aac*(6')-Ib; *aac(*6')-Ib-cr; *str*A; *str*B; *arm*A; *aad*A1; *aph*(3')-VI	*tet*A	*mph*A; *mph*E; *mrs*E	*fos*A6 (Q130P, Q139E)	*oqx*A; *oqx*B; *sul*1; *sul*2; *dfr*A5	*cat*A1	*kpn*E; *kpn*F; *kpn*G; *ompk*37	IncFIB; IncHI1B	366	IncL	67

ON-17	383	***bla*$_{NDM-5}$; *bla*$_{OXA-48}$;** *bla*$_{CTX-M-15}$; *bla*$_{TEM-1}$; *bla*$_{SHV-1}$; *bla*$_{\Delta OXA-9}$	*ble*$_{MBL}$	*oqx*A; *oqx*B; *qnr*S1	*aac*(6')-Ib; *aac(*6')-Ib-cr; *str*A; *str*B; *arm*A; *aad*A1; *aph*(3')-VI	-	*mph*A; *mph*E; *mrs*E	*fos*A6 (Q130P, Q139E)	*oqx*A; *oqx*B; *sul*1; *sul*2; *dfr*A5	*cat*A1	*kpn*E; *kpn*F; *kpn*G; *ompk*37	IncFIB; IncHI1B	366	IncL	67
ON-20	383	***bla*$_{NDM-5}$; *bla*$_{OXA-48}$;** *bla*$_{CTX-M-15}$; *bla*$_{TEM-1}$; *bla*$_{SHV-1}$; *bla*$_{\Delta OXA-9}$	*ble*$_{MBL}$	*oqx*A; *oqx*B; *qnr*S1	*aac*(6')-Ib; *aac(*6')-Ib-cr; *str*A; *str*B; *arm*A; *aad*A1; *aph*(3')-VI	*tet*A	*mph*A; *mph*E; *mrs*E	*fos*A6 (Q130P, Q139E)	*oqx*A; *oqx*B; *sul*1; *sul*2; *dfr*A5	*cat*A1	*kpn*E; *kpn*F; *kpn*G; *ompk*37	IncFIB; IncHI1B	331	IncL	67
ON-25	383	***bla*$_{NDM-5}$; *bla*$_{OXA-48}$;** *bla*$_{CTX-M-15}$; *bla*$_{TEM-1}$; *bla*$_{SHV-1}$; *bla*$_{\Delta OXA-9}$	*ble*$_{MBL}$	*oqx*A; *oqx*B; *qnr*S1	*aac*(6')-Ib; *aac(*6')-Ib-cr; *str*A; *str*B; *arm*A; *aad*A1; *aph*(3')-VI	*tet*A	*mph*A; *mph*E; *mrs*E	*fos*A6 (Q130P, Q139E)	*oqx*A; *oqx*B; *sul*1; *sul*2; *dfr*A5	*cat*A1	*kpn*E; *kpn*F; *kpn*G; *ompk*37	IncFIB; IncHI1B	331	IncL	67
ON-27	383	***bla*$_{NDM-5}$; *bla*$_{OXA-48}$;** *bla*$_{CTX-M-15}$; *bla*$_{SHV-1}$	*ble*$_{MBL}$	*oqx*A; *oqx*B; *qnr*S1	*str*A; *str*B; *arm*A; *aph*(3')-VI	*tet*A	*mph*A; *mph*E; *mrs*E	*fos*A6 (Q130P, Q139E)	*oqx*A; *oqx*B; *sul*1; *sul*2; *dfr*A5	*cat*A1	*kpn*E; *kpn*F; *kpn*G; *ompk*37	IncFIB; IncHI1B	244	IncL	67
ON-30	383	***bla*$_{NDM-5}$; *bla*$_{OXA-48}$;** *bla*$_{CTX-M-15}$; *bla*$_{TEM-1}$; *bla*$_{SHV-1}$; *bla*$_{\Delta OXA-9}$	*ble*$_{MBL}$	*oqx*A; *oqx*B; *qnr*S1	*aac*(6')-Ib; *aac(*6')-Ib-cr; *str*A; *str*B; *arm*A; *aad*A1; *aph*(3')-VI	*tet*A	*mph*A; *mph*E; *mrs*E	*fos*A6 (Q130P, Q139E)	*oqx*A; *oqx*B; *sul*1; *sul*2; *dfr*A5	*cat*A1	*kpn*E; *kpn*F; *kpn*G; *ompk*37	IncFIB; IncHI1B	366	IncL	67
ON-32	383	***bla*$_{NDM-5}$; *bla*$_{OXA-48}$;** *bla*$_{CTX-M-15}$; *bla*$_{TEM-1}$; *bla*$_{SHV-1}$; *bla*$_{\Delta OXA-9}$	*ble*$_{MBL}$	*oqx*A; *oqx*B; *qnr*S1	*aac*(6')-Ib; *aac(*6')-Ib-cr; *str*A; *str*B; *arm*A; *aad*A1; *aph*(3')-VI	*tet*A	*mph*A; *mph*E; *mrs*E	*fos*A6 (Q130P, Q139E)	*oqx*A; *oqx*B; *sul*1; *sul*2; *dfr*A5	*cat*A1	*kpn*E; *kpn*F; *kpn*G; *ompk*37	IncFIB; IncHI1B	331	IncL	67
ON-36	383	***bla*$_{NDM-5}$; *bla*$_{OXA-48}$;** *bla*$_{CTX-M-15}$; *bla*$_{SHV-1}$	*ble*$_{MBL}$	*oqx*A; *oqx*B; *qnr*S1	*str*A; *str*B; *arm*A; *aph*(3')-VI	*tet*A	*mph*A; *mph*E; *mrs*E	*fos*A6 (Q130P, Q139E)	*oqx*A; *oqx*B; *sul*1; *sul*2; *dfr*A5	*cat*A1	*kpn*E; *kpn*F; *kpn*G; *ompk*37	IncFIB; IncHI1B	244	IncL	67

Table 13. Genetic features of OXA-48-NDM-Kp sequenced achieved with WGS analysis.

Even if the epidemiological distance between clones was short, the phylogenetic tree showed that samples were organized in 3 subclusters [figure 24]. Cluster 1 was formed by ON-25, ON- 27, ON-32, and ON-36 and by three other samples (ON-5, ON-J, and ON-C) slightly more distant. Cluster 2 included ON-8 and ON-9 and the more different ON-1 and ON-30 while to the cluster 3 was associated ON-10, ON-11, ON-13, ON-17, and ON-20 with the slightly diverse ON-4. ON-1 was used as the reference sample and appeared to be closer to ON-5, while the more distant one was ON-30 (the unique sample sequenced belonging to B1 pulsotype), as shown by the longest branch tree. All these findings were confirmed by SNPs matrix, which detected from a minimum of 8 (between ON-13 and ON-17) to a maximum of 59 (among ON- 30 and ON-32) SNPs. More in detail, from 12 to 35 SNPs were detected among cluster 1, from 14 to 36 among cluster 2 and from 8 to 24 among cluster 3.

A

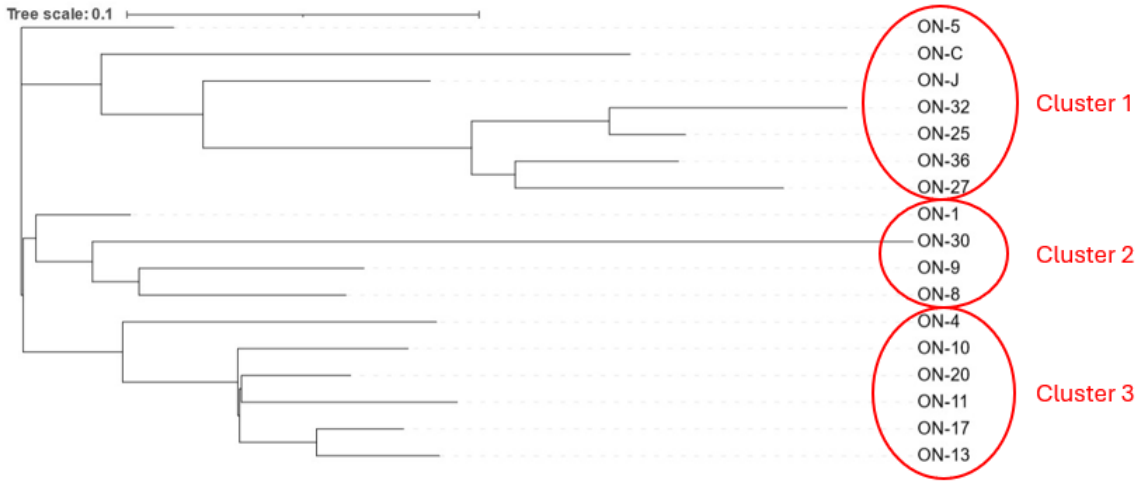

B

	ON-5	ON-4	ON-8	ON-J	ON-9	ON-C	ON-10	ON-11	ON-13	ON-17	ON-20	ON-25	ON-27	ON-30	ON-32	ON-36	ON-1
ON-5	0	21	18	21	14	24	20	17	17	19	15	29	29	34	35	29	10
ON-4	21	0	25	28	25	37	21	24	18	22	20	40	42	43	44	40	17
ON-8	18	25	0	23	16	32	26	27	21	27	25	37	39	36	43	37	14
ON-J	21	28	23	0	25	31	27	30	24	30	28	26	28	43	32	26	17
ON-9	14	25	16	25	0	26	20	21	21	19	19	31	37	34	35	33	16
ON-C	24	37	32	31	26	0	32	31	29	31	29	35	41	48	41	37	26
ON-10	20	21	26	27	20	32	0	15	13	13	11	37	39	44	41	37	18
ON-11	17	24	27	30	21	31	15	0	14	14	12	36	34	43	42	36	19
ON-13	17	18	21	24	21	29	13	14	0	8	10	34	38	37	40	36	13
ON-17	19	22	27	30	19	31	13	14	8	0	10	34	40	43	38	36	19
ON-20	15	20	25	28	19	29	11	12	10	10	0	34	38	43	38	34	17
ON-25	29	40	37	26	31	35	37	36	34	34	34	0	20	53	12	16	29
ON-27	29	42	39	28	37	41	39	34	38	40	38	20	0	57	24	16	31
ON-30	34	43	36	43	34	48	44	43	37	43	43	53	57	0	59	55	32
ON-32	35	44	43	32	35	41	41	42	40	38	38	12	24	59	0	22	35
ON-36	29	40	37	26	33	37	37	36	36	36	34	16	16	55	22	0	29
ON-1	10	17	14	17	16	26	18	19	13	19	17	29	31	32	35	29	0

Figure 24. (A) OXA-48-NDM-Kp phylogenetic tree. ON-1 was used as reference. (B) OXA-48-NDM-Kp SNPs matrix. Orange cells, maximum SNPs number; green cells, minimum SNPs number.

3.5. *Diffusion of non KPC-producing CR-KP*

Before 2021, the unique carbapenemase gene detected in CR-KP clinical strains circulating in our regional hospital was *bla*$_{KPC}$. For that reason, we decided to investigate the incidence and phylogenetic relations of non-KPC-producing *K. pneumoniae* in our study. Between 2021 and 2023 a total of 1,724 CP-KP clinical strains were collected at our regional hospital. Most of these (1,661 isolates, corresponding to 96.3%) were KPC-Kp, but the remaining 63 strains (3.7%) coded for at least one of *bla*$_{OXA-48}$ and *bla*$_{NDM}$ genes. More in detail, only 2 isolates (one coding for *bla*$_{OXA-48}$ and the other for *bla*$_{NDM}$) belonged to 2021 collection (3.2%), 26 Kp (7 *bla*$_{OXA-48}$ clones, 11 *bla*$_{NDM}$, and 8 positives for both these genes) were isolated in 2022 (41.3%) and the remaining 35 (5 *bla*$_{NDM}$ positives, and 30 coding for both *bla*$_{OXA-48}$ and *bla*$_{NDM}$) were harvested in 2023 (55.5%). OXA-48-Kp isolates represented a restricted event, with no more detection from June 2022, while a wide temporal diffusion involved the other carbapenemases. Indeed, NDM-Kp covered all the three years of study, with a 2022 peak, while OXA-48-NDM-Kp showed an increasing trend switching from 8 to 30 detections between 2022 and 2023 [figure 25].

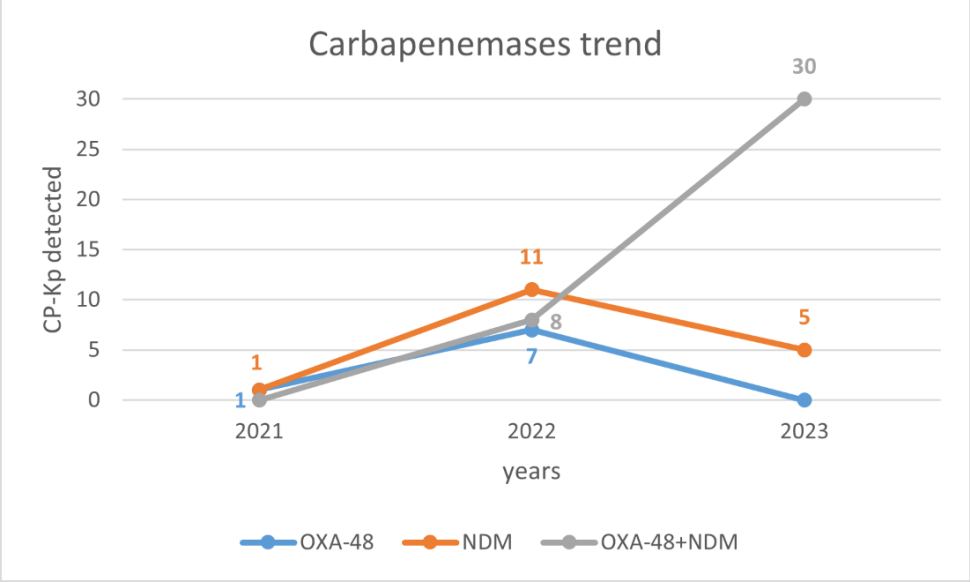

Figure 25. Carbapenemases trend during the study period.

As the phylogenetic tree showed, isolates belonging to ST395 were closer to each other, even if they harboured different carbapenemase genes. Anyway, they constituted two different clones, since OXA-48-Kp and NDM-Kp exhibited about 3,000 SNPs. ST383 clones, all coding for both types of carbapenemases studied, constituted a well-separated cluster, suggesting a different origin from OXA-48-Kp and NDM-Kp. These findings were confirmed by SNPs matrix, in which OXA-48-NDM-Kp featured at least 19,000 SNPs with isolates coding for different carbapenemases [figure 26].

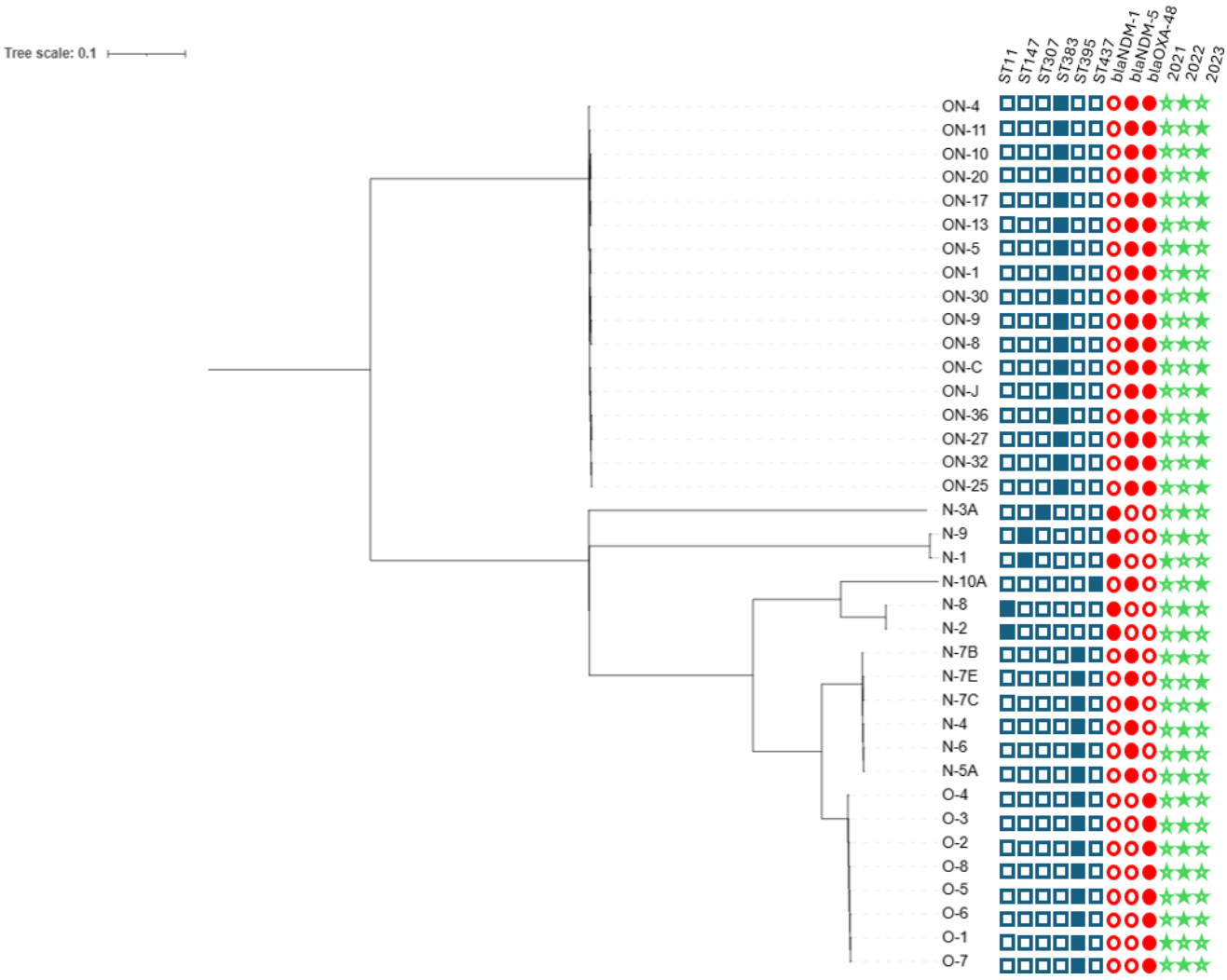

Figure 26. Phylogenetic tree of the 37 Kp sequenced coding for at least one carbapenemase gene between OXA-48 and NDM. O-1 was used as reference genome.

Even if these non-KPC-producing Kp represented the first detections in our region, the situation was different in other areas of our country. Indeed, already in 2016 two OXA-48-Kp ST395 were collected at hospital laboratories of Catania (KPN346) and Torino (KPN398) *(Di Pilato et al., 2021)*. Phylogenetic tree [figure 27] showed that although belonging to the same sequence type and harbouring the same carbapenemase gene, Ancona isolates built a well-separated cluster, and the two clones harvested in 2016 were slightly different from each other. From the SNPs matrix, indeed, the Catania and Torino isolates shared 377 SNPs, and both exhibited from 511 to 655 SNPs with the Ancona's ones.

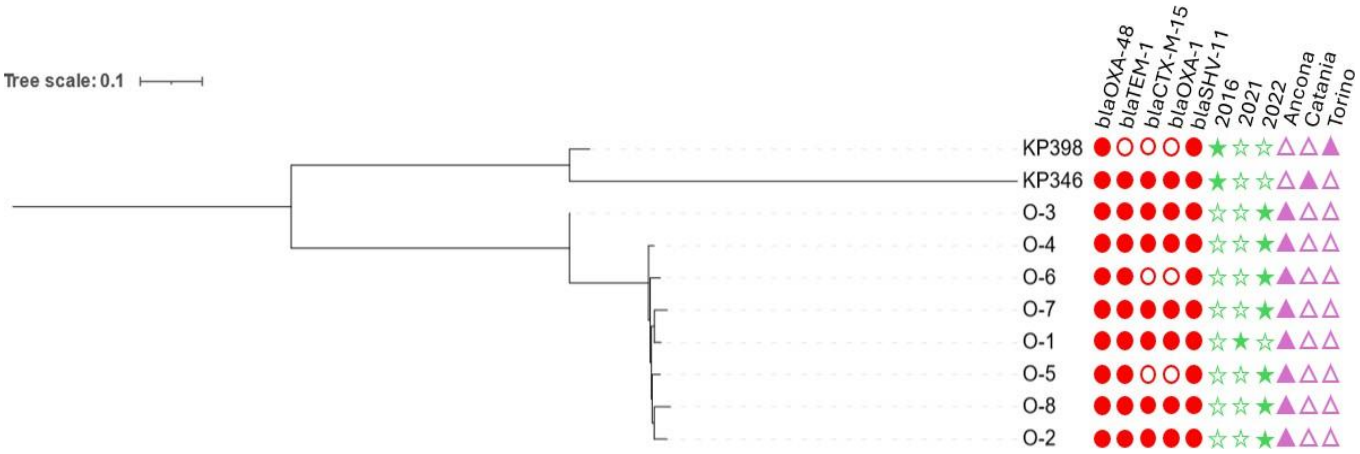

Figure 27. Phylogenetic tree of OXA-48-Kp circulating in Italy. KP346 was used as reference. KP346 and KP398 genomes were available at BioProject PRJEB22890.

Regarding NDM-Kp, since 2018 an endemic situation has been registered in Tuscany. Clones collected from hospitals of Pisa *(Falcone et al., 2020) (Di Pilato et al., 2022),* and Siena *(Martin et al., 2021)* belonged all to ST147 and coded for *bla*$_{\text{NDM-1}}$ or *bla*$_{\text{NDM-9}}$ allelic variants. Phylogenetic comparison [figure 28] of these strains with our NDM-Kp highlighted a major relatedness among all ST147, even if the Ancona isolates constituted a different epidemic clone, showing from 36 to 156 SNPs with the Tuscany ones.

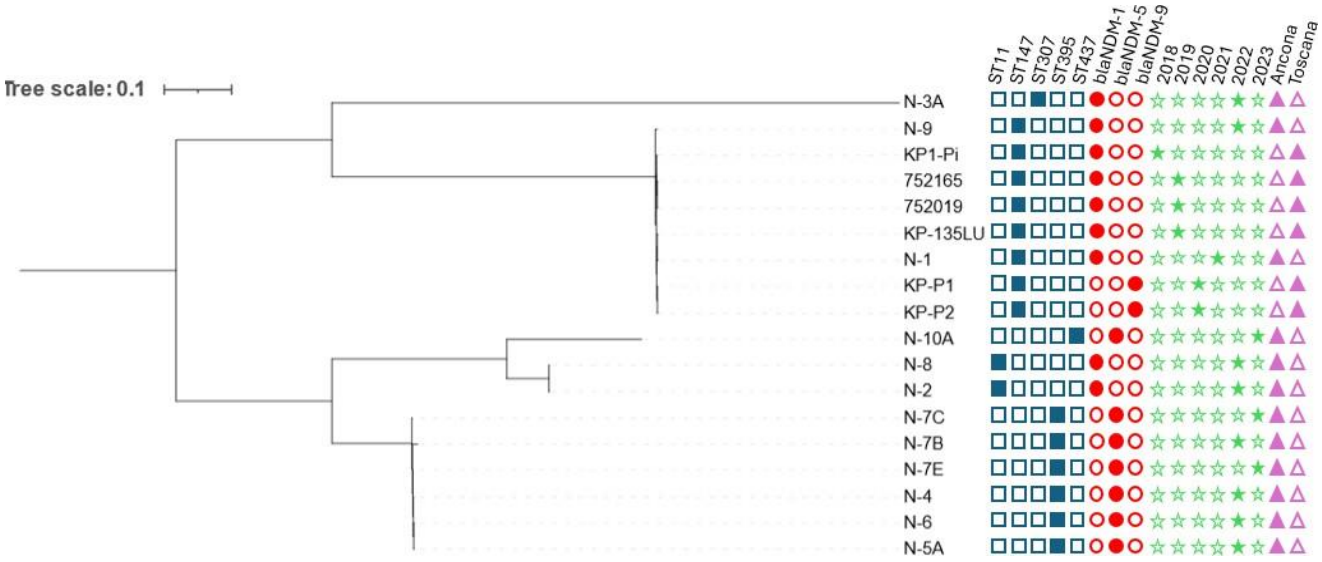

Figure 28. Phylogenetic tree of NDM-Kp circulating in Italy. KP-1Pi was used as reference. 752019 and 752165 genomes were available at BioProject PRJNA725484; KP-1Pi and KP-135LU genomes were available at BioProject PRJNA643814; KP-P1 and KP-P2 genomes were available at BioProject PRJNA667843.

To the Tuscany region belonged also the 4 OXA-48-NDM-Kp collected at the end of 2019, of which 2 (KP48 and KP50) shared the same sequence type of our isolates (ST383) while the remaining were ST15 (KP52) and ST147 (KP45) *(Lorenzin et al., 2022)*. These two clones coded for *bla*$_{\text{NDM-1}}$, KP48 for

bla$_{NDM-5}$ (as our clones), and KP50 for both allelic variants. From the phylogenetic tree [figure 29] we can see that the ST383 Kp were closer to each other, even if the Ancona isolates represented a distinct clonal event, showing from 213 to 381 SNPs with the Tuscany ones.

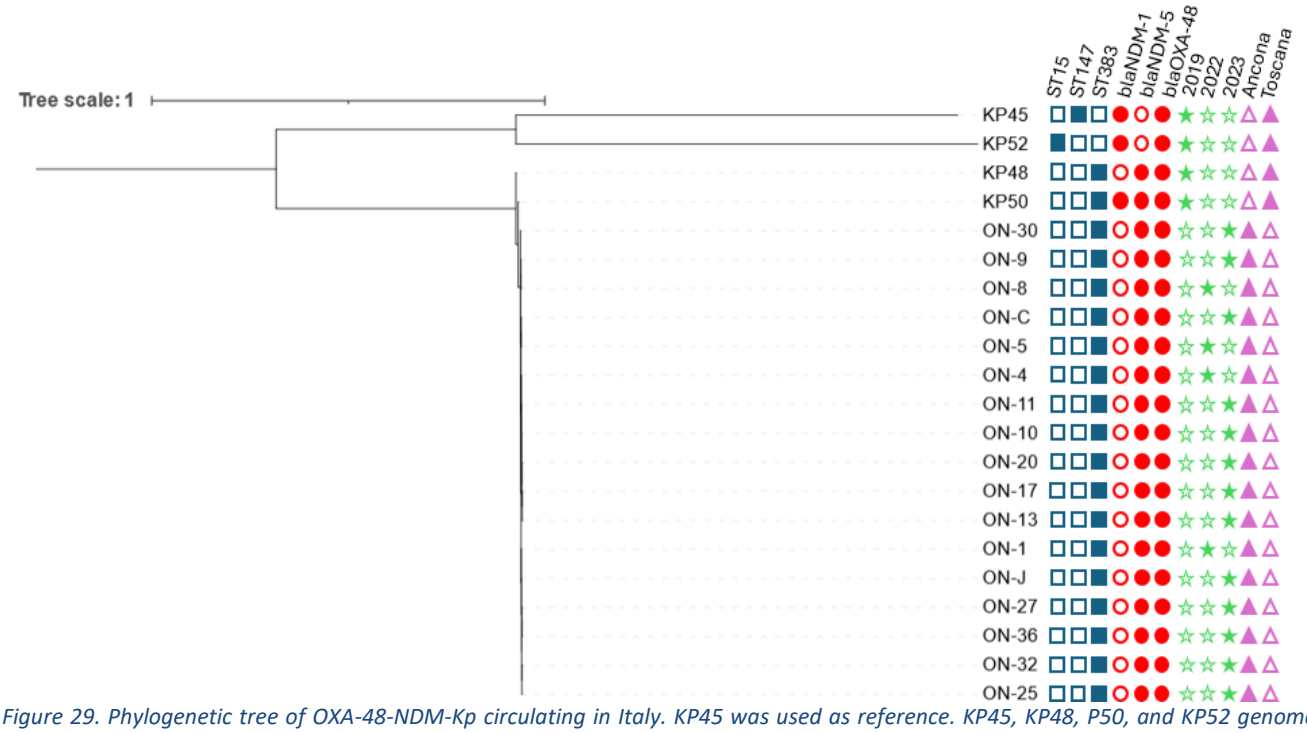

Figure 29. Phylogenetic tree of OXA-48-NDM-Kp circulating in Italy. KP45 was used as reference. KP45, KP48, P50, and KP52 genomes were available at BioProject PRJNA787449.

4. DISCUSSION

K. pneumoniae is one of the most critical nosocomial pathogens worldwide, responsible for several human pathologies such as urinary tract infections, pneumonia and bloodstream infections. The high propensity of this species to acquire multiple antimicrobial resistance genes, including those against carbapenems, makes these infections even harder to treat *(Ma et al., 2022)*. KPCR, indeed, has been included in the critical priority list by the World Health Organization (WHO) since 2017. Moreover, the resistance determinants to this class of drugs are mostly located on mobile elements which promoted a rapid and global spread of KPCR isolates. In fact, since the first KPCR clinical isolate detection in 1997 in the United States, their incidence was constantly growing *(Clegg and Murphy, 2016)*. Regarding the European situation, nowadays only some Northern regions like Denmark, Finland, Ireland, Iceland, Netherlands, Norway, and Sweden register a KPCR incidence lower than 1%. On the other hand, in Bulgaria, Greece, and Romania 50-75% of all isolates collected were KPCR. Italy is included, together with Cyprus and Croatia, in the group with 25-50% incidence of KPCR, counting 3,616 resistant isolates out of 13,654 total tested isolates (26.48% incidence) *(Atlas 2023)*. Differences in geographical distribution are reported depending on the type of carbapenemase encoded. In Italy,

the main cause of KPCR relies on KPC carbapenemase. More in detail, several epidemiological studies conducted in our country found out that from the first KPC-Kp detection in 2008 in Florence *(Giani et al., 2009)*, its spread was linked to a unique clonal group (CG), the CG258, which included the two high-risk clones ST258 and ST512. This situation was shared by all European countries. In the last years, however, this single lineage diffusion in Italy was replaced by a polyclonal distribution of several new high-risk clones. The last national survey conducted in Italy on *K. pneumoniae* revealed four major lineages circulating: CG258 (47.4%), CG307 (19.9%), ST101 (15.4%), and ST395 (5.1%) *(Di Pilato et al., 2021)*. Already in 2014, a multicentre study conducted in three different hospitals of Palermo, Sicily, Southern Italy, revealed that even if the CG258 was the most prevalent clone circulating in healthcare centers (40% incidence), other clones emerged and in particular one, the ST307, was in charge for 29% of KPC-Kp infections *(Bonura et al., 2015)*. This clone kept on circulating also in the following years. In fact, a study focused on BSIs caused by KPC-Kp conducted in our regional hospital between 2011 and 2015, revealed that 9% of the isolates collected belonged to ST307 *(Brescini et al., 2019)*. The ST101 is another concerning sequence type which is raising up its incidence. Between 2014 and 2016 at the University Hospital Policlinico of Bari, Puglia, Southern Italy, 20.3% of the 104 KPC-Kp collected belonged to ST101 *(Loconsole et al., 2020)*. In December 2016, the neonatal intensive care unit of a Palermitan hospital was the scenario of patient's colonization by KPC-Kp. Genomic analysis of the isolates collected highlighted that all belonged to the emerging ST395 epidemic clone, suggesting an outbreak occurrence *(Maida et al., 2018)*. All these reports are consistent with our data. In fact, in our study, ST512 was the main clone found (40%) but ST307 represented 30% of the isolates and 7 out of 50 strains sequenced (14%) were ST101. Only one isolate (2%), instead, belonged to ST395 and the same frequency featured the remaining 7 sequence types detected. Clones with major incidence were isolated in almost all the hospitals of the study: ST512 isolates were collected at all 4 hospitals, ST307 ones were detected in Ancona, Fano, and Perugia and ST101 clones were isolated in Ancona, Perugia, and Pesaro hospitals. The presence of strains belonging to the same sequence type and with short phylogenetic distances in different hospital settings that were not connected pointed out their high ability to spread and succeed as endemic clones in Italy. It is important to notice that during the study period, a decreasing trend in ST512 in favour of a growth in ST307 occurred. This finding is consistent with literature reports in which the genetic features of ST307 were considered a key role in its epidemic success *(Villa et al., 2017)*. Moreover, ST307 strains seem to be highly prone to colonize the human gut. In fact, a study conducted between 2018 and 2019 at "Ospedali Riuniti" regional hospital of Ancona, reported that

among 18 rectal swabs that tested positive for KPCR, 44.4% were classified as ST307 and 5% of these harboured the *bla*$_{KPC-2}$ gene *(Magi et al., 2021)*. Also in our study, the four cases of *bla*$_{KPC-2}$ allelic variant were harboured in strains belonging to ST307, while *bla*$_{KPC-3}$ allelic variant, which exhibited the highest incidence (90%) was shown up by all sequence types detected. Anyway, *bla*$_{KPC}$ genes were always carried by the Tn*4401* transposon, hosted in diverse plasmids with different replicon types, genetic content and size. It is already known this mobile element is crucial for *bla*$_{KPC}$ global dissemination and spread among diverse *K. pneumoniae* STs and also from *K. pneumoniae* to other bacterial species *(Hobson et al., 2022)*. Unlike all strains coding for *bla*$_{KPC-2}$ or *bla*$_{KPC-3}$ allelic variant, PR-11 featured *bla*$_{KPC-66.}$ This isolate was collected at Perugia's hospital in 2019, belonged to ST512 and showed a resistant phenotype to CZA. This KPC variant differs from KPC-3 for the L167ELdel, which was already known to characterize CZA-resistant clones. In fact, during a study conducted between 2019 and 2020 at the Clinical Microbiology Laboratory of the University Hospital Policlinico Umberto I of Rome, 32 KPC-Kp clinical isolates showed MIC values to CZA greater or equal to 8 mg/L. Of these, 3 isolates harboured the *bla*$_{KPC-66}$ allelic variant. More in detail, 2 of them were ST512, as in our study, while the remaining one was ST101. One of these 3 strains displayed CZA-resistance after exposure to this drug while the two others were isolated in patients not treated with CZA and showed susceptibility to meropenem *(Carattoli et al., 2021)*. In Perugia hospital, other 2 isolates were CZA-resistant but the equal PFGE pulsotype with PR-11 suggested that they were clonally related to this isolate and probably carried the same *bla*$_{KPC}$ gene. Regarding colistin resistance, we noticed a decreasing trend during the study period, with an incidence of 34% in the last year of investigation. This may be due to the reduction in colistin administration thanks to the development of the new effective combination CZA. Not surprisingly, the only 3 cases of CZA-resistance were detected in 2019, after the commercialization of CZA in 2016 *(Bush et al., 2018)*. The emergence of CZA-resistant clones is a concerning global matter since also point mutation on *bla*$_{KPC}$ genes could lead to CZA resistance. For example, the D179Y amino acid substitution in KPC-3 carbapenemase leads to KPC-31, known to confer resistance to CZA *(Di Pilato et al., 2024)*. Particular attention to therapy with new β-lactams and β-lactams inhibitors should be provided in order to minimize the bacterial chance to overcome them.

OXA-48-Kp is known to be endemic in Turkey, some other Middle Eastern countries, and North Africa, but in recent years it started to cause nosocomial outbreaks in non-endemic areas, such as Greece, Israel, United Kingdom, Spain, Germany and many others *(Pitout et al., 2019)*. Because of the increasing growth in KPCR incidence and the varying types of carbapenemases encoded, the European

prospective cohort study on *Enterobacterales* showing resistance to carbapenems (EURECA) collected carbapenem non-susceptible clinical samples between May 2016 and November 2018 to investigate the main KPCR circulating in Southern Europe *(Budia- Silva et al., 2024)*. Of the 683 isolates that made up the EURECA collection, 266 were OXA-48-like-Kp (39%) linked to several sequence types including ST11, ST15, and ST101 mainly circulating in Serbia, Spain, and Turkey. OXA-48-Kp detection occurred really seldom in Italy, and the bacterial strains described in this study represent the first case in our regional hospital. Moreover, the short time laps between strains' isolation and their phylogenetic neighbourhood (43 maximum SNPs number among isolates) suggested a clonal outbreak. The 8 OXA-48-Kp detected belonged to the ST395, renowned for being an emerging high-risk clone involved in bla_{KPC} spread in Italy, as previously described. In 2016, during the National Antimicrobial-Resistance Surveillance (AR-ISS) conducted in our country, two out of 156 clinical samples collected coded for bla_{OXA-48} and belonged to ST395 *(Di Pilato et al., 2024)*. Even though these two samples belonged to the same sequence type and derived from the same clinical sources (blood culture), they showed some differences as the origin, since one was collected at Catania hospital (Southern Italy) and the other at Turin hospital (Northern Italy), and β-lactams resistance genes other than $bla_{OXA-48.}$ The Catania isolate, indeed, coded also for $bla_{CTX-M-15,}$ and bla_{OXA-1} which were absent in the Turin one. Also in our study, 6 ST395 strains harboured these genes, while they were not present in the other 2 (O-5 and O-6). The lack of these genes together with the absence of *aac*(6')-Ib-cr explained the susceptibility of these two strains to aztreonam and ceftazidime. During the coronavirus pandemic, an outbreak sustained by *K. pneumoniae* coproducing bla_{OXA-48} and $bla_{CTX-M-15}$ genes was reported in Sydney, Australia *(Howard-Jones et al., 2022)*. Between September and October 2021, 7 clinical samples positive for CPE were obtained from patients admitted in an Intensive Care Unit (ICU) and affected by SARS-CoV-2 disease. All the strains tested positive for bla_{OXA-48} and $bla_{CTX-M-15}$ genes and showed a resistance phenotype close to one of our isolates, with susceptibility MIC values only to amikacin and CZA. WGS analysis assigned the ST16 to all strains and the plasmidome study localized bla_{OXA-48} and $bla_{CTX-M-15}$ genes on an IncL plasmid. This mobile element was widely described and known as pOXA-48a plasmid. Its high spread among *Enterobacteriaceae* relies on the presence of the Tn*1999* transposon inserted into the *tir* gene, involved in transfer inhibition mechanisms *(Potron et al., 2014)*. Unlike what was just described, our strains showed bla_{OXA-48} gene on the Tn*1999.2* transposon hosted on a well- conserved 57 kb long IncR plasmid. This is an uncommon bla_{OXA-48} element similar to one described by a Dutch 2014-2019 surveillance on OXA-48-producing *K. pneumoniae* and *E. coli (Hendrickx et al., 2021)*. During this study, 179 $bla_{OXA-48-like}$ carrying plasmids were analysed and most of

these, divided into five groups, were IncL plasmids similar to internationally reported elements. An additional cluster was genetically diverse from these and was characterized by many different replicon types. The pRIVM_C019523_2 plasmid (accession number CP068905.1) featured the IncR incompatibility group and its alignment on BLAST with our plasmid resulted in 99.93% identity. No other reports describing this plasmid have been published yet, and the presence of *bla*$_{OXA-48}$ in an unusual element supported the thesis of its high ability to diffuse among different *K. pneumoniae* strains. Moreover, since the majority of our clones were retrieved from rectal swabs, their spread may have occurred in the gut of healthy individuals. The detection in carriers of strains belonging to the high-risk clone ST395, underlined their ability to cause outbreaks also in non-endemic regions.

NDM-Kp data gained in our study confirmed the non-clonal dissemination of these carbapenemase and its location on different plasmids with several replicon types *(Logan et al., 2017)*. In fact, 5 different STs were assigned to the 12 NDM-Kp sequenced, with ST147, ST11, and ST395, considered high-risk clones, reporting the highest incidence. ST147 NDM-Kp was responsible for consecutive outbreaks in the Tuscany region, Italy, since 2018. The first outbreak occurred between 2018 and 2019 in the northern areas of the region and was sustained by ST147 strains responsible for BSIs *(Di Pilato et al., 2022)*. All strains coded for the *bla*$_{NDM-1}$ allelic variant and for two other β-lactamase genes (*bla*$_{CTX-M-15}$ and *bla*$_{OXA-1}$) which were detected also in our ST147 clones (N-1 and N-9). As in our study, strains were susceptible to colistin and cefiderocol. The Tuscany outbreak *bla*$_{NDM-1}$ genes were located on different plasmids, with a predominance of FIB(pQil) replicon but also the multireplicon FIB/HI1B and FII were detected. These 2 incompatibility groups featured on N-1 and N-9 isolates of our study, respectively. In 2020, in the same geographic area, a new outbreak sustained by ST147 NDM-Kp was reported *(Falcone et al., 2020)*. Differently from the previous one and from our situation, strains tested positive for the *bla*$_{NDM-9}$ allelic variant and acquired resistance to colistin. These findings suggested a high variability and heterogenicity among ST147 NDM-Kp, which was confirmed also in our study. In fact, the two ST147 strains showed NDM plasmids differing for genetic content, replicon type, size, and Tn*125-like* organization and they shared 159 SNPs which underlined a huge phylogenetic distance not referable to strains belonging to the same epidemiological clone. Between 2020 and 2021, another outbreak sustained by ST147 NDM-Kp was detected in the Apulia region, Southern Italy *(Loconsole et al., 2024)*. Phylogenetic analysis revealed a high correlation between the Apulia and the Tuscany first outbreak's isolates, with an average SNPs number of 49. This data highlighted the strong ability of this clone to spread and succeed in diverse healthcare settings, as it was found from north to south of our country and there were also international reports. For instance,

NDM-1-Kp ST147 was responsible for nosocomial outbreaks also in Chicago, United States *(Lapp et al., 2021)*, and Warsaw, Poland *(Biedrzycka et al., 2021)*. NDM-Kp ST11 is not frequently detected in our country, as it was predominantly linked to *bla*$_{KPC}$ spread worldwide *(Woodford et al., 2011)*. Anyway, in 2019 at the "Cardarelli" hospital of Molise, Central Italy, the first NDM-Kp ST11 was collected from blood and urine of an old man admitted to the ICU *(Ripabelli et al., 2020)*. This strain tested positive for *bla*$_{NDM-1}$ allelic variant, *bla*$_{SHV}$, and *bla*$_{TEM}$ genes (as our two ST11 strains N-2 and N-8), but the lack of WGS data prevented us from compare them with the strains of our study. ST11 NDM-Kp was detected also in other European regions, where it was responsible for prolonged outbreaks. For instance, between 2013 and 2016 eight Greek hospitals collected a total of 480 MBL-producing clinical strains, 341 of which tested positive for *bla*$_{NDM-1}$ and 97.6% were ST11 *(Politi et al., 2019)*. The two ST11 of our study coproduced the *bla*$_{NDM-1}$, *bla*$_{CTX-M-15}$, *bla*$_{TEM-1}$, and *bla*$_{OXA-1}$ genes as the Greek ones but also coded for *bla*$_{SHV-12}$. Moreover, *bla*$_{NDM-1}$ was located on a recombinant IncFII/repB plasmid 79 kb long while the Greek strains were characterized by a 95 kb long IncFII plasmid. In the last year of the Greek study (2016), the first outbreak of NDM-1-Kp was reported in Bulgaria *(Savov et al., 2018)*. 14 out of 17 clinical isolates belonged to ST11 and showed the same PFGE profile of the Greek cluster, even if *bla*$_{NDM-1}$ was found on a IncA/C plasmid instead of the IncFII one. These findings suggested that the ST11 could be a more conserved lineage compared to ST147 and also confirmed the ability of *bla*$_{NDM}$ genes to insert in different genetic environments, fostering its diffusion. Likewise, the phylogenetic analysis of our study revealed only 8 SNPs among N-2 and N-8 strains, suggesting the same epidemiological origin. The last NDM-Kp clone with significant incidence in our study was the ST395. More in detail, half of the isolates sequenced belonged to this ST, but three of them were collected from the same patient (patient 7 in this study). Kp ST395 is generally linked to *bla*$_{KPC}$ spread in our country, and no other episodes of its involvement in *bla*$_{NDM}$ spread in Italy were reported. All isolates harboured the *bla*$_{NDM-5}$ allelic variant, two isolates carried other β-lactams resistance encoding genes (*bla*$_{TEM-1,}$ and *bla*$_{SHV-11}$) while in strains not related to patients 7 also *bla*$_{CTX-M-15}$ and *bla*$_{OXA-1}$ were present. Even if all the ST395 strains showed a highly conserved *bla*$_{NDM}$ genetic context, Tn*125-like* transposon was chromosomally located in N-7C and N-7E isolates while localized on an IncFIB(pQil) 100 kb long plasmid in the remaining ones. The phylogenetic analysis pointed out that the ST395 cluster was established by strains belonging to different clonal events. Interestingly, ST395 isolates belonging to patients 4, 5, and 6 and the N-7E were close to each other, sharing a maximum of 14 SNPs suggesting a single clonal event. The remaining two isolates belonging to patient 7, instead, showed a higher genetic distance (266 maximum SNPs number) which implied a

different origin, even if all the ST395 clones constituted a well-defined cluster, separated from the other STs. As described previously, at the same time as NDM-Kp were detected in our regional hospital, an outbreak sustained by OXA-48-Kp ST395 occurred. This underlined the high ability of this clone to acquire and maintain different antibiotic resistance genes also in the same setting. Outside our country, sporadic events of *bla*$_{NDM}$ producing ST395 *K. pneumoniae* were reported. For instance, between 2017 and 2018, 13 NDM-Kp were collected at St. Petersburg hospital, Russia *(Lazareva et al., 2020)*. Seven of them were ST395, while the remaining were ST147. All tested positive for *bla*$_{NDM-1}$ allelic variant, while our ST395 clones harboured the *bla*$_{NDM-5.}$ Russian plasmids were not reconstructed but the replicon type detected did not include the IncFIB(pQil) of our ST395 *bla*$_{NDM}$ plasmids, suggesting a different carbapenemase localization. Even if ST307 is worldwide known as an endemic high-risk clone involved in *bla*$_{KPC}$ spread *(Loconsole et al., 2020)* its correlation also with *bla*$_{NDM}$ has already been reported. Between September and October 2017 three patients who were admitted to the ICU of the University Hospital of Nuevo Leon, Mexico, resulted positive for carbapenem-resistant *K. pneumoniae (Bocanegra-Ibarias et al., 2019).* Subsequent analysis revealed that all strains belonged to the ST307, coded for *bla*$_{NDM-1}$, *bla*$_{TEM}$, *bla*$_{SHV}$, and *bla*$_{CTX-M}$ genes and were susceptible only to colistin and tigecycline. Also in our ST307 strain (N-3A) the same phenotypic behaviour to colistin and β-lactams resistance genes (with an additional *bla*$_{OXA-1}$) was detected. Nine ST307 NDM-Kp with the same pattern of antibiotic susceptibility were collected in Shanghai, China, in 2022 *(Zhu et al., 2024)*. These strains, unlike our N-3A, harboured the *bla*$_{NDM-5}$ allelic variant and only the *bla*$_{CTX-M-15}$ and *bla*$_{DHA-1}$ β-lactams resistance genes. Moreover, the Chinese carbapenemases were located on an IncX3 type plasmid of 45 kb while in our study the *bla*$_{NDM-1}$ gene was hosted by a 360 kb long recombinant IncFIB/IncHI1B plasmid highly similar (99% identity) with the ST147 N-1 one. Moreover, the Tn*125-like* structure of N-1 and N-3A was the same, even if they belonged to distinct sequence types. The different *bla*$_{NDM}$ gene arrangement and localization among diverse ST307 strains and the ability of this sequence type to harbour different carbapenemases confirm its huge genome plasticity and explain its epidemiological success *(Villa et al., 2017).* The last NDM-Kp strain of our study (N-10A) was a ST437. This sequence type belongs to the GC258 but is not common in our country. Furthermore, when detected at Padua hospital, Northern Italy, between 2009 and 2011, ST437 *K. pneumoniae* strains were linked to *bla*$_{KPC-2}$ spread *(Ritcher et al., 2012)*. Also in other countries, ST437 was renewed for harbour carbapenemase other than *bla*$_{NDM}$. For instance, this strain has been linked to *bla*$_{KPC-2}$ in Brazil since 2006 *(Seki et al., 2011)* and to *bla*$_{OXA-245}$ in Spain since 2012

(Oteo et al., 2013). The first association between *bla*$_{NDM}$ and ST437 occurred in Madrid, Spain, in December 2013 *(Seara et al., 2015).* Seven patients from 3 different hospitals were infected by ST437 *K. pneumoniae* coding for *bla*$_{NDM-7}$ allelic variant, susceptible only to colistin (as N-10A). In our country, instead, the first identification of an NDM-Kp ST437 dates to April 2023 in Teramo, Abruzzo, Central Italy *(Ranieri et al., 2024)*. This strain co-harboured *bla*$_{NDM-5}$ (as N-10A) and *bla*$_{OXA-232}$ (missing in N-10A), and among the plasmids detected featured the IncFII replicon, which characterized the 84 kb *bla*$_{NDM-5}$ carrying plasmid of our ST437 strain. In September 2023, in the same region, two *K. pneumoniae* MDR strains were collected from urine samples of two patients hospitalized at San Salvatore hospital of L'Aquila, Central Italy *(Di Marcantonio et al., 2024).* Both strains tested positive for *bla*$_{NDM-5}$ allelic variant and carried resistance genes to β-lactams, macrolides, quinolones, rifamycin, and folate. Among these, *bla*$_{CTX-M-15}$, *arr*-2, *sul*1, and *dfrA*12 were present also in N-10A strain. Also the plasmidome analysis of the two Abruzzi strains highlighted several replicon types including IncFII. However, our strain, unlike the others, presented two tandem copies of the Tn*125-like* transposon that hosted the carbapenemase gene. The NDM-Kp polyclonal situation highlighted in our hospital during the study period is consistent with the epidemiological evolution already reported in our country. The rise of high-risk lineages coding for *bla*$_{NDM}$ is supported by the high plasticity of the Tn*125* that hosts the MBL gene. This mobile element allows the *bla*$_{NDM}$ to spread and helps its diffusion also among strains belonging to different sequence types.

K. pneumoniae co-producing *bla*$_{OXA-48}$ and *bla*$_{NDM-5}$ genes was never detected before in our regional hospital. The collection of these 38 strains occurred after the OXA-48-Kp outbreak and during the NDM-Kp prolonged detection previously described. Interestingly, all the OXA-48-NDM-Kp belonged to the ST383 which was not featured either in OXA-48-Kp and NDM-Kp strains. This finding suggested a different origin of the OXA-48-NDM-Kp strains even if they coded for the same two carbapenemases produced by the other *K. pneumoniae* strains circulating in the same hospital setting in the same time frame. This assumption was confirmed by both WGS and phylogenetic analysis conducted on 17 isolates chosen as described in *Result 4.1.2.* section. In fact, the *bla*$_{OXA-48}$ gene of this outbreak was located on a well-conserved 72 kb long IncL plasmid while the same carbapenemase gene in the OXA-48-Kp outbreak was hosted by an IncR plasmid of 57 kb. Moreover, also the *bla*$_{OXA-48}$ genetic environment was different: in OXA-48-NDM-Kp strains the gene was localized on a 5.6 kb transposon flanked by two IS10A inverted sequences while in the OXA-48-Kp ones was integrated in a 7 kb element flanked by IS903 by one side and IS10A by the other. The *bla*$_{NDM-5}$ gene was plasmid located

on 10 out of 17 isolates and chromosomally located in the remaining 7 ones. The MBL-carrying plasmid was a recombinant IncFIB/IncHI1B element of 367 kb which showed 99% identity with the plasmids of N-1 and N-3A strains of NDM-Kp isolates, even if they coded for *bla*$_{NDM-1}$ allelic variant. Unlike the NDM-Kp clones, the Tn*125-like* transposon housing the *bla*$_{NDM-5}$ gene was highly conserved in all OXA-48-NDM-Kp strains. In fact, even in those isolates with a chromosomal MBL location, the carbapenemase gene was always inserted on a 10 kb mobile element flanked by IS110A by one side and ISAba125 by the other. Moreover, we found this MBL carrying IncFIB/IncHI1B plasmid in ST147, ST307, and ST383 *K. pneumoniae* isolates. ST383 was recently included in the high-risk clone group together with ST147 and ST15 *(Palmieri et al., 2021)*. Already in 2019, at "Spedali Civili" hospital of Brescia, Italy, a *K. pneumoniae* ST383 isolate coding for the same carbapenemases highlighted in this study was detected *(Scaltriti et al., 2021)*. Moreover, in the same year, also in Tuscany, Italy, two samples with identical features were collected from rectal swabs of hospitalized patients *(Lorenzin et al., 2022)*. Both Brescia and Tuscany isolates hosted the carbapenemase genes in two plasmids with the same features as ours and showed susceptibility only to colistin, to which our isolates exhibited heterogeneous behaviour. These episodes underline the ability of this clone to spread among different Italian regions. Looking outside of our country, in 2018 another isolate with the same characteristics was identified from a patient with bacteraemia in a London hospital *(Turton et al., 2019)*. However, the *bla*$_{NDM-5}$ flanking regions showed some differences: the London isolate presented the *bla*$_{CTX-M-15}$ and *bla*$_{OXA-1}$ encoding genes inside the mobile element while in the Italians samples the first gene was chromosomally located in the 7 strains with a shorter IncFIB/IncHI1B plasmid, and the second gene was missing. The distribution of this clone seemed to also involve countries outside Europe. Indeed, another study conducted in an Egyptian hospital in 2020 detected the same clone with similar plasmids *(Edward et al., 2022)*. In this case, the *bla*$_{OXA-48}$ gene was located on a IncL/M plasmid along with *bla*$_{CTX-M-14}$ which is not present in the samples studied. The *bla*$_{NDM-5}$ gene, instead, was hosted in the same IncFIB/IncHI1B plasmid of our study, together with *bla*$_{CTX-M-15}$. Moreover, plasmids detected in our outbreak showed high nucleotide identity (99.96%) and coverage (100%) with those of a recent Qatar study, conducted in 2022 *(Tsui et al., 2022)*. Qatari plasmids had short regions that are missing on Italian ones: IncFIB/IncHI1B Qatar element had additional transpositional sequences while IncL had both transposon and two antibiotic resistance genes lacking in our study (*bla*$_{CTX-M-15}$ and *aph* (3'')-IV). Besides the small differences between isolates and mobile elements, the presence of NDM-5 and OXA-48 producing *K. pneumoniae* belonging to ST383 in different hospitals worldwide underlines the extremely high spread and global dissemination of this clone, facilitated

also by international travels.

5. CONCLUSIONS

Data acquired on KPCR during this three-year study show an evolving epidemiological scenario at the three university hospitals in Central Italy. In fact, even if KPC is the carbapenemase still predominantly detected, other carbapenems-hydrolysing enzymes were first-time observed. Moreover, since 2019 KPC-Kp belonging to sequence types other than ST512 started to emerge and rise. In particular, we noticed a huge percentage of ST307 and ST101 isolates, considered emerging high-risk clones worldwide. Regarding OXA-48-Kp, their recovery from rectal swabs, their belonging to ST395 (another high-risk clone) and the localization of $bla_{\text{OXA-48}}$ in an unusual plasmid are of particular concern. In fact, all these findings underline the chance of healthy carriers to spread these high-risk clones outside the nosocomial settings and the ability of $bla_{\text{OXA-48}}$ to cause outbreaks also in non-endemic areas. Even if bla_{NDM} has already been circulating in our country since 2018, we reported the detection of 5 different *K. pneumoniae* sequence types (4 of which are considered high-risk clones) in a very short time frame (less than two years), supporting the common concept of non-clonal success of these MBL strains. In addition, the high ability of Tn*125* transposon to rearrange itself and integrate both in chromosomes and in a huge number of different plasmids underlines the epidemiological potential spread of these carbapenemase-carrying strains. The co-expression of NDM and the serine carbapenemase OXA-48 lowers the few effective therapeutic options available. In fact, the development and commercialization of CZA in 2016 allowed public health services to efficiently overcome severe infections sustained by MDR strains producing some serine carbapenemases, including KPC and OXA-48. As explained before, however, point mutations on KPC can lead to CZA resistance and these bla_{KPC} allelic variants are constantly increasing. Anyway, this β-lactam-β-lactamase inhibitor combination shows no activity against MBLs *(Sharma et al., 2016)*, against which is effective the monobactam aztreonam. On the other hand, really seldom carbapenem-resistant pathogens coded for the bla_{NDM} gene alone. In most cases, the MBL gene is co-expressed with other ESBLs, such as CTX-M-15, which makes aztreonam ineffective. The same thing applies to OXA-48-NDM-Kp. Indeed, even if aztreonam is effective against NDM carbapenemase, it is hydrolizable by OXA-48 enzymes. A successful treatment is the combination of aztreonam (active against MBL) with avibactam (effective against serine-carbapenemase), approved by the European Commission for MBL treatment in April 2024. Another option available and effective against all three types of carbapenemases detected in this study is the siderophore cephalosporin cefiderocol, even if strains

resistant to this drug were already detected.

In conclusion, this report highlights a changing KPCR epidemiology in our regional hospitals, with the emergence of carbapenemases never detected before, capable of causing outbreaks and spreading among different high-risk lineages. Active surveillance on carbapenem-resistant *Enterobacteriaceae* is essential to monitor the clones already circulating and immediately detect new potential worrisome lineages. Moreover, a mindful use of the few therapeutic options working against this group of pathogens is essential, in order to preserve their efficacy and confine the emergence of new resistance phenotypes.

6. REFERENCES

1. Arena F, Di Pilato V, Vannetti F, et al. Population structure of KPC carbapenemase-producing Klebsiella pneumoniae in a long-term acute-care rehabilitation facility: identification of a new lineage of clonal group 101, associated with local hyperendemicity. *Microbial Genomics.* 2020;6. DOI: 10.1099/mgen.0.000308.
2. Armstrong T, Fenn SJ, Hardie KR. JMM Profile: Carbapenems: a broad-spectrum antibiotic*. J Med Microbiol*. 2021 Dec; 70(12):001462. DOI: 10.1099/jmm.0.001462.
3. Aurilio C, Sansone P, Barbarisi M, et al. Mechanisms of Action of Carbapenem Resistance. *Antibiotics*. 2022; 11(3):421. DOI: 10.3390/antibiotics11030421.
4. Bialek-Davenet S, Lavigne JP, Guyot K, et al. Differential contribution of AcrAB and OqxAB eflux pumps to multidrug resistance and virulence in Klebsiella pneumoniae. *J Antimicrob Chemother.* 2015 Jan; 70(1):81-8. DOI: 10.1093/jac/dku340.
5. Biedrzycka M, Urbanowicz P, Guzek A, et al. Dissemination of Klebsiella pneumoniae ST147 NDM-1 in Poland, 2015–19. *J Antimicrob Chemother.* 2021; 76: 2538–2545 DOI: 10.1093/jac/dkab207.
6. Birgy A, Nnabuife C, Palzkill T. The mechanism of ceftazidime and cefiderocol hydrolysis by D179Y variants of KPC carbapenemases is similar and involves the formation of a long-lived covalent intermediate. *Antimicrob Agents Chemother.* 2024 Mar 6; 68(3):e0110823. DOI: 10.1128/aac.01108-23.
7. Biswas S, Burnel JM, Dubus JC, et al. Colistin: an update on the antibiotic of the 21st century. *Expert Rev. Anti Infect. Ther.* 2012. DOI: 10.1586/eri.12.78.
8. Bocanegra-Ibarias P, Garza-Gonzalez E, Padilla-Orozco M, et al. The successful containment of a hospital outbreak caused by NDM-1-producing Klebsiella pneumoniae ST307 using active surveillance. *PLoS ONE.* 2019; 14(2):e0209609. DOI: 10.1371/journal. pone.0209609.
9. Bonura C, Giuffrè M, Aleo A, et al. An Update of the Evolving Epidemic of blaKPC Carrying Klebsiella pneumoniae in Sicily, Italy, 2014: Emergence of Multiple Non-ST258 Clones. *PLoS ONE*. 2015; 10(7): e0132936. DOI: 10.1371/journal.pone.0132936.
10. Boyd SE, Holmes A, Peck R, et al. OXA-48-Like β-Lactamases: Global Epidemiology, Treatment Options, and Development Pipeline. *Antimicrob Agents Chemother*. 2022; 66:e00216-22. DOI: 10.1128/aac.00216-22.
11. Brescini L, Morroni G, Valeriani C, et al. Clinical and epidemiological characteristicsof KPC-producing Klebsiella pneumoniae from bloodstream infections in a tertiaryre ferral center in Italy. *Infectious Diseases*. 2019; 19:611. DOI: 10.1186/s12879-019-426.

12. Brolund A, Lagerqvist N, Byfors S, et al. Worsening epidemiological situation of carbapenemase-producing Enterobacteriaceae in Europe, assessment by national experts from 37 countries, July 2018. *Euro Surveill.* 2019; 24(9):pii=1900123. DOI: 10.2807/1560- 7917.ES.2019.24.9.1900123.
13. Budia-Silva, M., Kostyanev, T., Ayala-Montaño, S. et al. International and regional spread of carbapenem-resistant *Klebsiella pneumoniae* in Europe. *Nat Commun*. 2024. DOI: 10.1038/s41467-024-49349-z.
14. Bush K. Past and Present Perspectives on β-Lactamases. *Antimicrob Agents Chemother.* 2018; 62:e01076-18. DOI: 10.1128/AAC.01076-18 2018.
15. Cannatelli A, D'Andrea MM, Giani T, et al. In Vivo Emergence of Colistin Resistance in Klebsiella pneumoniae Producing KPC-Type Carbapenemases Mediated by Insertional Inactivation of the PhoQ/PhoP mgrB Regulator. Antimicrob Agents Chemother. 2013; 57. DOI: 10.1128/aac.01480-13.
16. Cannatelli A, Giani T, D'Andrea MM, et al. MgrB Inactivation Is a Common Mechanism of Colistin Resistance in KPC-Producing Klebsiella pneumoniae of Clinical Origin. *Antimicrob Agents Chemother*. 2014; 58. DOI: 10.1128/aac.03110-14.
17. Carattoli A, Arcari G, Bibbolino G, et al. Evolutionary Trajectories toward Ceftazidime- Avibactam Resistance in Klebsiella pneumoniae Clinical Isolates. *Antimicrob Agents Chemother*. 2021; 65(10):e0057421. DOI:10.1128/AAC.00574-21.
18. Clegg S, Murphy CN. Epidemiology and virulence of Klebsiella pneumoniae. *Microbiol Spectrum.* 2016; 4(1):UTI-0005-2012. DOI: 10.1128/microbiolspec.UTI-0005-2012.
19. Conte V, Monaco M, Giani T, et al. Molecular epidemiology of KPC-producing Klebsiella pneumoniae from invasive infections in Italy: increasing diversity with predominance of the ST512 clade II sublineage. *J Antimicrob Chemother*. 2016; 71: 3386 –3391 DOI: 10.1093/jac/dkw337.
20. Davido B, Fellous L, Lawrence C, et al. Ceftazidime-avibactam and aztreonam, an interesting strategy to overcome β-lactam resistance conferred by metallo-β-lactamases in Enterobacteriaceae and Pseudomonas aeruginosa. *Antimicrob Agents Chemother*. 2017; 61:e01008-17. DOI: 10.1128/AAC .01008-17.
21. Di Marcantonio S, Perilli M, Alloggia G, et al. Coexistence of *bla*NDM-5, *bla*CTX-M-15, *bla*OXA-232, *bla*SHV-182 genes in multidrug-resistant *K. pneumoniae* ST437-carrying OmpK36 and OmpK37 porin mutations: First report in Italy. *Journal of Global Antimicrobial Resistance.* 2024; 24–27. DOI: 10.1016/j.jgar.2024.02.015.
22. Di Pilato V, De Angelis LH, Aiezza N, et al. Resistome and virulome accretion in an NDM-1-

producing ST147 sublineage of Klebsiella pneumoniae associated with an outbreak in Tuscany, Italy: a genotypic and phenotypic characterisation. *Lancet Microbe.* 2022; 3:e224–34. DOI: 10.1016/S2666-5247(21)00268-8.

23. Di Pilato V, Errico G, Monaco M, et al. The changing epidemiology of carbapenemase- producing Klebsiella pneumoniae in Italy: toward polyclonal evolution with emergence of high-risk lineages. *J Antimicrob Chemother.* 2021; 76: 355–361. DOI: 10.1093/jac/dkaa431.
24. Di Pilato V, Pollini S, Miriagou V, et al. Carbapenem-resistant *Klebsiella pneumoniae*: the role of plasmids in emergence, dissemination, and evolution of a major clinical challenge. *Expert Rev Anti Infect Ther.* 2024 Jan-Jun; 22(1-3):25-43. DOI: 10.1080/14787210.2024.2305854.
25. Diene SM, Rolain JM. Carbapenemase genes and genetic platforms in Gram-negative bacilli: Enterobacteriaceae, Pseudomonas and Acinetobacter species. *Clin Microbiol Infect.* 2014; 20: 831–838. DOI: 10.1111/1469-0691.12655.
26. Ding L, Shen S, Chen J, et al. Klebsiella pneumoniae carbapenemase variants: the new threat to global public health. *Clin Microbiol Rev.* 2023 Dec 20; 36(4):e0000823. DOI: 10.1128/cmr.00008-23.
27. Dobias J, Dénervaud-Tendon V, Poirel L, et al. Activity of the novel siderophore cephalosporin cefiderocol against multidrug-resistant Gram-negative pathogens. *Eur J Clin Microbiol Infect Dis*. 2017; 36:2319–2327. DOI 10.1007/s10096-017-3063-z.
28. Docquier JD, Calderone V, De Luca F, et al. Crystal structure of the OXA-48 beta-lactamase reveals mechanistic diversity among class D carbapenemases. *Chem Biol.* 2009 May 29; 16(5):540-7. DOI: 10.1016/j.chembiol.2009.04.010.
29. Dong H, Li Y, Cheng J, et al. Genomic Epidemiology Insights on NDM-Producing Pathogens Revealed the Pivotal Role of Plasmids on *bla*NDM Transmission. *Microbiol Spectr.* 2022 Apr 27; 10(2):e0215621. DOI: 10.1128/spectrum.02156-21.
30. Duin D, Doi Y. The global epidemiology of carbapenem maseproducing Enterobacteriaceae. *Virulence*. 2017; 4:460–469. DOI: 10.1080/21505594.2016.1222343.
31. Duin D, Paterson D.L. Multidrug-Resistant Bacteria in the Community: An Update. *Infectious Disease Clinics of North America.* 2020. DOI: 10.1016/j.idc.2020.08.002.
32. Edward EA, Mohamed NM, Zakaria AS. Whole Genome Characterization of the High-Risk Clone ST383 Klebsiella pneumoniae with a Simultaneous Carriage of blaCTX-M-14 on IncL/M Plasmid and blaCTX-M-15 on Convergent IncHI1B/IncFIB Plasmid from Egypt. *Microorganisms.* 2022; 10,

1097. DOI: 10.3390/ microorganisms10061097.

33. Ehmann DE, Jahić H, Ross PL, et al. Avibactam is a covalent, reversible, non–β-lactam β- lactamase inhibitor. *Proc. Natl. Acad. Sci. U.S.A.* 2012; 109 (29) 11663-11668. DOI: 10.1073/pnas.1205073109.
34. European Centre for Disease Prevention and Control. Antimicrobial resistance in the EU/EEA (EARS-Net) - Annual Epidemiological Report 2022. Stockholm: ECDC; 2023. https://www.ecdc.europa.eu/en/publications-data/surveillance-antimicrobial-resistance- europe-2022.
35. European Centre for Disease Prevention and Control. Carbapenem-resistant Enterobacteriaceae, second update – 26 September 2019. ECDC: Stockholm; 2019. https://www.ecdc.europa.eu/sites/default/files/documents/carbapenem-resistant-enterobacteriaceae-risk-assessment-rev-2.pdf.
36. European Centre for Disease Prevention and Control. Rapid risk assessment: Carbapenem-resistant Enterobacteriaceae - first update 4 June 2018. Stockholm: ECDC; 2018. https://www.ecdc.europa.eu/en/publications-data/rapid-risk-assessment-carbapenem- resistant-enterobacteriaceae-first-update.
37. European Centre for Disease Prevention and Control. Surveillance Atlas of Infectious Diseases. 2023. http://atlas.ecdc.europa.eu/public/index.aspx.
38. Falcone M, Giordano C, Barnini S, et al. Extremely drug-resistant NDM-9-producing ST147 Klebsiella pneumoniae causing infections in Italy, May 2020. *Euro Surveill.* 2020;25(48):pii=2001779. DOI: 10.2807/1560-7917.ES.2020.25.48.2001779.
39. Feng H, Liu X, Wang S, et al. The mechanism of NDM-1-catalyzed carbapenem hydrolysis is distinct from that of penicillin or cephalosporin hydrolysis. *Nat Commun.* 2017 Dec 21; 8(1):2242. DOI: 10.1038/s41467-017-02339-w.
40. Galdadas I, Lovera S, Pérez-Hernández G, et al. Defining the architecture of KPC-2 Carbapenemase: identifying allosteric networks to fight antibiotics resistance. *Sci Rep.* 2018 Aug 27; 8(1):12916. DOI: 10.1038/s41598-018-31176-0.
41. Giani T, D'Andrea MM, Pecile P, et al. Emergence in Italy of Klebsiella pneumoniae sequence type 258 producing KPC-3 Carbapenemase. *J Clin Microbiol*. 2009 Nov; 47(11):3793-4. DOI: 10.1128/JCM.01773-09.
42. Gupta N, Limbago BM, Patel JB, et al. Carbapenem-resistant Enterobacteriaceae: epidemiology and prevention. *Clin Infect Dis*. 2011 Jul 1; 53(1):60-7. DOI: 10.1093/cid/cir202.

43. Hansen G.T. Continuous Evolution: Perspective on the Epidemiology of Carbapenemase Resistance Among Enterobacterales and Other Gram-Negative Bacteria. *Infect Dis Ther.* 2021; 10: 75–92. DOI:10.1007/s40121-020-00395-2.
44. Havenga B, Ndlovu T, Clements T, et al. Exploring the antimicrobial resistance profiles of WHO critical priority list bacterial strains. *BMC Microbiology.* 2019; 19:303. DOI: 10.1186/s12866-019-1687-0.
45. Hendrickx APA, Landman F, de Haan A, et al. bla OXA-48-like genome architecture among carbapenemase-producing Escherichia coli and Klebsiella pneumoniae in the Netherlands. *Microbial Genomics*. 2021. DOI: 10.1099/mgen.0.000512.
46. Hidalgo L, de Been M, Rogers MRC, et al. Sequence-based epidemiology of an OXA-48 plasmid during a hospital outbreak. *Antimicrob Agents Chemother.* 2019; 63:e01204-19. DOI: 10.1128/AAC.01204-19.
47. Hobson CA, Pierrat G, Tenaillon O, et al. Klebsiella pneumoniae Carbapenemase Variants Resistant to Ceftazidime-Avibactam: an Evolutionary Overview. *Antimicrob Agents Chemother.* 2022; 66:e00447-22. DOI: 10.1128/aac.00447-22.
48. Hornsey M, Phee L, Wareham DW. A novel variant, NDM-5, of the New Delhi metallo-β-lactamase in a multidrug-resistant Escherichia coli ST648 isolate recovered from a patient in the United Kingdom. *Antimicrob Agents Chemother.* 2011 Dec; 55(12):5952-4. DOI: 10.1128/AAC.05108-11.
49. Howard-Jones AR, Sandaradura I, Robinson R, et al. Multidrug-resistant OXA-48/CTX-M-15 Klebsiella pneumoniae cluster in a COVID-19 intensive care unit: salient lessons for infection prevention and control during the COVID-19 pandemic. *Journal of Hospital Infection*. 2022; 64-69. DOI: 10.1016/j.jhin.2022.05.001.
50. Jeon JH, Lee JH, Lee JJ, et al. Structural basis for carbapenem-hydrolyzing mechanisms of carbapenemases conferring antibiotic resistance. *Int J Mol Sci*. 2015 Apr 29; 16(5):9654-92. DOI: 10.3390/ijms16059654.
51. Karakonstantis S, Rousaki M, Kritsotakis EI. Cefiderocol: Systematic Review of Mechanisms of Resistance, Heteroresistance and In Vivo Emergence of Resistance. *Antibiotics (Basel).* 2022 May 27; 11(6):723. DOI: 10.3390/antibiotics11060723.
52. Lapp Z, Crawford R, Miles-Jay A, et al. Regional Spread of blaNDM-1-Containing Klebsiella pneumoniae ST147 in Post-Acute Care Facilities. *Clinical Infectious Diseases.* 2021; 73(8):1431–9. DOI: 10.1093/cid/ciab457.

53. Lazareva I, Ageevets V, Sopova J, et al. The emergence of hypervirulent blaNDM-1-positive Klebsiella pneumoniae sequence type 395 in an oncology hospital. *Infection, Genetics and Evolution.* 2020. DOI: 10.1016/j.meegid.2020.104527.
54. Loconsole D, Sallustio A, Sacco D, et al. Genomic surveillance of carbapenem-resistant Klebsiella pneumoniae reveals a prolonged outbreak of extensively drug-resistant ST147 NDM-1 during the COVID-19 pandemic in the Apulia region (Southern Italy). *Journal of Global Antimicrobial Resistance.* 2024; 260-266. DOI: 10.1016/j.jgar.2024.01.015.
55. Logan LK, Weinstein RA. The Epidemiology of Carbapenem-Resistant Enterobacteriaceae: The Impact and Evolution of a Global Menace. *The Journal of Infectious Diseases*. 2017; 215(S1):S28–36. DOI: 10.1093/infdis/jiw282.
56. López Montesinos I, Carot-Coll A, Montero M.M. *et al.* A case–control study of the clinical and economic impact of infections caused by Carbapenemase-producing Enterobacterales (CPE). *Infection.* 2024. DOI: 10.1007/s15010-024-02268-z.
57. Lorenzin G, Gona F, Battaglia S, et al. Detection of NDM-1/5 and OXA-48 co-producing extensively drug-resistant hypervirulent Klebsiella pneumoniae in Northern Italy. *Journal of Global Antimicrobial Resistance*. 2022; 146–150. DOI: 10.1016/j.jgar.2022.01.001.
58. Ma J, Song X, Li M, et l. Global spread of carbapenem-resistant Enterobacteriaceae: Epidemiological features, resistance mechanisms, detection and therapy. *Microbiol Res.* 2023 Jan; 266:127249. DOI: 10.1016/j.micres.2022.127249.
59. Magi G, Tontarelli F, Caucci S, et al. High prevalence of carbapenem-resistant Klebsiella pneumoniae ST307 recovered from fecal samples in an Italian hospital. *Future Microbiol.* 2021. DOI: 10.2217/fmb-2020-0246.
60. Magiorakos AP, Srinivasan A, Carey RB, et al. Multidrug-resistant, extensively drugresistant and pandrug-resistant bacteria: an international expert proposal for interim standard definitions for acquired resistance. *Clin Microbiol Infect*. 2012; 18:268–281. DOI: 10.1111/j.1469-0691.2011.03570.x.
61. Magiorakos AP, Suetens C, Monnet DL, et al. The rise of carbapenem resistance in Europe: just the tip of the iceberg? *Antimicrobial Resistance and Infection Control.* 2013; 2:6. http://www.aricjournal.com/content/2/1/6.
62. Maida CM, Bonura C, Geraci DM, et al. Outbreak of ST395 KPC-Producing Klebsiella pneumoniae in a Neonatal Intensive Care Unit in Palermo, Italy. *Infection Control & Hospital Epidemiology*. 2018. DOI: 10.1017/ice.2017.267.

63. Martin MJ, Corey BW, Sannio F, et al. Anatomy of an extensively drug-resistant Klebsiella pneumoniae outbreak in Tuscany, Italy. *Proc. Natl. Acad. Sci. U.S.A.* 2021. DOI: 10.1073/pnas.2110227118.

64. Matesanz M, Mensa J. Ceftazidime-avibactam. *Rev Esp Quimioter.* 2021; 34 (Suppl. 1): 38-40. DOI: 10.37201/req/s01.11.2021.

65. Meletis G. Carbapenem resistance: overview of the problem and future perspectives. *Ther Adv Infect Dis*. 2016 Feb; 3(1):15-21. DOI: 10.1177/2049936115621709.

66. Oteo J, Hernandez JM, Espasa M, et al. Emergence of OXA-48-producing Klebsiella pneumoniae and the novel carbapenemases OXA-244 and OXA-245 in Spain. *J Antimicrob Chemother*. 2013; 68: 317 –321. DOI: 10.1093/jac/dks383.

67. Palmieri M, Wyres KL, Mirande C, et al. Genomic evolution and local epidemiology of Klebsiella pneumoniae from a major hospital in Beijing, China, over a 15 year period: dissemination of known and novel high-risk clones. *Microbial Genomics*. 2021; 7:000520. DOI: 10.1099/mgen.0.000520.

68. Papp-Wallace KM, Endimiani A, Taracila MA, et al. Carbapenems: past, present, and future. *Antimicrob Agents Chemother.* 2011 Nov; 55(11):4943-60. DOI: 10.1128/AAC.00296-11.

69. Pérez-Vázquez M, Sola Campoy PJ, Ortega A, et al. Emergence of NDM-producing Klebsiella pneumoniae and Escherichia coli in Spain: phylogeny, resistome, virulence and plasmids encoding blaNDM-like genes as determined by WGS. *J Antimicrob Chemother.* 2019 Dec 1; 74(12):3489-3496. DOI: 10.1093/jac/dkz366.

70. Petrosillo N, Taglietti F, Granata G. Treatment Options for Colistin Resistant Klebsiella pneumoniae: Present and Future. *J. Clin. Med.* 2019; 8, 934. DOI:10.3390/jcm8070934.

71. Pitout JDD, Peirano G, Kock MM, et al. The global ascendency of OXA-48-type carbapenemases. *Clin Microbiol Rev*. 2019; 33:e00102-19. DOI: 10.1128/CMR.00102-19.

72. Pitout JDD, Peirano G, Kock MM, et al. The global ascendency of OXA-48-type carbapenemases. *Clin Microbiol Rev*. 2019; 33:e00102-19. DOI: 10.1128/CMR.00102-19.

73. Poirel L, Héritier C, Tolün V, et al. Emergence of Oxacillinase-Mediated Resistance to Imipenem in Klebsiella pneumoniae. *Antimicrob Agents Chemother*. 2004; 48: DOI: 10.1128/aac.48.1.15-22.2004.

74. Poirel L, Potron A, Nordmann P. OXA-48-like carbapenemases: the phantom menace. *J Antimicrob Chemother*. 2012; 67: 1597 –1606. DOI: 10.1093/jac/dks121.

75. Politi L, Gartzonika K, Spanakis N, et al. Emergence of NDM-1-producing Klebsiella pneumoniae in Greece: evidence of a widespread clonal outbreak. *J Antimicrob Chemother*. 2019; 74: 2197–2202. DOI: 10.1093/jac/dkz176.

76. Potron A, Poirel L, Nordmann P. Derepressed Transfer Properties Leading to the Efficient Spread of the Plasmid Encoding Carbapenemase OXA-48. *Antimicrob Agents Chemother*. 2014 DOI: 10.1128/aac.01344-13.

77. Queenan AM, Bush K. Carbapenemases: the versatile beta-lactamases. *Clin Microbiol Rev.* 2007 Jul; 20(3):440-58. DOI: 10.1128/CMR.00001-07.

78. Ranieri SC, Fabbrizi V, D' Amario AM, et al. First report of a blaNDM-producing extensively drug resistant Klebsiella pneumoniae ST437 in Italy. *Front. Cell. Infect. Microbiol*. 2024; 14:1426817. DOI: 10.3389/fcimb.2024.1426817.

79. Richter SN, Frasson I, Franchin E, et al. KPC-mediated resistance in Klebsiella pneumoniae in two hospitals in Padua, Italy, June 2009-December 2011: massive spreading of a KPC-3- encoding plasmid and involvement of non-intensive care units. *Gut Pathog.* 2012 Jul 16; 4(1):7. DOI: 10.1186/1757-4749-4-7.

80. Ripabelli G, Sammarco ML, Salzo A, et al. New Delhi metallo-b-lactamase (NDM-1)- producing Klebsiella pneumoniae of sequence type ST11: first identification in a hospital of central Italy. *Applied Microbiology.* 2020; 652-659. DOI: 10.1111/lam.13384.

81. Sabnis A, Hagart KLH, Klöckner A, et al. Colistin kills bacteria by targeting lipopolysaccharide in the cytoplasmic membrane. *eLife*. 2021; 10:e65836. DOI: 10.7554/eLife.65836.

82. Savov E, Politi L, Spanakis N, et al. NDM-1 Hazard in the Balkan States: Evidence of the First Outbreak of NDM-1 Producing Klebsiella pneumoniae in Bulgaria. *Microbial Drug Resistance*. 2018. DOI: 10.1089/mdr.2017.0230.

83. Sawa T, Kooguchi K, Moriyama K. Molecular diversity of extended-spectrum β-lactamases and carbapenemases, and antimicrobial resistance. J *Intensive Care*. 2020. DOI: 10.1186/s40560-020-0429-6.

84. Scaltriti E, Piccinelli G, Corbellini S, et al. Detection of a hypermucoviscous Klebsiella pneumoniae co-producing NDM-5 and OXA-48 carbapenemases with sequence type 383, Brescia, Italy. *International Journal of Antimicrobial Agents.* 2020; 106130. DOI: 10.1016/j.ijantimicag.

85. Seara N, Oteo J, Carrillo R, et al. Interhospital spread of NDM-7-producing Klebsiella pneumoniae belonging to ST437 in Spain. *International Journal of Antimicrobial Agents*. 2015; 169-173. DOI:

10.1016/j.ijantimicag.2015.04.001.

86. Seki LM, Pereira PS, de Souza MPAH, et al. Molecular epidemiology of KPC-2-producing Klebsiella pneumoniae isolates in Brazil: the predominance of sequence type 437. *Diagnostic Microbiology and Infectious Disease.* 2011; 274-277. DOI: 10.1016/j.diagmicrobio.2011.01.006.
87. Sharma R, Park TE, Moy S. Ceftazidime-Avibactam: A Novel Cephalosporin/β-Lactamase Inhibitor Combination for the Treatment of Resistant Gram-negative Organisms. Clin Ther. 2016; 38(3):431-44. DOI: 10.1016/j.clinthera.2016.01.018.
88. Shirley M. Ceftazidime-Avibactam: A Review in the Treatment of Serious Gram-Negative Bacterial Infections*. Drugs.* 2018; 78:675–692. DOI: 10.1007/s40265-018-0902-x.
89. Simner PJ, Mostafa HH, Bergman Y, et al. Progressive Development of Cefiderocol Resistance in Escherichia coli During Therapy is Associated With an Increase in blaNDM-5 Copy Number and Gene Expression. *Clinical Infectious Diseases*. 2022;75(1):47–54. DOI: 10.1093/cid/ciab888.
90. Strydom KA, Chen L, Kock MM, et al. Klebsiella pneumoniae ST307 with OXA-181: threat of a high-risk clone and promiscuous plasmid in a resource-constrained healthcare setting*. J Antimicrob Chemother*. 2020; 75: 896–902. DOI: 10.1093/jac/dkz550.
91. Tavoschi L, Forni S, Porretta A, et al. Prolonged outbreak of New Delhi metallo-beta- lactamase-producing carbapenem-resistant Enterobacterales (NDM-CRE), Tuscany, Italy, 2018 to 2019. *Euro Surveill*. 2020; 25(6):pii=2000085. DOI: 10.2807/1560-7917.ES.2020.25.6.2000085.
92. Tenover FC, Arbeit RD, Goering RV, et al. Interpreting chromosomal DNA restriction patterns produced by pulsed-field gel electrophoresis: criteria for bacterial strain typing. *J Clin Microbiol*. 1995 Sep;33(9):2233-9. DOI: 10.1128/jcm.33.9.2233-2239.1995.
93. Tsai YK, Fung CP, Lin JC, et al. Klebsiella pneumoniae outer membrane porins OmpK35 and OmpK36 play roles in both antimicrobial resistance and virulence. *Antimicrob Agents Chemother*. 2011 Apr; 55(4):1485-93. DOI: 10.1128/AAC.01275-10.
94. Tsui CKM, Abid FB, McElheny CL, et al. Genomic epidemiology revealed the emergence and worldwide dissemination of ST383 carbapenem-resistant hypervirulent *Klebsiella pneumoniae* and hospital acquired infections of ST196 *Klebsiella quasipneumoniae* in Qatar. *bioRxiv*. 2022; 06.02.494628. DOI: 10.1101/2022.06.02.494628.
95. Tumbarello M, Trecharichi EM, De Rosa FG, et al. Infections caused by KPC-producing Klebsiella pneumoniae: differences in therapy and mortality in a multicentre study. *J Antimicrob Chemother.* 2015; 70: 2133 –2143. DOI: 10.1093/jac/dkv086.

96. Turton J, Davies S, Turton J, et al. Hybrid Resistance and Virulence Plasmids in “High-Risk” Clones of Klebsiella pneumoniae, Including Those Carrying blaNDM-5. *Microorganisms*. 2019; 7, 326. DOI: 10.3390/microorganisms7090326.

97. Villa L, Feudi C, Fortini D, et al. Diversity, virulence, and antimicrobial resistance of the KPC-producing Klebsiella pneumoniae ST307 clone. *Microbial Genomics*. 2017; 3. DOI: 10.1099/mgen.0.000110.

98. Wise MG, Karlowsky JA, Mohamed N, et al. Global Trends in Carbapenem- and Difficult-to- Treat-Resistance Among World Health Organization Priority Bacterial Pathogens: ATLAS Surveillance Program 2018-2022. *Journal of Global Antimicrobial Resistance.* 2024. DOI: 10.1016/j.jgar.2024.03.020.

99. Woodford N, Turton JF, Livermore DM. Multiresistant Gram-negative bacteria: the role of high-risk clones in the dissemination of antibiotic resistance. *FEMS Microbiol Rev*. 2011; 736–755. DOI: 10.1111/j.1574-6976.2011.00268.x.

100. Wu W, Feng Y, Tang G, et al. NDM metallo-β-lactamases and their bacterial producers in health care settings. *Clin Microbiol Rev.* 2019; 32:e00115-18. DOI: 10.1128/CMR .00115- 18.

101. Yao J, Wang J, Chen M, et al. Cefiderocol: An Overview of Its *in-vitro* and *in-vivo* Activity and Underlying Resistant Mechanisms. *Front Med (Lausanne).* 2021 Dec 7; 8:741940. DOI: 10.3389/fmed.2021.741940.

102. Yigit H, Queenan AM, Anderson GJ, et al. Novel carbapenem-hydrolyzing beta-lactamase, KPC-1, from a carbapenem-resistant strain of Klebsiella pneumoniae. *Antimicrob Agents Chemother.* 2001 Apr; 45(4):1151-61. DOI: 10.1128/AAC.45.4.1151-1161.2001.

103. Young D. Toleman M.A., Giske C.G., et al. Characterization of a New Metallo-β-Lactamase Gene, blaNDM-1, and a Novel Erythromycin Esterase Gene Carried on a Unique Genetic Structure in Klebsiella pneumoniae Sequence Type 14 from India. *Antimicrob Agents Chemother.* Dec 2009; 5046–5054. DOI: 10.1128/AAC.00774-09.

104. Zhanel GG, Lawrence CK, Adam H, et al. Imipenem–Relebactam and Meropenem–Vaborbactam: Two Novel Carbapenem-b-Lactamase Inhibitor Combinations. *Springer Nature.* 2017; 78:65–98. DOI: 10.1007/s40265- 017-0851-9.

105. Zhu J, Wang G, Li M. Outbreak of NDM-5-producing Klebsiella pneumoniae ST307: an emerging high-risk antimicrobial resistance clone in Shanghai, China. *mSystem.* 2024. DOI: 10.1128/msystems.01369-23.